КРИСТАЛЛОГРАФИЯ

SOVIET PHYSICS

Crystallography

VOLUME 2 NUMBER 6

A Translation

of the journal

Crystallography

of the

Academy of Sciences of the USSR

(RUSSIAN ORIGINAL VOL. 2, NO. 6)

Published by the

AMERICAN INSTITUTE OF PHYSICS

INCORPORATED

SOVIET PHYSICS

Crystallography

A translation of the journal "Crystallography" of the Academy of Sciences of the USSR

A publication of the
AMERICAN INSTITUTE OF PHYSICS

Governing Board

FREDERICK SEITZ, *Chairman*

Members

WALTER S. BAIRD
JAMES G. BAKER
JESSE W. BEAMS
R. H. BOLT
J. W. BUCHTA
J. H. DILLON
VERNET E. EATON
HERBERT A. ERF
S. A. GOUDSMIT
W. W. HAVENS, JR.
C. KITTEL
WINSTON E. KOCK
R. BRUCE LINDSAY
WALTER C. MICHELS
C. J. OVERBECK
G. E. PAKE
JOSEPH B. PLATT
RALPH A. SAWYER
JOHN STRONG
GEORGE E. UHLENBECK
VICTOR F. WEISSKOPF

Officers and Staff

ELMER HUTCHISSON
Director
HENRY A. BARTON
Associate Director
WALLACE WATERFALL
Secretary and Treasurer
EDWARD P. TOBER
Mgr., Production and Distribution
THEODORE VORBURGER
Advertising Manager
RUTH F. BRYANS
Publication Manager
KATHRYN SETZE
Assistant Treasurer
ALICE MASTROPIETRO
Circulation Manager
EUGENE H. KONE
Director of Public Relations
WILLIAM C. KELLY
Director of Education Projects

American Institute of Physics Advisory Board on Russian Translations

ROBERT T. BEYER, *Chairman*

FREEMAN DYSON, DWIGHT GRAY, MORTON HAMMERMESH, DAVID HARKER, VLADIMIR ROJANSKY, HAROLD F. WEAVER

Advisory Editor, Soviet Physics – Crystallography: DAVID HARKER, Protein Structure Project, Polytechnic Institute of Brooklyn, Brooklyn 2, New York.

"Soviet Physics – Crystallography" is published by the American Institute of Physics, with the cooperation of the American Crystallographic Association, for the purpose of making available in English reports of current Soviet research in crystallography as contained in the journal "Crystallography" of the Academy of Sciences of the USSR. The translation begins with the 1957 issues.

Transliteration of the names of Russian authors follows the system employed by the Library of Congress.

This translating and publishing project was undertaken by the Institute in the conviction that dissemination of the results of research everywhere in the world is invaluable to the advancement of science. The National Science Foundation of the United States encouraged the project initially and is supporting it in large part by a grant. Translation and printing are being handled by Consultants Bureau, Inc.

The American Institute of Physics and its translators propose to translate faithfully all of the scientific material in the "Crystallographic Journal of the Academy of Sciences of the USSR" appearing after January 1, 1957. The views expressed in the translated material, therefore, are intended to be those expressed by the original authors, and not those of the translators nor of the American Institute of Physics.

One volume is published annually. The volume numbering coincides with that of the original Russian journal.

Subscription Prices:

Per year (6 issues), starting with Vol. 2, No. 1

General: United States and Canada	$25.00
Elsewhere	27.00
Libraries of non-profit academic institutions:	
United States and Canada	10.00
Elsewhere	12.00
Back numbers, all issues	5.00

Subscriptions should be addressed to the American Institute of Physics, 335 East 45th Street, New York 17, New York.

Copyright American Institute of Physics Incorporated, 1959

SOVIET PHYSICS

Crystallography

VOLUME 2, NUMBER 6 NOVEMBER-DECEMBER 1957

IN MEMORY OF OSIP MARKOVICH ANSHELES

Soviet crystallographic science has sustained a great loss. Professor Osip Markovich Ansheles, head of the Department of Crystallography at the Leningrad State University, died after a serious illness on July 23, 1957, in his seventy-second year.

Death removed from our ranks one of the most prominent Soviet crystallographers, the talented carrier of the traditions of the Fedorov school of crystallography. We lost the oldest Soviet crystallographer, who trained several generations of crystallographers and was a sensitive and painstaking person.

O. M. Ansheles was born on October 5 (17), 1885, in the town of Penza in an artisan's family. He graduated from the 2nd Penza Gymnasium in 1904. Following his father's death, Osip Markovich was forced, beginning with his sophomore year, to earn his living by giving private lessons.

In 1906 O. M. Ansheles enrolled in the physicomathematical department of the Kharkov University, and in 1907 transferred to the natural science division of the physicomathematical department of the St. Petersburg University in the geology and mineralogy group. In 1911, the students of the University, among whom were O. M. Ansheles, B. P. Orelkin and G. V. Pigulevskii, organized a group and began to attend a special course of crystallography by E. S. Fedorov at the Mining Institute. From then on, O. M. Ansheles became fascinated with crystallography and with Fedorov's ideas and decided to devote himself entirely to this science.

While still a student, he carried out a series of researches at E. S. Fedorov's suggestion, and took part in editing the manual on Fedorov's method, which at that time was being compiled by Fedorov's student, V. V. Nikitin. On completing the University course in 1913, Osip Markovich was retained there to continue his studies towards a professorship. At that time he was conducting, under B. A. Popov's direction, crystallo-optical researches by the universal method on feldspar and other minerals form the ores of the Kolskii peninsula. In 1915, E. S. Fedorov invited Osip Markovich to become an assistant in the department of crystallography of the Mining Institute.

Here he lectured on Fedorov's crystallochemical analysis, and worked out important questions of method essential for its application (methods for determining recticular density, methods of calculation, and graphic solution of goniometric problems). Later he extended these studies and compiled an important monograph "Computational and Graphic Methods of Crystallography" (1939), which is widely known. After E. S. Fedorov's death, O. M. Ansheles lectured for many years on Fedorov's crystallochemical analysis at the Mining Institute.

In 1924 O. M. Ansheles established an independent chair of crystallography in the geology department of the Leningrad University. From then on until the last days of his life he devoted all his strength and all his scientific and pedagogical talent to his department. Through his efforts, the department of crystallography of the Leningrad University became an important and well-equipped establishment for the teaching of scientific crystallography. In this department, crystallization, crystallo-optical, goniometric and x-ray laboratories were set up. Students and followers, many of whom became prominent scientists, grouped themselves around Osip Markovich. Intensive research and study went on in these laboratories, in which O. M. Ansheles participated most actively. He created in the department Fedorov's circle of scientific crystallography, which attracted to its meetings crystallographers from Leningrad, Moscow, and other cities. The circle discussed the essential questions of modern crystallography and the basic problems of this science.

It is impossible to do justice to Osip Markovich's many-faceted scientific activity. More than 70 published works are the product of his pen, among them a series of important monographs and textbooks, which are universally known.* Osip Markovich's creative interests were diverse and touched upon almost all the divisions of modern crystallography.

He worked out the most convenient method for the calculations and graphic solutions of the problems of goniometry which arise in using Fedorov's theodolite goniometer. His method of direct substitution, his exceptionally simple and graceful graphic methods, and his approach have all become part of the practice of experimental goniometric research. O. M. Ansheles' method of calculating the relative reticular density of crystal faces simplifies considerably the treatment of the data when solving some structural problems.

O. M. Ansheles was greatly interested in problems of crystal genesis. In this area he carried out a series of experimental studies of the mechanism of crystal growth; he confirmed E. S. Fedorov's hypothesis that the growth of crystals is possible by means of the precipitation of small crystals – embryos – on their faces, he elucidated the mechanism of the formation of inclusions of the mother solution in the growing crystal, established the wide distribution of laminar crystal growth, which often appears as steps on crystal faces, and finally showed that rounded growth forms are as characteristic of crystals under certain growth conditions as is flat-facedness. His work in the field of crystal genesis led him, independently of the corresponding assumptions of other authors, to the idea of developing an accelerated method, the so-called dynamic one, of growing large single crystals which has been in wide use in industry and technology.

Recently, on the basis of his experimental and theoretical studies of crystal growth without a framework, Osip Markovich showed that the rounded forms characteristic of crystals of native quartz can arise as a result of growth, and not of solution, as had been assumed by some mineralogists. These studies are of great practical significance for the understanding of the genesis of native quartzes and for the development of methods of synthesizing them.

Of great significance is O. M. Ansheles' work in the field of perfecting crystallo-optic methods of analysis of substances. It must be noted here first that, even in the beginning of the twenties, he was the first in our country to apply the immersion method to the study of sedimentary rock. His development of this method was original and found general application. Secondly, it is to O. M. Ansheles that belongs the idea of perfecting and simplifying microchemical analysis by means of a consistent use of the crystallo-optical constants of the products obtained in the course of microchemical reactions. To him belongs a series of brilliant studies, in which he showed how new possibilities arise in using his methods of optical analysis in studying crystalline substances.

Osip Markovich was always exceptionally modest, accessible and self-critical, and inculcated a similar high personal standard of achievement in his students. Meticulous adherence to principle in scientific work was

* For the bibliography of O. M. Ansheles' works, see "Vestnik Leningrad Univers." 10, 120-122 (1955), and also Zapiski Vsesoiusnogo Mineralog. Obshchestva 86 (1957).

his outstanding trait. The research of his students and co-workers always interested him deeply. Everyone could obtain from him objective criticism and attentive consideration, as well as advice and assistance.

In the last years of his life, already seriously ill, Osip Markovich continued to develop successfully his ideas in the field of crystal genesis, re-edited the classical works of his great teacher, E. S. Fedorov, and was engaged in compiling the original manual "Goniometry of Crystals with and without Faces," which, unfortunately remains unfinished. O. M. Ansheles retained his energy and freshness of thought to the last days of his life.

Everyone who knew him will always remember him as an indefatigable scientific worker, a great scientist and a wonderful person.

Osip Markovich Ansheles' name will live in the history of crystal science. His works will occupy an honored place in the treasury of the crystallographic literature of his country.

V. A. Frank-Kamenetskii

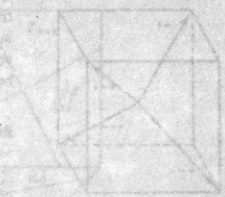

CONCERNING THE TETRAHEDRAL (T = 23) AND GYROHEDRAL (O = 432) GROUPS

N. V. Belov

It is well known that the presence of 4 triad axes parallel to the body diagonals of the cube gives rise to a set of three mutually perpendicular diad axes, parallel to the edges of the same cube. Sometimes it is said that the "coordinate" diad axis is the product of the two triad axes which have an included angle of 109°28'16". More precisely, if one were to "cross multiply" not the axes, but the corresponding operations – rotations in this case – we would obtain less usual products. The result of two consecutive rotations around the two triad axes with an included angle of 109°28'16" (arccos $-\frac{1}{3}$) will be a rotation about one of the coordinate diad axes if the triad rotations are opposite in sign (one right-handed, the other left-handed), and a rotation about a triad axis if both rotations have the same sign. A left-hand rotation about the "derivative" triad axis corresponds to two right-hand rotations about the different triad axes, and a right-hand rotation corresponds to two left-hand ones. A change in the order of the rotation factors leads to a rotation about the fourth triad axis (see below).

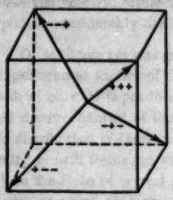

Fig. 1. Denotation of the four triad axes of the cube.

The denotation of the four triad axes and their mutual arrangement are shown in Fig. 1.

If one were to proceed from the three mutually perpendicular tetrad axes of the cubic classes O = 432 or $O_h = \frac{4}{m}\bar{3}\frac{2}{m}$, then the product of 2 tetrad rotations about the two tetrad axes would be a rotation about the corresponding triad axis. But if rotations of 180° (double) were made about the same derivative axes, then, as is well known, the result would be again a double rotation about the third tetrad axis. If the rotation about one of the tetrad axes is 90° (four-fold), and then immediately 180° (two-fold) about the other tetrad, then the resulting rotation will be two-fold about the "diagonal" diad axis, which is in the plane perpendicular to that axis about which the 90° rotation is performed and makes a 45° angle with the second factor, that is, with the second tetrad axis.

All these peculiarities, in particular the noncommutability of the products of the rotations in the (tetrahedral) T = 23 and (gyrohedral) O = 432 groups, can be established very simply if, for the first group, two tetrahedra closest to the cube are used analogously [1] (in the hkl symbol the first index is much larger than the two other), and, for the second group, two gyrohedra of the same sort. In other words, we shall have 2 cubes with the faces of each (Fig. 2) divided by an oblique "edge," and two other cubes, the faces of which are divided by two mutually perpendicular oblique edges (Fig. 3).

We find without difficulty by the method recommended in [1] (actually a simpler one, inasmuch as here there are neither planes of symmetry, nor centers):

$$a\ 3_{+++} \times 3_{+--} = 3^{-1}_{-+-} \qquad a'\ 3_{+--} \times 3_{+++} = 3_{-++}$$

$$a''\ 3_{+++} \times 3^{-1}_{+--} = 2_y \qquad a'''\ 3_{+--} \times 3^{-1}_{+++} = 2_z$$

$$b\ 4_x \times 4_y = 3^{-1}_{--+} \qquad b'\ 4_y \times 4_x = 3_{+++}$$

$$b'\ 4_x^{-1} \times 4_y^{-1} = 3_{+++}^{-1} \qquad b''\ 4_y^{-1} \times 4_x^{-1} = 3_{--+}$$
$$b^{IV}\ 4_x \times 4_y^{-1} = 3_{+--}^{-1} \qquad b^{V}\ 4_y^{-1} \times 4_x = 3_{+--}$$
$$c\ 2_z (= 4_z^2) \times 2_y (= 4_y^2) = 2_x$$
$$d\ 4_x \times 2_y = 2_{o+-} \quad d'\ 2_y \times 4_x = 2_{o++}$$

Of course, all these results can be interpreted if one writes out the coordinates of the intermediate and final positions of the point mnp which is subjected to subsequent rotations. Thus, for the product a we shall have: mnp, pmn, $\overline{pmn}$, $\overline{npm}$, $\overline{npm}$. Comparing the last term with the first one, we find that the final result is a left-

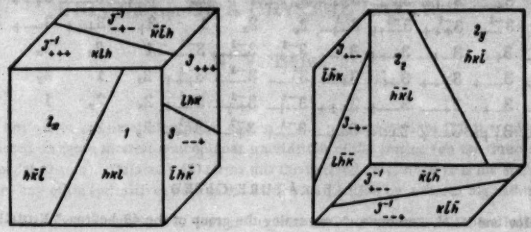

a b

Fig. 2. The simplest tetrahedron (pentagondihexahedron).

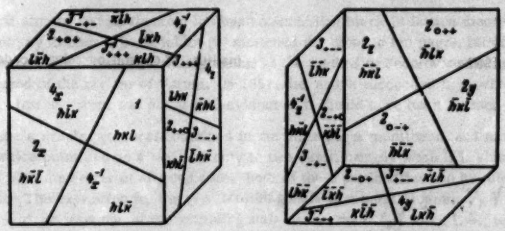

a b

Fig. 3. The simplest gyrohedron (pentagontetrahexahedron).

hand rotation about the axis 3_{-+-}. For the product d we obtain the following points: mnp, $\overline{mpn}$, $\overline{mpn}$. The last set of three is obtained from the first one by the action of the diagonal axis in the Oyz* quadrant.

Inasmuch as group T=23 contains only 12 operations, we shall write out here the corresponding Cayley's square, in which the first factor is always taken from the left vertical column and the second one from the upper horizontal line.

Cayley's square for the tetrahedron T = 23 group

---

* The points obtained from mnp as a result of right-handed and lef-handed rotations about the triad axes (see Fig. 2) are

$$3_{+++}\ pmn;\ npm\ \ 3_{+--}\ \overline{pmn};\ \overline{npm}$$
$$3_{-+-}\ pmn;\ \overline{npm}\ \ 3_{--+}\ \overline{pmn};\ npm$$

Points obtained as a result of the action of the diagonal diad axes are

$$2_{o++}\ \overline{mpn}\ \ 2_{o+-}\ \overline{mpn}$$

1	3^{-1}_{+++}	3^{-1}_{+--}	3^{-1}_{-+-}	3^{-1}_{--+}	2_x	2_y	2_z	3_{--+}	3_{-+-}	3_{+--}	3_{+++}
3_{+++}	1	2_y	2_z	2_x	3_{+-}	3_{--+}	3_{+--}	3^{-1}_{+--}	3^{-1}_{--+}	3^{-1}_{-+-}	3^{-1}_{+++}
3_{+--}	2_y	1	2_x	2_z	3_{--+}	3_{-+-}	3_{+++}	3^{-1}_{-+-}	3^{-1}_{+++}	3^{-1}_{+--}	3^{-1}_{--+}
3_{-+-}	2_z	2_x	1	2_y	3_{+++}	3_{+--}	3_{--+}	3^{-1}_{+++}	3^{-1}_{+--}	3^{-1}_{--+}	3^{-1}_{+--}
3_{--+}	2_x	2_z	2_y	1	3_{+--}	3_{+++}	3_{-+-}	3^{-1}_{--+}	3^{-1}_{+--}	3^{-1}_{+++}	3^{-1}_{-+-}
2_x	3^{-1}_{+-}	3^{-1}_{--+}	3^{-1}_{+++}	3^{-1}_{+--}	1	2_z	2_y	3_{+++}	3_{+--}	3_{-+-}	3_{--+}
2_y	3^{-1}_{+--}	3^{-1}_{+-}	3^{-1}_{+--}	3^{-1}_{+++}	2_z	1	2_x	3_{-+-}	3_{--+}	3_{+++}	3_{+--}
2_z	3^{-1}_{--+}	3^{-1}_{+++}	3^{-1}_{--+}	3^{-1}_{+-}	2_y	2_x	1	3_{+--}	3_{+++}	3_{--+}	3_{-+-}
3^{-1}_{--+}	3_{+--}	3_{-+-}	3_{+++}	3_{--+}	3^{-1}_{+++}	3^{-1}_{-+-}	3^{-1}_{+--}	1	2_z	2_x	2_y
3^{-1}_{-+-}	3_{--+}	3_{+++}	3_{-+-}	3_{+--}	3^{-1}_{+--}	3^{-1}_{--+}	3^{-1}_{+++}	2_z	1	2_y	2_x
3^{-1}_{+--}	3_{-+-}	3_{+--}	3_{--+}	3_{+++}	3^{-1}_{--+}	3^{-1}_{+++}	3^{-1}_{--+}	2_x	2_y	1	2_z
3^{-1}_{+++}	3_{+++}	3_{--+}	3_{+--}	3_{-+-}	3^{-1}_{--+}	3^{-1}_{+--}	3^{-1}_{--+}	2_y	2_x	2_z	1

LITERATURE CITED

[1] N. V. Belov and T. N. Tarkhova, "Concerning the group of the 48-hedron," Kristallografiia 1, 2, 360-361 (1956).

[2] N. V. Belov, "Concerning a course of geometric crystallography for physicists," Kristallografiia 2, 5, 678-685 (1957).*

Received October 7, 1957

Institute of Crystallography, Academy of Sciences, USSR

* [Soviet Physics – Crystallography, p. 667].

A THEOREM ON THE PRIMITIVENESS (EMPTINESS) OF THE UNIT CELL OF A CRYSTAL LATTICE

N. V. Belov

In a crystal lattice (in the parallelepipedal system of the mathematicians [1]) it is always possible to find a unit cell constructed on three shortest noncoplanar translations of the lattice (on the three consequent minima of the parallelepipedal system). Delaunay [2] terms this the derived cell, since it is the standard which it is possible to derive from any other (primitive) cell of the lattice in question by a direct algorithm.

If it is desired to construct this lattice for some crystal and, maintaining self-parallelism, to place one of its lattice points at any point (atom) in the crystal in which we are interested, then all other homologous points [1] must be situated at the vertices of the repeating unit cell, and no homologous point may appear inside the cell, nor on its face, nor on its edge.

This simple and almost obvious theorem has been a stumbling block in lattice theory [2]. It was first proved, at considerable length, by Zeeber [2]. Dirichlet [2] shortened the proof to ten pages, introducing the method which subsequently came to be known among crystallographers as the method of Fedorov's parallelahedra, and to mathematicians as the method of the regions of Varoni. In 1951, the author succeeded in proving this theory in three pages [3], but nonetheless the proof was not as self-evident as it should have been for such an obvious theorem.

In the meantime a simple proof was contained in the three pages mentioned, and turns out to be, essentially, that an additional lattice point can be a real one only in two cases, namely when it is at the body center of the unit cell, or when it is in the center of any one face. Both of these possibilities can be ruled out immediately for the fundamental cell. The expression for the two semidiagonals of a parallelogram $\frac{1}{2}\sqrt{a^2+b^2 \pm 2ab\cos\gamma}$ shows that (where $a \leq b$), at least one of the semidiagonals is less than $\frac{1}{2}\sqrt{2b^2}$, i. e., less than 0.72 b, contrary to the original assumption.*

In the same way from the expression for the four space semidiagonals of the unit cell,

$$\frac{1}{2}d = \frac{1}{2}\sqrt{a^2+b^2+c^2+2bc\cos\alpha+2ca\cos\beta+2ab\cos\gamma},$$

$$\frac{1}{2}d' = \frac{1}{2}\sqrt{a^2+b^2+c^2+2bc\cos\alpha-2ca\cos\beta-2ab\cos\gamma} \quad \text{etc.},$$

it follows that (where $a \leq b \leq c$), one of the $\frac{1}{2}d$ is less than $\frac{1}{2}\sqrt{3c^2} \approx 0.87\,c$, contrary to the original assumption.

From the properties of a translational lattice, two additional lattice points are possible on one diagonal, which they divide into three equal parts.

Corresponding to the formula given above (where $60° \leq \alpha, \beta, \gamma \leq 120°$) a third of the largest diagonal $\leq \frac{1}{3}\sqrt{6c^2} \approx 0.8\,c$, i. e., this possibility is also excluded.

---

* Insofar as in a primitive parallelogram $60° \leq \gamma \leq 120°$ (cf. [1]), then both semidiagonals even appear to be less than $b(\frac{1}{2}b\sqrt{3})$.

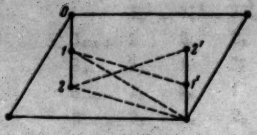

Fig. 1. Family of additional lattice points in the unit cell.

Three additional lattice points are possible only in the centers of the three faces, and this possibility is excluded, reducing itself to the plane case. In all other cases the additional lattice point gives rise to at least three more lattice points, as is shown schematically in Fig. 1. If they are all in one plane xy, then the coordinates of one of them satisfy the condition $x < \frac{a}{2}$, $y < \frac{b}{2}$, and consequently the corresponding radius vector is smaller than the semidiagonal, the largest of which is equal to $\frac{1}{2}\sqrt{a^2 + b^2 + 2|ab|\cos 60^\circ} \leq \frac{1}{2}\sqrt{3b^2} \approx 0.87b$. If four additional lattice points do not lie in one plane then, together with the lattice points of the unit cell system, they give rise, simultaneously, to $\frac{1}{2} \cdot 5 \cdot 4 = 10$ vectors. If at least one has a component along x, y, or z, expressible as an irreducible simple fraction p/m, then the m-repetition of this vector produces a complementary lattice point on one of the fundamental faces of the unit cell under consideration, and the theorem is proved. If this is not the case for any of the vectors, then on three of them, A, B, C, with coordinates (x_1, y_1, z_1), (x_2, y_2, z_2), (x_3, y_3, z_3) construct a lattice originating from the origin of the fundamental lattice.

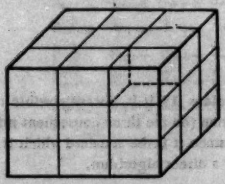

Fig. 2. The 27 small cells in the basic unit cell.

A vector from the origin to any lattice point of the new lattice can be expressed in the form $mA + nB + pC$, where m, n, and p are integers. Resolving the system into three inequalities,

$$\text{fractional part } \{mx_1 + nx_2 + px_3\} \leqslant \frac{1}{3}$$
$$\text{fractional part } \{my_1 + ny_2 + py_3\} \leqslant \frac{1}{3}$$
$$\text{fractional part } \{mz_1 + nz_2 + pz_3\} \leqslant \frac{1}{3}$$

we find the lattice point which is situated in the first (the nearest to O) of the 27 small cells into which the unit cell is divided, as a result of dividing each edge into three equal parts and tracing through these points planes parallel to the faces of the unit cell (Fig. 2). No vector from the origin which terminates inside this small cell can have a length greater than $\frac{1}{3}$ of the diagonal of the unit cell, i. e., at most $\frac{1}{3}\sqrt{6c^2} \approx 0.82c$, and the theorem is proved.

If a proof is required without a system of inequalities, then consider the case where all three coordinates of the additional lattice point are irrational. Having set up the appropriate fractions for one of them, we shall be able, with a corresponding repetition of the vector, to adjust an alternate lattice point to be so near to the net of the unit cell that the additional component 0.87c (see above) gives for $\sqrt{(0.87c)^2 + \delta^2}$ less than c.

The case where all the coordinates of the additional lattice point are represented by irreducible fractions of common denominator m, and which had appeared difficult, may be solved in this way.[3].

If m is even, then all three numerators p, q, r, are odd and the $\frac{1}{2}$-m lattice point falls in the center of the central cell of the large p × q × r net, which, as was shown, proves the theorem.

If m is odd, and p, q, r are all even, then the vector between the $\frac{1}{2}(m + 1)$ lattice point and the $\frac{1}{2}(m - 1)$ one is divided into two halves, one on either side of the lattice point of the unit cell, i. e., there must be one additional lattice point in the unit cell, at a distance from the origin half as great, and the value of m is doubled. If, after this, the doubly reduced numerators p', q', r' remain even, then consider the lattice point which (by inversional symmetry) must be present in the unit cell $\frac{m-p}{m}$, $\frac{m-q}{m}$, $\frac{m-r}{m}$ in which all the numerators are even. A lattice point with all numerators even can easily be chosen in two adjacent cells if part of the numerators remain odd. In this way the process of successive division by two of the residue from the origin to the additional lattice point becomes infinite, and one of the translations grows infinitely smaller, which is impossible.

LITERATURE CITED

[1] N. V. Belov, Structural Crystallography [in Russian] (1951).

[2] B. N. Delaunay, Uspekhi Matematicheskikh Nauk 3 (1937); 4 (1938).

[3] N. V. Belov, "A theorem on the primitiveness of a particular cell," Doklady Akad. Nauk SSSR 78, 1 (1951).

Received October 7, 1957

Institute of Crystallography, Academy of Sciences, USSR

THE POINT GROUPS OF SYMMETRY OF CRYSTALS AND THEIR PHYSICAL INTERPRETATION

I. S. Zheludev

It is shown that the 32 crystallographic point groups can be obtained by means of scalar, vector, and tensor operations on a cube. The hypothesis is put forward that the differences in the properties of crystals having the same symmetry group correspond to the diverse ways in which these groups may be obtained.

One of the most important tasks of crystal physics lie in establishing a link between the symmetry and the physical properties of crystals. At the present day, the solution to this problem takes the form of "prediction" of the physical properties of crystals which derive from their symmetry. Thus it is possible, for example, to "predict" the possibility of pyro- and piezoelectric properties, of pyromagnetic properties, of rotation of the plane of polarization, etc. However, in this direction crystal physics runs into a series of fundamental difficulties. The most important of these is that the knowledge of symmetry allows only the "prediction" of the possibility of some property or other of the crystal, and does not allow us to assert that this property is necessarily present in it. In other words only the necessary conditions for the presence of some physical property or other in the crystal follow from the symmetry, and not sufficient conditions.

This situation in crystal physics is historically conditioned by the fact that, on the one hand, the study of symmetry in itself developed from purely geometrical concepts, devoid of any direct link with real physical phenomena, and, on the other hand, that the laying of the foundations of that study preceded the direct study of the physical properties of crystals.

It seems to us that the development of modern science enables us, at least in crystal physics, to supplement this purely analytical-geometrical approach to symmetry by a physical approach. From our point of view, the study of symmetry should concern itself with the study of the geometrical links between physical processes, rather than with the study of the interrelationships between geometrical figures, with the physical processes which are found in natural environments, and in particular, in crystals. Clearly this change from the symmetry of figures to the symmetry of processes and phenomena permits a closer approach to the question of the physical properties, of crystals. As will be shown below, the multiplicity of physical processes and phenomena is richer and wider than the manifold symmetry of figures (we have in mind the symmetry of finite figures, which as a rule is also used in the description of the physical properties of crystals). This circumstance readily allows us to understand more fully why, for instance, crystals belonging to the same symmetry point group can possess different physical properties.

The method of deducing the symmetry of finite figures by geometrical analysis is found in the works of Gadolin [2], Fedorov [3], Curie [4], Wulff [5], Shubnikov [6], and others. In these works it is shown that the number of crystallographic point groups is 32.

In a previous work of the author [7] an attempt was made to deduce point groups of symmetry, starting from representations of the geometrical link between physical processes. It was shown in this work that homogeneous, continuous, isotropic environments in poles described by polar and axial tensors of the second order belong to 17 point groups of symmetry namely: $\infty/\infty \cdot m$; ∞/∞; $m \cdot \infty : m$; $\infty : m$; $\infty : 2$; $\infty \cdot m$; ∞; $\bar{4} \cdot m$; $\bar{4}$; $m \cdot 2 : m$; m; $2 : 2$; $2 : m$; $2 \cdot m$; 2; $\bar{2}$; 1. A table of so-called elementary operations on the environment describing

physically different processes is given in this same work (e. g., for mechanical operations: stretching-compression, translation, rotation, torsion, and multilateral compression).

We shall show that the 32 crystallographic point groups can also be obtained by the method used in that work [7]. As is customary [6], we shall understand by this those groups which contain as elements of symmetry, only simple 1, 2, 3, 4 and 6-fold axes, and mirrors, inasmuch as five-fold axes and axes higher than 6-fold are excluded for such groups since their existence in crystals is incompatible with the theories of the crystal lattice.

Let us consider the arrangement adopted by small particles having the highest symmetry and forming the extended lattice of highest symmetry. The point group of symmetry (point symmetry) of this extension will be described as the group $\overline{6}/4$. It is clear that such symmetry will be possessed, for instance, by a simple cubic lattice, at the lattice points of which are situated isotropic spheres. We shall take the unit cell corresponding to such a lattice (in this case a cube) and shall observe what point groups of symmetry describe this cube after its symmetry is changed under different physical operations.

We mean by operation in this context an operation which is external with relation to the cube. The position remains the same, however, if instead of an external operation, we look at the change of symmetry as resulting from a change in the forces of interaction between the particles. This presentation of the situation allows us to consider real crystals not only as crystals deformed from the cubic, but also as crystals formed noncubically as a result of the operation of anisotropic forces between their particles.

In considering the symmetry of the cube subjected to some operation we shall assume (analogously to what was done in deducing the point groups of symmetry of continuous, homogeneous, isotropic environments [7]) that this operation itself may be described by 2nd order polar and axial tensors, which in their turn describe scalar and pseudo-scalar, polar- and axial-vectoral, polar- and axial-tensoral quantities, and also any combination of these quantities. These quantities, in their turn, can describe processes of a different nature: a polar vector, for instance, describes the translation of a body and an electrical polarization, an axial vector may describe rotation of a body and magnetization, etc.

There exist, as is known [8], seven systems of extended lattices: cubic, tetragonal, orthorhombic, monoclinic, triclinic, trigonal, and hexagonal. The forms of the unit cells corresponding to these lattices, and their symmetry, can be easily derived by considering the deformation of the cube described earlier, of symmetry $\overline{6}/4$. It is clear that a scalar operation (e. g., multilateral compression, symmetry $\infty/\infty \cdot m$) does not change the symmetry of the cube. A pseudo-scalar operation (e. g., multilateral torsion, symmetry ∞/∞) leads to a new symmetry group 3/4 (Fig. 1).

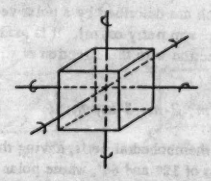

Fig. 1. Pseudo-scalar operations on a cube symmetry group 3/4.

Let us now consider polar-tensor operations on the cube. By stretching the cube (symmetry of this operation $m \cdot \infty : m$) along the four-fold axis, a cell of the tetragonal system results (symmetry $m \cdot 4 : m$); along the two-fold axis, an orthorhombic cell (symmetry $m \cdot 2 : m$); along the three-fold axis, a trigonal cell (symmetry $\overline{6} \cdot m$); stretching the cube in any direction which lies in a plane of symmetry but does not coincide with any of the axes, a monoclinic cell (symmetry $2 : m$) results; stretching the cube in a complete arbitrary direction, a triclinic cell results (symmetry $\overline{2}$). A hexagonal cell is also obtained by deformation of the cube but it is not simple, consisting of three rhombohedral cells, whose rhombuses have origin angles of 120 and 60°. In this sense the hexagonal system is not independent and simple, but represents a special case of the rhombohedral system.* The form of the unit cells of all classes is shown in Fig. 2.

Thus by considering only the polar-tensor operations on the unit cube of a simple cubic lattice, the following crystal symmetry groups have been obtained:

$$\overline{6}/4,\ m \cdot 4 : m,\ m \cdot 2 : m,\ \overline{6} \cdot m,\ 2 : m,\ \overline{2}\ \text{и}\ m \cdot 6 : m.$$

* The fact that the presence of a 6-fold axis is not excluded in an extended lattice, allows the hexagonal system to be regarded as independent also.

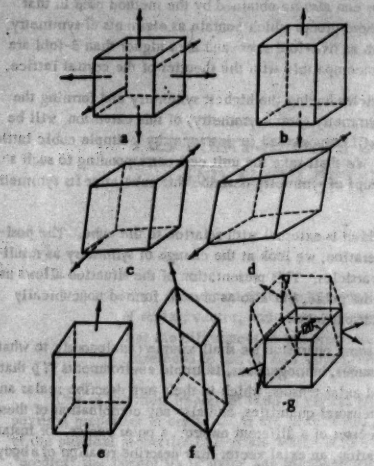

Fig. 2. Unit cells of all systems resulting from a polar-tensoral operation on a cube. a) Cubic, b) tetragonal, c) orthorhombic, d) trigonal, e) monoclinic, f) triclinic, g) hexagonal cells.

There is no need to prove the completeness of the groups obtained, since all cases of orientation of a polar-tensor operation were considered.

Consider now the greatest symmetry changes in the cells, found under conditions where they undergo axial-tensoral operations (torsion), in the same directions as those in which the stretching (or compression) was carried out. It can be readily be seen that torsion (symmetry $\infty:2$) in the direction of the 4-, 2- and 3-fold axes, along directions lying in the planes of symmetry of the original cube, and in arbitrary directions, lead in similar fashion, to the following new symmetry groups: $4:2$, $2:2$, $3:2$, $2, 1$. In addition, analogously to what has been said above, the combination of three rhombohedral cells (having origin angles of 120 and 60°) leads to the symmetry group $6:2$. It is easily seen that all the groups just mentioned can give both left- and right-hand forms, depending on the sign of the rotation.

Among those axial-tensoral operations of symmetry $\infty:2$ (torsion in one direction), there also exist torsions of different magnitudes in two directions but of the same sign (symmetry $2:2$), torsions of the same magnitude and of different sign in two directions (symmetry $\bar{4}\cdot m$), and of different torsions in all three directions (symmetry $2:2$). The first and third of these cases yield nothing new in the way of symmetry. However, the second case – torsions similar in magnitude and of different sign – leads to a new symmetry group $\bar{4}\cdot m$ which corresponds to torsion on two mutually perpendicular two-fold axes, extended in the direction of the 4-fold axis of the cube.

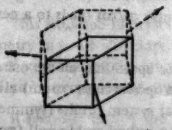

Fig. 3. Polar-vectoral operations. Symmetry group $m\cdot 3:m$.

Consider now the operations which are described by a polar vector (e. g., the electrical polarization of the cube; symmetry $\infty\cdot m$). It is readily seen that such operations, coinciding in direction with the direction of stretching, lead to the following symmetry groups:

$$4\cdot m;\ 2\cdot m;\ 3\cdot m;\ m;\ 1.$$

A group of three rhombohedral cells, having rhombuses with origin angles of 120 and 60°, whose polar vectors are directed along the 2-fold axis (perpendicular to the rhombuses) and oriented in the same direction, leads to the symmetry group $6\cdot m$, and the group of cells whose polar vectors coincide in direction with the direction of stretching (compression) leads to the group $m\cdot 3:m$ (Fig. 3).

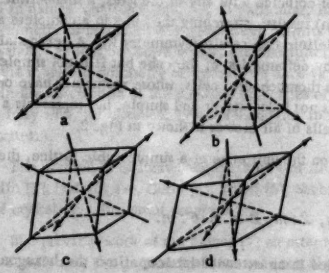

Fig. 4. Polar-vectoral operations. Symmetry groups: a) $\bar{3}/4$; b) $\bar{4}\cdot m$; c) $2:2$; d) $3\cdot m$.

Cases have been examined up to now where the unit cells contain one polar vector. In addition to this it is possible to imagine an operation consisting of a combination of four polar vectors. Such a combination in the case of a cube, leads to the symmetry group $3/4$, in the case of a tetragonal cell to the group $\bar{4}\cdot m$, for

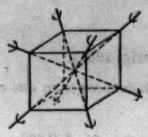

Fig. 5. Axial-vectoral operations on a cube. Symmetry group $\overline{6}/2$.

an orthorhombic cell to the group 2:2, and for a rhombohedron to the group 3·m, etc. (Fig. 4).*

The operations described by an axial vector, e. g., rotation (symmetry ∞:m), may be examined in an analogous fashion. The groups 4:m (rotation about the 4-fold axis of the cube stretched along the same axis); 2:m (rotation about the 2-fold axis of the cube stretched along the same direction); $\overline{6}$ (rotation about the $\overline{6}$ axis of the cube stretched along the same direction); 6:m (rotation of the group of cells forming the group m·6:m about the 6-fold axis); $\overline{6}/2$ derived from a combination of four axial-vectoral operations oriented in the direction of the $\overline{6}$ axis of the cube (see Fig. 5), can be gotten in this way.

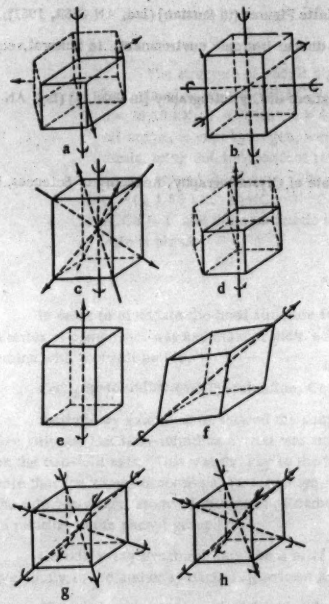

Fig. 6. Combined operations. Symmetry groups: a) 3:m; b) $\overline{4}$; c) 4; d) 6; e) 4; f) 3; g) 3/2; h) 3/2.

This concludes the consideration of the point groups of symmetry obtained by one operation of one type (insofar as these operations were performed on a cube deformed in various ways). The cases where operations of different types are combined will now be considered (let us say the combination of polar-vectoral operations with axial-tensoral ones, etc.). The multiplicity of such cases will not be considered in this work, and attention will be paid only to those cases which result in new symmetry groups. Thus the new group 3:m may be derived from the group m·3:m, formed by the operation described by polar vectors, by means of an additional rotation about the 3-fold axis (Fig. 6, a); a new group $\overline{4}$ may be obtained either from the group $\overline{4}$·m, formed by an axial-tensoral operation plus a rotation about the 4-fold inversion axis of the group $\overline{4}$·m, or from the same group $\overline{4}$·m, formed by a polar-vectoral operation plus rotation about the same $\overline{4}$ axis (Fig. 6, b and c).

New groups 6, 4 and 3, may be gotten by various means. In particular they may be derived from the groups 6·m; 4·m; 3·m; plus rotation about the 6, 4, and 3-fold axes, respectively (Fig. 6, d, e, f), plus torsion about the same axes, etc. In addition, combination of the groups $3/\overline{4}$ and $\overline{6}/2$; $3/\overline{4}$ and 3/4, etc., leads to the group 3/2 (Fig. 6, g, h).

The total number of groups considered is 32, and this exhausts all the groups usually derived geometrically. Careful consideration of any other combinations of operations shows that there are no new groups apart from those enumerated above. The groups of symmetry obtained may be grouped into classes, as is usually done, on the basis that crystals of one class have the same form of unit cell.

It has already been noted that one and the same symmetry group may be derived by different methods, i. e., by the combination of different physical operations. There exists in this sense a diversity in the same point group of symmetry of crystals. By this diversity it is possible, obviously, to explain the difference in the physical properties of crystals of the same point symmetry.

The writer is grateful to Academician A. V. Shubnikov for considering many of the points mentioned in this article.

* It may be mentioned that the group 3·m, like other groups commonly counted as belonging to the trigonal system, may be derived from a combination of the three rhombohedral cells considered above.

LITERATURE CITED

[1] J. Hessel, Krystall. Gehler's Phys. Wörterbuch (1830); Krystallometrie (Leipzig, 1831).

[2] A. V. Gadolin, "The derivation of all crystallographic systems and their subdivisions from one common source," Notes Russian Min. Soc. 4 (1869).

[3] E. S. Fedorov, "Symmetry of regular systems of figures," Notes Russian Min. Soc. 25, 1 (1889).

[4] P. Curie, Sur la Symètrie, Bul. de la Soc. Min. de France 9 (1884).

[5] G. V. Wulff, Selected Works in Crystal Physics and Crystallography [in Russian] (State Technical and Theoretical Press, 1952).

[6] A. V. Shubnikov, Symmetry and Antisymmetry in Finite Figures [in Russian] (Izd. AN SSSR, 1951).

[7] I. S. Zheludev, "The symmetry of homogeneous continuous isotropic environments in tensoral, vectoral and scalar fields," Kristallografiia 2, 3, 334-339 (1957).*

[8] A. V. Shubnikov, E. E. Flint, and G. B. Bokii, Foundations of Crystallography [in Russian] (Izd. AN SSSR, 1940).

Received August 7, 1957

Institute of Crystallography, Academy of Sciences, USSR

* [Soviet Physics – Crystallography, pp. 330-333.]

X-RAY DIFFRACTION STRUCTURE DETERMINATION OF COBALT DIPARATOLUIDINE DICHLORIDE

T. I. Malinovskii

The structure of cobalt diparatoluidine dichloride crystals was determined to be molecular. $CoCl_2 \cdot 2H_2NC_6H_4CH_3$ crystals are monoclinic: a = 12.30, b = 4.59, c = 26.10 kX, $\beta = 93°45'$, n = 4, the space group is $C_{2h}^5 = I^2/a$. The coordinates of all atoms, except hydrogen, were determined by a three-dimensional Patterson synthesis, using 556 independent reflections, taken from 5 layer lines when rotating the crystal around the Y axis. The distances are: Co—Cl 2.26, Co—N 1.95, $N—C_1$ 1.45, $C_4—C_7$ 1.50 kX. The Co—N—C_1 valence angle is 105°. The coordination number of Co is 4 and the coordination polyhedron is a tetrahedron. The paratoluidine molecule is planar.

INTRODUCTION

In order to elucidate the bond structure in compounds of the type $CoX_2 2A$, an x-ray structure analysis of a series of compounds was undertaken, these compounds being the result of joining two molecules of an organic amine with a cobalt halide.

$CoCl_2$ 2p-toluidine, CoI_2 2p-toluidine, $CoCl_2$ 2p-iodoaniline and CoI_2 2p-aniline [1] were studied.

Preliminary examination showed the similarity of the structure types of the compounds under study; therefore only the $CoCl_2$ 2p-toluidine cyrstal was analyzed, in which the heavy atom (cobalt) is in a special position on the two-fold axis. This was the key to the interpretation of the Patterson synthesis. The fact was also favorable that the three-dimensional Patterson synthesis, even when cobalt and chloride atoms were present, showed the relatively light atoms of nitrogen and carbon. This was important in finding the direction of the Co—N bond in relation to the phenyl group.

Certain x-ray structural data and a brief description of the structure of $CoCl_2$ 2p-toluidine have appeared previously in the author's article [2], written jointly with G. B. Bokii and A. V. Ablov.

The present article describes the experimental material and the refined data relating to the interpreted structure.

Preparation of Crystals and Crystallographic Data

The cobalt diparatoluidine dichloride crystals ($CoCl_2 \cdot 2H_2NC_6H_4CH_3$) were obtained by evaporating a mixture of ethanol solutions of anhydrous cobaltous chloride and p-toluidine. Pink crystals of $CoCl_2 \cdot 2C_7H_9N$ dialcoholate are formed at the bottom of the beaker, and blue elongated plates of $CoCl_2 \cdot 2C_7H_9N$ [1] gradually grow on the walls.

Chemical analysis gave Co 17.21, Cl 20.67, N 8.13%. Co 17.12, Cl 20.60, N 8.14% was calculated. The crystals are optically biaxial (the interaxial angle $2v \approx 90°$). The indices of refraction in white light are $n_g = 1.701$, $n_m = 1.652$, $n_p = 1.610$.

The imperfection of the crystals hampered the goniometric measurements. Diffraction patterns were taken by the Laue method. To protect the crystal from moist air, it was enclosed in a cellophane capsule. The monoclinic lattice constants were found with the aid of the oscillation camera (RKOP):

$$a = 12.30 \pm 0.05\ kX.$$
$$b = 4.59 \pm 0.01\ kX. \qquad \beta = 93°45'.$$
$$c = 26.10 \pm 0.10\ kX.$$

The pycnometric density is 1.483, which gives n = 3.83 ≈ 4 formula units per unit cell. The x-ray density is 1.55.

The indexing of the x-ray diffraction patterns showed the following extinctions: hkl present only if $h + k + l = 2n$, $h0l$ present only if $h = 2n$ and $l = 2n$, $0k0$ present only if $k = 2n$. These laws correspond to the space groups $I^2/a = C_{2h}^5$ and $Ia = C_s^4$.

Analysis of the Intensities

The structural analysis was performed on the basis of data obtained from the KFOR reciprocal lattice camera, using MoK radiation. Crystals 0.2-0.4 mm in size were adjusted on the KFOR with the aid of an illuminator, were enclosed in cellophane, and, after trial exposures, were subjected to prolonged photography.

Photographs of five layer lines were obtained ($h0l$, $h1l$, $h2l$, $h3l$, $h4l$). The numbers of independent reflections were: $h0l$ — 108, $h1l$ — 153, $h2l$ — 148, $h3l$ — 85, $h4l$ — 62. The total number of independent reflections used in the three-dimensional Patterson synthesis was 556. To increase the intensity range, multiple film photography was used. The intensities were visually estimated by comparison with prepared scales. The F^2 values were calculated, using the kinematic and polarization factors.

The structure factors obtained from the five layer lines turned out to be on the same scale, according to Wilson's method [3], and also later, when the coordinates of the cobalt and chlorine atoms were known, by comparing the average values of $|F_{exp}(hkl)|$ and $|F_{calc}(hkl)|$ [4].

Determination of the Projected Molecular Shape

When studying a structure consisting of one heavy atom M and light atoms N_1, N_2, N_3, . . ., N_n, the locations of which are unknown, the Patterson synthesis can be considered as consisting approximately of vectors of the types M—N and N—M. In case the heavy atom is in a special position, on a center or axis of symmetry, the locations of the light atoms can be found directly from the positions of the Patterson peaks.

The structure under study presents such a case. The heavy atom (Co) is on a two-fold axis of symmetry. This situation determined the choice of the method of structure determination. Inasmuch as the interatomic vector function has peak heights proportional to the products of the atomic numbers involved, and the cobalt atom lies on a two-fold rotation axis, the peaks corresponding to the 18 interatomic vectors between the cobalt atom and the other atoms must stand out sharply on the F^2 series projected on the (010) plane.

On the basis of these considerations, an interatomic vector function projected on the x0z plane was constructed, from which the first information concerning the compound under study was obtained (Fig. 1).

From the x0z projection it is obvious that a rather definite picture of the molecule appears. It is possible here to determine the x and z coordinates of the interatomic vectors Co—Cl and, consequently, of the Cl atoms. The Co—N and Co—C peaks are also present, but are somewhat diffuse and, therefore, are unsuitable for refining the N and C coordinates.

Although no final conclusion concerning the molecular structure can be made, it is obvious that two chlorine atoms and two organic groups, $H_2NC_6H_4CH_3$, surround the cobalt atom — a fact not in disagreement with modern thinking concerning the complexes under study. However, it is impossible to obtain evidence in favor of either four-fold or six-fold coordination of the cobalt atom.

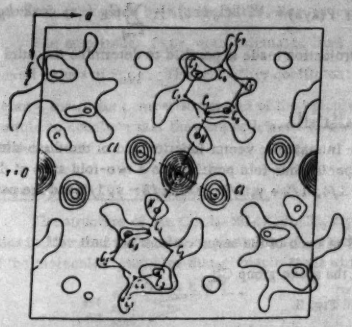

Fig. 1. Projection of the interatomic vector function of $CoCl_2 \cdot 2H_2NC_4H_4CH_3$ on the (010) plane.

If one assumes that the cobalt atom has six-fold coordination, then the structure must be composed of chains of octahedra in which the vertices of the square cross sections are occupied by chlorine atoms, and the edges of the squares are common to two neighboring octahedra, as in the structure of $CoCl_2 \cdot 2H_2O$ [5]. If one considers that the length of the Y axis is 4.59 kX, and that the Co–Cl distance is, in the x0z projection, 1.89 kX, then the Co–Cl distance is, in the three-dimensional structure, equal to 3.0 kX, which is larger than the sum, 2.59 kX, of the ionic radii of Co and Cl. This means that six-fold coordination of cobalt is improbable.

If the cobalt atom is considered to be in four-fold coordination, two variants of the structure are possible: planar or tetrahedral. In the planar variant the molecule must be centrosymmetric, while in the tetrahedral variant it must have a two-fold symmetry axis.

In order to resolve this question, an attempt was made to determine the chlorine coordinates from Patterson projections on two other faces of the unit cell (xy and yz). For this purpose reciprocal lattice photographs were obtained about the X and Z axes, using the KFOR camera. However, the unfortunate shape of the crystal caused such poor diffraction patterns that no answer to this question could be obtained.

The Three-Dimensional Patterson Synthesis

Using the values of F^2_{hkl} obtained from all the planes of the crystal, the Harker-Patterson section was constructed for the plane y = 0 (Fig. 2).

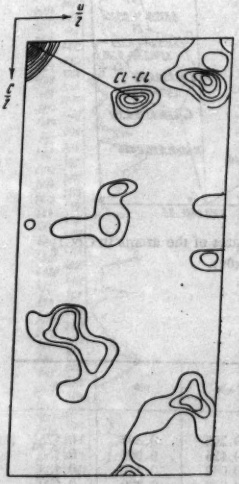

Fig. 2. Harker-Patterson section on the plane y = 0.

Inasmuch as the Harker-Patterson section for the zero plane gives all the interatomic distances parallel to this plane, two-fold axes should, of necessity, appear in this synthesis. Since there is a maximum in this synthesis which corresponds to the Cl–Cl interatomic vector, as shown in Fig. 2, the fact that the chlorine atoms are related by a two-fold axis is confirmed, which shows that there is a greater probability that the structure belongs to the space group C^4_{2h}. Eventually this group was accepted.

The three-dimensional Patterson synthesis was constructed to determine the location of the atoms in space. The computation of the synthesis was carried out by summing the two-dimensional series:

$$C_k(xz) = \sum_h^{\infty} \sum_l \{(F^2_{hkl} + F^2_{\bar{h}kl}) \cos 2\pi hx \cdot \cos 2\pi lz - (F^2_{hkl} - F^2_{\bar{h}kl}) \sin 2\pi hx \cdot \sin 2\pi lz.$$

The matrices of the coefficients $C_k(xz)$ were obtained for the 5 values of k and for all the values of the x and z coordinates when the edges a and c were divided into 48 parts. They represent weighted projections of the interatomic vector function. The quantities C_k served

as coefficients for the vertical one-dimensional synthesis: $P(xyz) = 1/2C_0(xz) + \sum_{k=1}^{4} C_k(xz)\cos 2\pi ky$.

These "samplings" in the regions of the maxima on the projection made it possible to determine the third coordinate of each atom individually.

The Atomic Coordinates of $CoCl_2 \cdot 2H_2NC_6H_4CH_3$

It follows from the analysis of the projection of the interatomic vector function and of the three-dimensional series of this function, that the cobalt occupies a special four-fold position (on a two-fold axis) of the space group C_{2h}^5, with coordinates 1/4, y, 0; 3/4, y, 0; 1/4, 1/2 + y, 1/2; 1/4, 1/2 − y, 1/2, and the parameter y = 0.386.

There are 8 chlorine atoms, 8 nitrogen atoms and 8 of each of the seven carbons per unit cell.

These atoms occupy the 8-fold general position of the space group C_{2h}^5.

The atomic coordinates are given in Table 1 and in Fig. 3.

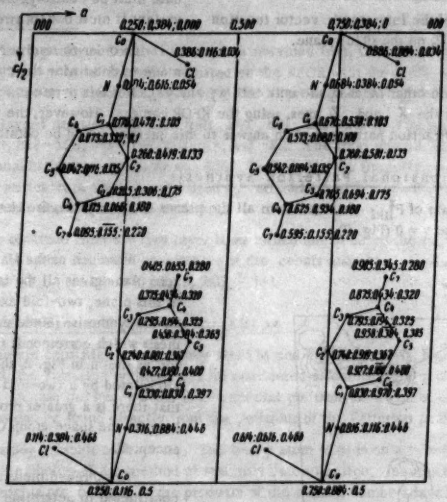

Fig. 3. Molecular arrangement and coordinates of the atoms in $CoCl_2 \cdot 2H_2NC_6H_4CH_3$. Projection on the plane (x0z).

TABLE 1

Atomic Coordinates of $CoCl_2$ 2p-Toluidine

Atom	x/a	y/b	z/c	Atom	x/a	y/b	z/c
Co	0.250	0.384	0.000	C_3	0.205	0.306	0.175
Cl	0.386	0.116	0.034	C_4	0.125	0.066	0.180
N	0.184	0.616	0.054	C_5	0.042	0.116	0.135
C_1	0.170	0.470	0.103	C_6	0.073	0.320	0.100
C_2	0.260	0.419	0.133	C_7	0.095	0.155	0.220

The coordinates of the maxima of the three-dimensional Patterson synthesis were refined by the interpolation method proposed by Kitaigorodskii, Khotsianova, and Struchkov [6].

The amplitudes F_{hkl} were calculated from the atomic coordinates and were compared with the experimental values of F_{hkl}. The reliability coefficient $R = \frac{\Sigma \left| |F_{exp}| - |F_{calc}| \right|}{|F_{exp}|}$ proved to be equal to 0.22.

Figure 4 shows the comparison graphs of the calculated and experimental amplitudes, on the basis of which it is possible to conclude that they are satisfactorily similar, inasmuch as the locations of the hydrogen atoms were not determined.

Description of the Structure

The structure of the $CoCl_2 \cdot 2H_2NC_6H_4CH_3$ crystals is molecular. The $CoCl_2 \cdot 2H_2NC_6H_4CH_3$ molecule contains in its turn 2 molecules of paratoluidine, which are joined to the cobalt atom by nitrogen atoms. The shape of the molecules resembles that of maple seeds which have petals turned like the blades of a propeller (Fig. 5).

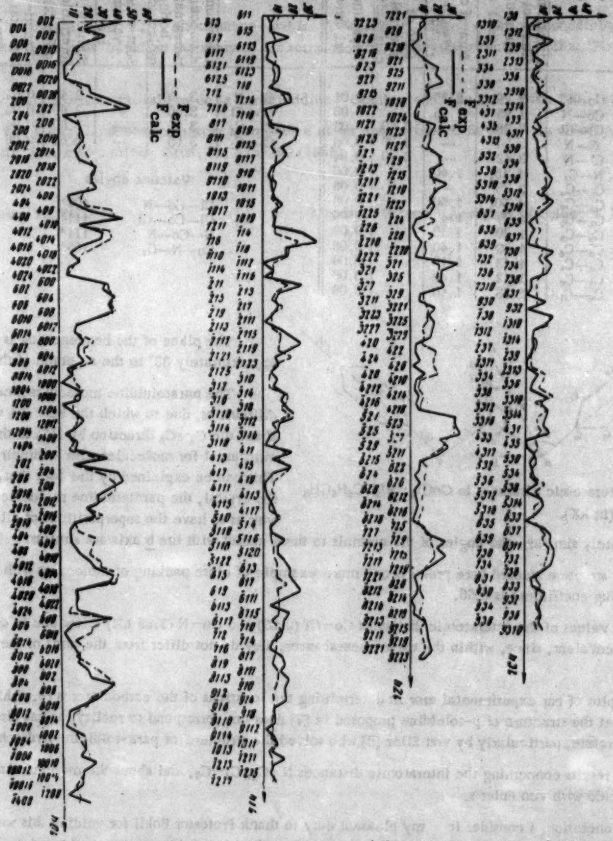

Fig. 4. Comparison graph of the calculated (F_{calc}) and the experimental (F_{exp}) structure amplitudes.

The Co atom is located in the center of an almost regular tetrahedron, the vertices of which are occupied by Cl and N atoms. It is on a two-fold axis, and the whole molecule has the symmetry 2. The Cl and N atoms, located around the cobalt atom, are close packed, as is indicated by the fact that their interatomic distances are equal to the sums of the intermolecular radii. The nitrogen atom is joined directly to the carbon (C_1) of the benzene ring. The CH_3 group is joined to the diametrically opposed carbon atom (C_4). The interatomic distances in the benzene ring do not differ from those described in the literature within the experimental error. The Cl—Co—Cl, N—Co—N and Cl—Co—N angles are tetrahedral within the limits of error. The values of the interatomic distances, the experimental errors, and the valence angles are given in Table 2.

TABLE 2

Interatomic Distances in the $CoCl_2 \cdot 2H_2NC_6H_4CH_3$ Structure

	Interatomic distances in molecule (kX)	Sum of covalent radii	Sum of intermolecular radii	Experimental error		Interatomic distances between neighboring molecules	Sum of covalent radii	Sum of intermolecular radii	Experimental error
Co—Cl	2.26	2.25	—	0.01	Cl—N	3.40	—	3.40	0.04
Co—N	1.95	1.95	—	0.03	C—Cl	3.50	—	3.60	0.03
Cl—Cl	3.78	—	3.60	0.02	Cl—C_1	3.80	—	3.60	0.04
N—N	3.26	—	3.20	0.06	C_7—C_7	3.65	—	3.60	0.06
Cl—N	3.42	—	3.40	0.04					
N—C_1	1.45$_5$	1.40	—	0.06					
C_1—C_4	2.78	—	—	0.06					
C_4—C_7	1.50$_5$	1.50	—	0.06					
C_1—C_2	1.37	1.40	—	0.06					
C_2—C_3	1.30	1.40	—	0.06					
C_3—C_4	1.39	1.40	—	0.06					
C_4—C_5	1.43	1.40	—	0.06					
C_5—C_6	1.42	1.40	—	0.06					
C_6—C_1	1.38	1.40	—	0.06					

Valence angles

Cl—Co—N	109°
Cl—Co—Cl	111°
N—Co—N	111°
Co—N—C_1	105°

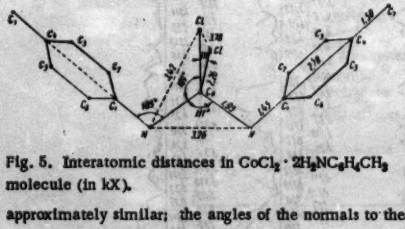

Fig. 5. Interatomic distances in $CoCl_2 \cdot 2H_2NC_6H_4CH_3$ molecule (in kX).

The plane of the benzene ring is inclined at approximately 33° to the ac plane of the cell.

The paratoluidine molecules meet minor space difficulties, due to which the benzene nuclei are turned about the C_1—C_4 direction by 15°, so that the symmetry mm, usual for molecules with symmetry 2, disappears. This can be explained by the fact that, in packing into the crystal, the paratoluidine molecules turn in such a way as to have the superpositions of all benzene nuclei approximately similar; the angles of the normals to these nuclei with the b axis are similar.

The structure studied here presents one more example of close packing of molecules with the symmetry 2. The packing coefficient is 0.66.

The values of the interatomic distances Co—Cl (2.26) and Co—N (1.95 kX) allow one to conclude that these bonds are covalent, since, within the experimental error, they do not differ from the sums of the covalent atomic "radii."

In spite of our experimental eror in determining the locations of the carbon atoms (0.03 kX), it is quite obvious that the structure of p-toluidine proposed in [7] does not correspond to reality, as has already been noted in the literature, particularly by von Eller [8], who solved the structure of para-toluidine hydrochloride.

Our results concerning the interatomic distances N—C_1, C_4—C_7, and about the molecular shape of paratoluidine coincide with von Euler's.

In conclusion, I consider it my pleasant duty to thank Professor Bokii for guiding this work, Professor A. V. Ablov for furnishing the crystals, and M. A. Porai-Koshits for giving much valuable advice and for his interest in the work.

LITERATURE CITED

[1] A. V. Ablov, Z. P. Burnasheva, and E. G. Levitskaia, "Addition compounds of aniline and of its derivatives with cobalt halides, Zhur. Neorg. Khim. 1 (1956).

[2] G. B. Bokii, T. I. Malinovskii, and A. V. Ablov, "The structure of the dihalide of cobalt diamine," Kristallografiia 1, 1, 49-52 (1956).

[3] A. J. C. Wilson, "Determination of absolute from relative x-ray intensity data," Nature 150, 152-153 (1942).

[4] M. A. Porai-Koshits, "Concerning the reduction of structure amplitudes to the absolute scale," Trudy Institute Krist. 9, 305-312 (1954).

[5] B. K. Vainshtein, "Electron diffraction determination of $CoCl_2 \cdot 2H_2O$," Doklady Akad. Nauk 68, 301-304 (1949).

[6] A. I. Kitaigorodskii, T. L. Khotsianova and Iu. T. Struchkov, "Some questions concerning the methods of x-ray structural analysis based on the study of the tetraiodoethylene crystal structure," Zhur. Fiz. Khim. 27, 1490-1502 (1953).

[7] J. Wyart, "Structure cristalline de la paratoluidine," Compt. rend. Acad. Sci. Paris 200, 1862-1864 (1935).

[8] G. von Eller, "Le photosommateur harmonique et ses possibilités II. Structure du chlorhydrate de paratoluidine," Bull. Soc. franç. minér. Crist. 78, 275-300 (1955).

Received January 12, 1957

Moldavia Branch, Academy of Sciences, USSR

CRYSTAL STRUCTURE OF THE COMPOUNDS $MoBe_{12}$, WBe_{12} and $TaBe_{12}$

E. I. Gladyshevskii and P. I. Kripiakevich

In our studies of the alloys of beryllium with the transition metals, we established that in the systems R–Be, where R = Cr, V, or Nb, compounds RBe_{12} are formed which have a structure of the $ThMn_{12}$ type [1]. The goal of the present work is to establish whether compounds of an analogous type exist in the systems Mo–Be, W–Be, and Ta–Be.

In the system Mo–Be, beside the compound $MoBe_2$ of the $MgZn_2$ type, the compound T is known with a higher but not accurately determined beryllium content, tetragonal in structure and with the lattice constants

TABLE 1

X-ray Powder Patterns of $MoBe_{12}$, WBe_{12}, and $TaBe_{12}$. Cr Radiation (Unfiltered) Camera Diameter 57.4 mm

hkl	$MoBe_{12}$				WBe_{12}		
	$\sin^2\theta$ obs.	$\sin^2\theta$ calc.	I obs.	I calc.	$\sin^2\theta$ obs.	$\sin^2\theta$ calc.	
110	0.051	0.050	50	134	0.051	0.050	
101	0.100	0.098	80	176	0.099	0.098	
200		0.100		80 → 256		0.100	
211	0.200	0.198	80	207	0.200	0.199	
220		0.200		49 → 256		0.201	
310	0.250	0.250	40	72	0.253	0.251	
002	0.297	0.292	10	20	0.298	0.293	
301	0.301	0.298	40	71	0.302	0.299	
112	0.346	0.342	20	38	0.345	0.343	
202	0.392	0.392	40	71	0.398	0.393	
321	0.401	0.398	80	125	0.403	0.399	
400		0.399		42 → 167		0.401	
330	0.451	0.449	15	22	0.454	0.451	
222	0.496	0.492	5	9	0.498	0.494	
411	0.500	0.498	30	36	0.505	0.500	
420		0.499		14 → 50		0.501	
312	0.543	0.541	40	73	0.546	0.544	
510	0.648	0.649	30	44	0.654	0.652	
103	0.682	0.683	20	30	0.686	0.685	
402	0.693	0.691	20	36	0.697	0.694	
501	0.696	0.696	80	69	0.703	0.699	
431		0.696		34 → 103		0.699	
332	0.744	0.741	50	50	0.746	0.745	
213	0.783	0.781	80	95	0.789	0.784	
422	0.794	0.791	80	116	0.795	0.794	
521	0.796	0.795	90	106	0.804	0.800	
440		0.798		37 → 143		0.802	
530	0.847	0.849	60	81	0.854	0.852	
303	0.882	0.881	70	121	0.883	0.885	
600	0.897	0.898	50	51	0.902	0.903	
512 (α_1)	0.941	0.940	100	323	0.943	0.945	
323 (α_1)							
611 (α_1)							
620 (α_1)							

Notes on Table 1. Only α-lines are given. $\sin^2\theta_{MoBe_{12}} = 0{,}0250\ (h^2 + k^2 + 2{,}932\, l^2)$;

a = 10.12 and c = 4.22 kX (Misch [2]). Gordon and his co-workers [3] confirmed the existence of the compound $MoBe_2$, and ascribed to the second the composition $MoBe_{13}$. According to their data, the latter compound has a tetragonal lattice (the space group is $D_4^1 - P42$) with the constants a = 10.27 and c = 4.29 kX; the unit cell contains 56 atoms with an unknown arrangement. Comparing the constants of $MoBe_{13}$ with those of $NbBe_{12}$ (a = 7.357,* c = 4.247 kX) [1], we see that $a_{MoBe_{13}} \approx \sqrt{2} a_{NbBe_{12}}$ and $c_{MoBe_{13}} \approx c_{NbBe_{12}}$; consequently, it is quite possible that the compound $MoBe_{13}$ actually has a structure of the $ThMn_{12}$ type (like $NbBe_{12}$) and correspondingly the composition $MoBe_{12}$.

We studied the alloy obtained by melting molybdenum (pure Kahlbaum) with beryllium (99.7% pure) in a crucible of BeO in a high-frequency furnace under argon*; analysis showed it to contain 92.3 at.% Be. The study showed that the alloy held for 10 days at t = 400°C and quenched from this temperature is microstructurally homogeneous, and the arrangement of lines on its x-ray diffraction pattern (Table 1) is analogous to that on the $NbBe_{12}$ pattern. Thus, the alloy is a compound with the structure type of $ThMn_{12}$; we ascribed to it the formula $MoBe_{12}$. The $MoBe_{12}$ x-ray diffraction pattern leads to the following lattice constants: a = 7.237 ± 0.004, c = 4.233 ± 0.002 kX. The ratio c/a (equal to 0.584) differs from that characteristic of the structures of the previously studied compounds RBe_{12} (0.577 = $1/\sqrt{3}$). This is indicated by the splitting of some lines; for example, lines 002 and 301, which coincide in $CrBe_{12}$, are observed separately (Table 1) in $MoBe_{12}$. The intensities computed for the structure type $ThMn_{12}$ (space group $D_{4h}^{17} - I4/mmm$, atomic arrangement: 2Mo in (a), 8 Be in (f), 8 Be in (i) with $x_i = 0.361$, 8 Be in (j) with $x_j = 0.277$) agree well with those observed experimentally.

TABLE 1 (continued)

WBe_{12}			$TaBe_{12}$			
I obs.	*I* calc.	$\sin^2\theta$ obs.	$\sin^2\theta$ calc.	*I* obs.	*I* calc.	
50	500	0.048	0.048	30	485	
90	645 + 312 = 957	0.096	0.096 0.097	60	618 + 296 = 914	
90	710 + 172 = 882	0.193	0.194 0.195	60	692 + 170 = 862	
40	252	0.242	0.243	30	247	
10	58	0.288	0.289 0.291	30	58 + 216 = 274	
40	219					
30	148	0.335	0.338	20	144	
40	200	0.388	0.387 0.388 0.389	70	195 + 362 + 107 = 664	
80	368 + 110 = 478					
15	81	0.437	0.438	15	72	
15	74	0.483	0.484 0.486 0.486	50	71 + 186 + 83 = 340	
50	192 + 87 = 279					
60	273	0.531	0.533	40	266	
40	155	0.630	0.633	30	150	
25	128	0.678	0.676 0.679 0.681 0.681	70	125 + 137 + 266 + 132 = 660	
25	140					
90	272 + 136 = 408					
40	172	0,728	0.728	30	169	
80	370	0 778	0.773 0.776 0.778 0.779	90	362 + 401 + 383 + 114 = 1260	
90	409					
90	398 + 116 = 514					
60	285	0.827	0.828	40	285	
70	404	0.870	0.870	40	392	
30	198	0.877	0.876	40	193	
100	1175	0·920	0.922	70	1120	
		0.968	0.968	80	1420	
		0.973	0.973 0.974	100	1820 + 710 = 2530	

$\sin^2\theta_{WBe_{12}} = 0{,}0251\ (h^2 + k^2 + 2{,}922\, l^2)$; $\sin^2\theta_{TaBe_{12}} = 0{,}0243\ (h^2 + k^2 + 2{,}972\, l^2)$.

* At first the alloy was prepared by the powder method (heating in vacuum or in molten KCl at t = 1000°C).

The existence of the compound $MoBe_{12}$ in the system Mo–Be with a structure of the $ThMn_{12}$ type confirms our assumption of the true composition and structure of the compound $MoBe_{13}$ described by Gordon and his co-workers. The erroneous conclusion of these authors was based on the fact that they mistook the $MoBe_{12}$ and $MoBe_2$ lines (α and β) present on the x-ray diffraction pattern for those of the compound $MoBe_{13}$; all these lines are observed at such angles θ that they all can be indexed on the basis of a tetragonal primitive lattice with the constants $c = c_{MoBe_{12}}$ and $a = \sqrt{2}a_{MoBe_{12}}$.

The structure of the compound $MoBe_{12}$ was also studied by Raeuchle and von Batchelder [4], with whose work we became acquainted after concluding our study. The results that we obtained agree with those of these authors; according to their data, $MoBe_{12}$ has a structure of the $ThMn_{12}$ type with the constants $a = 7.271 \pm 0.005$ and $c = 4.234 \pm 0.005$ A.

TABLE 2

Interatomic Distances (d) in the Structures $MoBe_{12}$, WB_{12} and $TaBe_{12}$

№		d (kX)	Coordination number
1	R*– 8Be (f)	2.77 2.76 2.80	20
2	R — 4Be (i)	2.61 2.60 2.64	
3	R — 8Be (j)	2.91 2.90 2.94	
4	Be (f) — 2Be (f)	2.11 2.11 2.12	12
5	Be (f) — 4Be (i)	2.24 2.24 2.27	
6	Be (f) — 4Be (j)	2.10 2.10 2.12	
7	Be (f) — 2R	see № 1	
8	Be (i) — 1Be (i)	2.00 2.00 2.02	14
9	Be (i) — 4Be (i)	2.54 2.54 2.56	
10	Be (i) — 2Be (j)	2.34 2.34 2.36	
11	Be (i) — 2Be (j)	2.24 2.24 2.27	
12	Be (i) — 4Be (f)	see № 5	
13	Be (i) — 1R	see № 2	
14	Be (j) — 2Be (j)	2.28 2.28 2.31	12
15	Be (j) — 2Be (i)	see № 10	
16	Be (j) — 2Be (i)	see № 11	
17	Be (j) — 4Be (f)	see № 6	
18	Be (j) — 2R	see № 3	
	Be — Be (average)	2.24 2.24 2.27	

* R = Mo, W, Ta.

In the W–Be system the compounds WBe_2 and T are known, isostructural to the compounds of Mo with Be, and in the system Ta–Be one beryllium-rich compound is known, with a structure akin to that of T [2]. Taking into account what has been said before, we assumed that compounds rich in beryllium have a structure of the $ThMn_{12}$ type and a composition RBe_{12}. Our assumptions were correct. As is shown in Table 1, the diffraction patterns of the WBe_{12} and $TaBe_{12}$, obtained by sintering tungsten powder (pure Kahlbaum) and tantalum (99.9% pure) with beryllium, held for 10 days at t = 400° and quenched, are analogous to the $MoBe_{12}$ diffraction pattern. The locations of the lines and their intensities also correspond to the $ThMn_{12}$ type; thus it is possible to conclude that the alloys studied are the compounds WBe_{12} and $TaBe_{12}$ of the structural type mentioned above. The lattice constants of these compounds have the following values: in WBe_{12} $a = 7.220 \pm 0.004$, $c = 4.224 \pm 0.002$ kX, $c/a = 0.585$; in $TaBe_{12}$, $a = 7.322 \pm 0.004$, $c = 4.247 \pm 0.002$ kX, $c/a = 0.580$.

Thus, the presence of RBe_{12} compounds with a structure of the $ThMn_{12}$ type is characteristic of six transition metal–beryllium systems, namely the systems with vanadium, niobium, tantalum, chromium, molybdenum and tungsten.

The interatomic distances in the structures of the compounds $MoBe_{12}$ and $TaBe_{12}$ are given in Table 2.

Besides the compounds RBe_{12}, we studied alloys with a higher Be content in the Mo–Be, W–Be, and Ta–Be systems. In the Ta–Be system all these alloys contain only a mixture of $TaBe_{12}$ and Be, but the Mo–Be and W–Be systems contain new compounds, richer in beryllium than $MoBe_{12}$ and WBe_{12}. The Be content in these compounds is close to 98 at.%, the structure is face-centered cubic with the lattice constants $a = 11.60$ and 11.59 kX for the Mo and W compounds, respectively. These compounds are in equilibrium with beryllium.

LITERATURE CITED

[1] P. I. Kripiakevich and E. I. Gladyshevskii, Doklady Akad. Nauk 104, 82 (1955).

[2] L. Misch, Metallwirtsch. 15, 163 (1936).

[3] S. G. Gordon, J. A. McGurthy, G. S. Klein and W. J. Koshuba, J. Metals 3, 637 (1951).

[4] R. F. Raeuchle and F. W. von Batchelder, Acta Cryst. 8, 691 (1955).

Received October 1, 1957

I. Franko Lvovsk State University

CONCERNING A METHOD OF TESTING SMALL SAMPLES IN COMPRESSION AND STRESS RELAXATION

G. A. Dubov and V. R. Regel'

The possibilities of applying a new apparatus for testing single crystals in compression are evaluated in this article. It is shown that on samples with a height-to-diameter ratio h/d = 2-3, it is possible to determine from the compression curve the yield point and the coefficient of hardening, without applying an extrapolation method to $h/d \rightarrow \infty$. The parameters of the compression and extension curves are compared. The advantages of compression testing methods are stressed. From analysis of compression curves for TlBr–TlI crystals of different orientations it is concluded that "the limit of fault formation" is subject to the law of shearing stresses.

The apparatus designed for mechanical testing of small samples by compression and extension [1, 2] has been described in preceding articles. The photoelectro-optic dynamometer used in the apparatus is very rigid (under a force of 100 kg the deformation of the dynamometer is $\sim 1\,\mu$), which makes it possible to use it for measuring relaxation stresses. Compression curves, extensions and relaxations are automatically recorded by photorecording. It is especially convenient to use this apparatus for obtaining compression curves and the subsequent relaxation of stresses.

Compression tests have in many instances advantages over extension tests. These are: a smaller amount of work to prepare samples, the possibility of determining the plastic characteristics of fragile materials, and the use of smaller samples than in extension. In studying the properties of single crystals, the above-mentioned advantages are decisive in choosing the method of testing.

On the other hand, the results of compression tests require special analysis in order to separate the plasticity characteristics inherent in uniaxial stress from side effects connected with the appearance of elongated bends in high samples, and from the influence of friction and stress inhomogeneity in short samples. The simplest way of carrying out this analysis is to base it on a series of samples with different height h to diameter d ratios (cylindrical samples are assumed), and also on comparisons with the results of extension tests. Such studies are well known [3, 4] for polycrystalline materials, however none have as yet been carried out on single crystals.

In this connection, studies were made of the dependence of the parameters of the compression and relaxation curves of TlBr–TlI single crystals on their h/d ratio. Some measurements were also made on plastic materials, the homogeneity of which made it possible to use them as standards for verifying the reproducibility of the measurements.

Sample Preparation and Reproducibility Checks

Oriented samples, in the shape of square prisms, were cut from a large crystal, using a milling cutter. Then, cylindrical samples with a diameter of 2.5 mm of different heights were carefully turned on a watchmaker's lathe. For finishing these specimens, special chucks were used: steel disks with 2.5 mm diameter holes. The samples were inserted into these holes and polished; this insured great accuracy in obtaining parallel surfaces on the specimens. All samples were annealed at 280°C for one before testing.

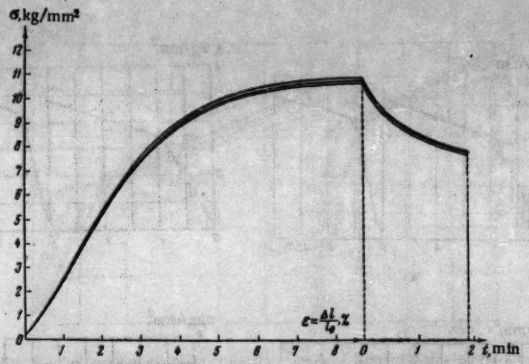

Fig. 1. Compression and relaxation stress curves for 8 similar samples of polymethylmethacrylate (h/d = 2).

To evaluate the quality of the apparatus, the repoducibility of the results of measurements on samples of homogeneous material was first checked to eliminate the possibility of scatter due to changes in the properties of samples.

Figure 1 shows curves for the compression and subsequent relaxation of stresses obtained for 8 samples of polymethylmethacrylate with h/d = 2 under completely stable testing conditions. It is obvious that the curves diverge from one another by no more than 1% of the ordinates. A similar reproducibility as in Fig. 1 is observed for other samples of plastic materials when $1 < h/d < 4$. For samples when $h/d < 1$ the reproducibility diminishes, which apparently is connected with the increase of the influence on the measurements of the condition of the end faces of the sample.

The reproducibility of the results of measurements on crystals of TlBr–TlI was less satisfactory than that on plastic materials; but at least was no worse than that in extension testing using a different apparatus [5-7]. Figure 2 shows the averaged compression curves of samples of the same orientation [110] with different h/d ratios. For each point of measurement the maximum scatter is given. To check the influence of the treatment of the end faces of the samples, each sample was tested twice. Repeated compression was done at definite intervals following the relieving of loading after the first compression.

As Figure 2 shows, the curves for the samples when $h/d > 1.5$ diverge no more than by 2-3% in the ordinates. A greater scatter appears for samples when $h/d < 1.5$, especially for the initial curve in the first stage of compression. With repeated compression the reproducibility of the results of the measurements is improved. This indicates that the scatter of the data in the first testing stage on samples when $h/d < 1.5$ is basically connected with defects in the treatment of the sample surface. Naturally, these defects are more pronounced when testing short samples.

The Influence of the h/d Ratio on the Parameters of the Compression Curves

The average compression curves for different h/d are shown on one graph in Fig. 3. Compression curves similar to those in Figs. 2 and 3, can be characterized by 3 parameters: 1) the slope α of the initial region of the curve; 2) the yield point σ_T; 3) the slope β of the curve after passing beyond the yield point. Comparison of the compression curves with different h/d shows that the parameters σ_T and β for samples when $h/d > 1.5$ are practically independent of h/d. On the other hand, for samples when $h/d < 1.5$, σ_T and β increase appreciably as h/d decreases. Such a dependence of σ_T and β on h/d indicates that the influence of the friction force on the end faces has a practical effect on these parameters which starts only when $h/d \approx 1$.

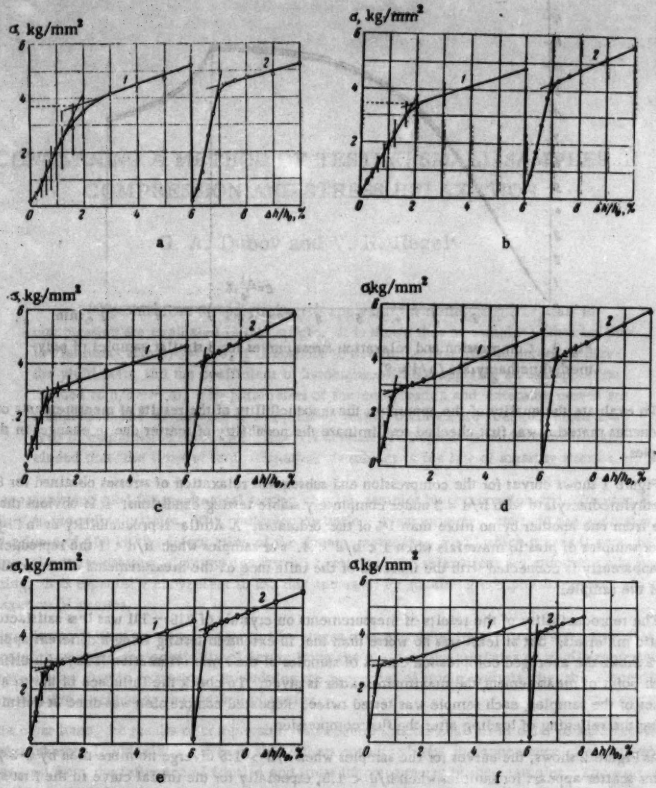

Fig. 2. Compression curves of monocrystals of TlBr–TlI for samples with different h/d ratios. a) h/d = 0.5, b) h/d = 0.8, c) h/d = 1.2, d) h/d = 2, e) h/d = 3, f) h/d = 4. Orientation [110].

The curves in Figs. 2 and 3 show that the parameter α is quite dependent on h/d – it decreases as h/d decreases. This can be explained by the increase of the relative influence of the defects found on the end faces, or by the deviation of their surfaces from parallelism. At the first compression the surfaces are partially "corrected," therefore the slope α becomes appreciably steeper at the second compression. Thus the comparison of the slope α for the curves obtained at the first and second compressions makes it possible to evaluate the degree of perfection of the preparation of the samples.

The fact that the dependence of α on h/d is also partially manifested at the second compression can be due not only to the fact that the defects of the end faces are not entirely eliminated at the first compression (this partially takes place for samples with h/d < 1.5), but also to the fact that during automatic recording of the compression curves (also in Figs. 2 and 3) the sum of the deformations of the sample, the dynamometer, and the apparatus is recorded (see the description of the apparatus in article [2]). In testing short samples of hard materials it is essential to take this circumstance into account. Calculations have shown that introducing the corresponding

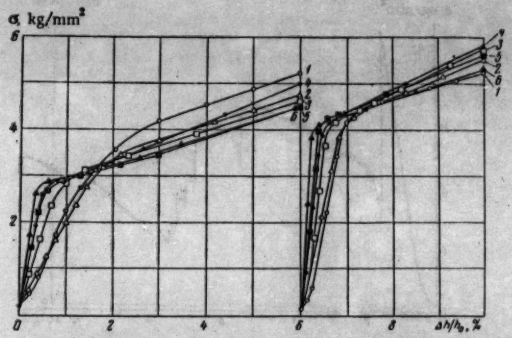

Fig. 3. Comparison of the compression curves of TlBr–TlI single crystals for samples with different h/d ratios. 1) h/d = 0.5, 2) h/d = 0.8, 3) h/d = = 1.2, 4) h/d = 2, 5) h/d = 3, 6) h/d = 4. Orientation [110].

corrections for the rigidity of the apparatus leads to complete agreement of the α values for samples with different h/d. Such corrections are not included in Figs. 2 and 3; therefore it is impossible to judge the rigidity of the apparatus by the dependence of α on h/d during the second compression.

It can be added to what has been said about the dependence of σ_T, β and α on h/d in crystals, that for plastic materials (for example, for polymethylmethacrylate) the constrained elastic limit σ_B for compression testing remains constant in the range of h/d ratios from 1.5–6. The independence of σ_B from h/d is observed up to values h/d = 6, in spite of the fact that even when h/d = 4, after the transition across σ_B the influence of buckling is already apparent. This experimental fact disproves the commonopinion that the characteristics of the σ_B type obtained from compression experiments cannot be compared with the σ_B values from extension experiments, since during compression the stressed condition is distinctly inhomogeneous [8]. Actually, the influence of end face friction and the inhomogeneity of the stressed condition on the magnitude of σ_B appears to be important in practice only when testing short samples with h/d < 1.5. But in testing samples when h/d > 1.5, quite reliable σ_B values are obtained independent of h/d.

The data on the dependence of σ_T, β and α on h/d prove that in determining these compression curve parameters it is not necessary to carry out tests on several samples with different h/d and then to extrapolate the data obtained to $h/d \longrightarrow \infty$. Samples with h/d > 1.5 and one measurement are sufficient.

As to large h/d values, there is a limitation connected with the necessity of eliminating buckling. In samples with h/d = 4, the first traces of buckling already appear for deformations $\epsilon \approx 10\%$. Hence, for experiments to determine σ_T as well as β (keeping in view that in order to determine β it is necessary to deform a sample by at least 10%), samples with h/d ratios from 2 to 3 are necessary.

Comparison of Parameters for Compression and Extension Curves

For materials in which the emergence and development of plastic deformation are determined only by the action of shearing stresses independently of normal ones, the compression and extension curves must coincide. But in materials in which normal stresses influence the development of plastic deformation (for example, as a consequence of cracks) the compression and extension curves must differ. From this point of view, plastic materials and crystals behave differently.

Judging by our experiments, the polymethylmethacrylate compression curves, if drawn on the same graph, are located considerably higher than the extension curves. The σ_B during compression up to 1.5 times or more exceed the σ_B values during extension.

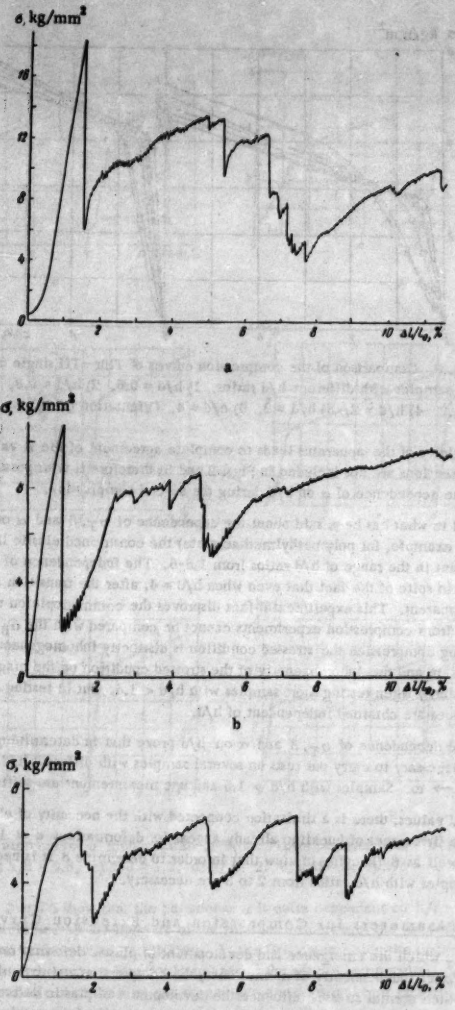

Fig. 4. Compression curves of single crystals of TlBr—TlI of different orientations. a) $\lambda_0 \approx 90°$, b) $\lambda_0 = 82.5°$, c) $\lambda_0 = 75°$.

(cont'd)

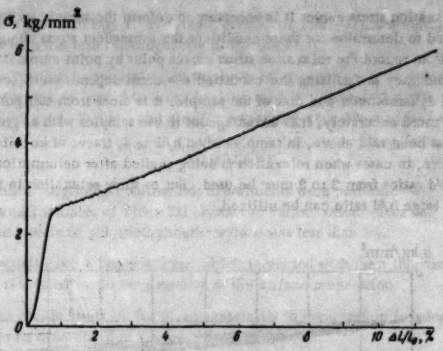

d

Fig. 4. (cont'd). d) $\lambda_0 = 45°$.

In single crystals of TlBr–TlI, oriented along [110], the compression curves also lie somewhat higher than the extension curves, so that the difference in the σ_T and β values is about 10%. However, this effect almost does not exceed the limits of the experimental data, and more experiments, in addition to the present work, are needed to establish it. It can be considered that in comparison with polymethylmethacrylate, the compression and extension curves coincide in single crystals of TlBr–TlI for a given orientation.

A more noticeable difference in the results of compression and extension experiments is apparent in samples whose axes are oriented along or near the direction [100]. Such samples burst at stresses of 6-10 kg/mm² during extension experiments, without revealing, prior to that, any perceptible traces of plastic deformation. During compression, samples of such orientations are deformed elastically to much greater stresses (16-20 kg/mm²); moreover, after the transition through σ_T, the plastic deformation in these samples is developed by means of fault formation. In this connection, during compression experiments, the determination of the dependence of σ_T on orientation should show whether "the fault formation limit" is subject to the law of the critical shearing stress. To clarify this question the present work gives the compression curves for samples of different orientation (h/d = 2) obtained at 20 and 90°C. Several such curves obtained at 20°C are given in Fig. 4. It is easy to see that after the transition beyond the yield point (Fig. 4, a) a sharp stress drop appears in the curves. Observation of samples in the process of deformation showed that this stress drop appears in curves at the same time as fault formation in the sample. The table gives the σ_T values determined from the compression curves, and also values of the critical τ_{cr} shearing stress, calculated from the formula $\tau_{cr} = \sigma_T \sin\chi_0 \cos\lambda_0$. (Here χ_0 is the angle between the axis of the sample and its projection on the glide surface (110) and λ_0 is the angle between the axis of the sample and the glide direction [100].)

TABLE

λ_0, deg		90	82,5	75	45
χ_0, deg		45	45	43	30
20° C	σ_T	18.2	10.7	5.7	2.7
	τ_{cr}		0.98	1.00	0.96
90° C	σ_T	13.7	9.0	4.6	2.4
	τ_{cr}	—	0.83	0.81	0.85

In calculating the set of possible surfaces and directions, the most favorably located ones were chosen.

The data of the table show that in the case of compression, as in that of extension, the law of shearing stresses is sufficiently well observed both at 20 and at 90°C. This means that the emergence of faults and of gliding is determined by the magnitude of the shearing stresses active in the glide surface along the glide direction. This must be taken into account in discussing the mechanism of fault emergence.

The data given show that experiments with crystals in compression have, in many cases, advantages over those with crystals in extension.

The Relaxation Stress Curves of Samples with Different h/d Ratios

To obtain the relaxation stress curves it is necessary to deform the sample up to the ϵ value, to retain it constant at this value and to determine for these conditions the subsequent stress changes with time. The apparatus used made it possible to record the relaxation stress curves point by point automatically with the aid of photorecording [1, 2]. The accuracy in fulfilling the condition ϵ = const depends on the correlation between the rigidity of the apparatus and dynamometer and that of the sample. It is clear from this point of view that, to fulfill the condition ϵ = const more accurately, it is advantageous to use samples with as great an h/d ratio as possible. On the other hand, as has been said above, in samples when $h/d \geq 4$, traces of buckling already begin to appear when $\epsilon \approx 10\%$. Therefore, in cases when relaxation is being studied after deformation of the order of 10% and greater, samples with h/d ratios from 2 to 3 must be used. But to study relaxation in the region of small deformations, samples with a large h/d ratio can be utilized.

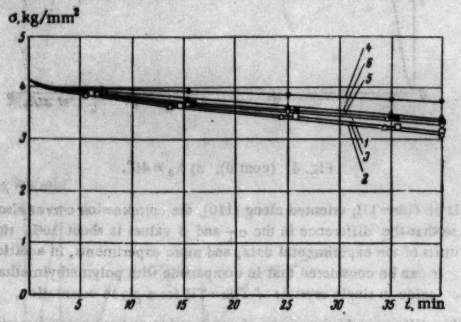

Fig. 5. Average stress relaxation curves for single crystals of TlBr—TlI, for samples with different h/d ratios. 1) h/d = 2; 2) h/d = 4; 3) h/d = = 3; 4) h/d = 0.5; 5) h/d = 1.2; 6) h/d = 0.8. Orientation [110].

It is also desirable to use samples with as great an h/d ratio as possible, since, in experiments with high samples, the influence of defects in the treatment of the plane surfaces and their deviation from mutual parallelism will be less pronounced. The influence of these defects should be very pronounced in experiments with short samples.

On the other hand, it is possible to assume that after preliminary deformation these defects should disappear. If the influence of the defects in the treatment of the plane surfaces really substantially affected the relaxation speed, then one could expect this speed to be greater in short samples than in long ones. Experiment shows the opposite. Figure 5 presents the stress relaxation curves measured at room temperature on samples with different h/d ratios for the same degree of initial deformation: $\epsilon \approx 5\%$. As is apparent from Fig. 5, the relaxation speed when $h/d > 1$ increases linearly with h/d. It follows then, that the influence of defects in the plane surfaces is not so substantial as to affect the results of the measurements of the degree of relaxation, if the sample is first deformed beyond the yield point. It is another matter if stress relaxation not exceeding the yield point is being studied. In this case, the defects in the plane surfaces can be of great influence. Therefore the plane surfaces of the sample must be prepared very carefully for such studies.

As has been said before, it is possible to judge the quality of the surfaces from the change in the slope α between the first and second compressions. Using this method, it is possible to show that the use of special chucks in preparing the surfaces of the samples guarantees such surface perfection that the slopes α for the first and second compressions differ by no more than 1%.

Such surface treatment practically eliminates scatter in the relaxation curves measured for any values of σ and ϵ. For homogeneous materials of the polymethylmethacrylate type, this scatter does not exceed 1% for

samples with h/d = 2, as is shown in Fig. 1. For single crystals of TlBr–TlI, the corresponding scatter increases to 3%; this is connected with the lesser homogeneity of the material.

On the whole, it is possible to ascertain that the stress relaxation curves obtained after compression of differently oriented samples with h/d from 2 to 3 can be fully used for comparative studies of the dependence of the degree of relaxation on σ, ϵ, T, etc., and also for comparing with the results of relaxation after extension.

SUMMARY

1. On the apparatus as originally constructed, experiments were performed on the compression, extension, and stress relaxation of small samples of TlBr–TlI crystals in various orientations and of polymethylmethacrylate. The scatter of the measurements on polymethylmethacrylate was less than 1%.

Experiments on crystals gave a larger scatter, which increased with their inhomogeneity. For samples of small height the scatter is related to the poor quality of the surface preparation.

2. The constrained elastic limit σ_B for plastic materials in compression is independent of the ratio of the height h of the sample to its diameter d in the range h/d = 1.5–6.0.

3. The yield point σ_T of TlBr–TlI crystals oriented along [110] is independent of h/d in the range 1.5–4. When h/d is smaller than 1.5, the σ_T increases as h/d decreases. When h/d = 4 and ϵ is about 10%, indications of buckling appear.

4. The compression curves obtained on this apparatus by means of photorecording show the intermittent process of deformation of crystals in cases where fault formation occurs.

5. The law of shearing stresses is observed in compression testing. "The limit of fault formation" is subject to that law.

6. The limit of constrained elasticity σ_B of polymethylmethacrylate obtained from compression experiments under stable testing conditions exceeds σ_B obtained from extension experiments by a factor of about 1.5.

7. The degree of relaxation in crystals of TlBr–TlI (orientation [110]), measured on samples with different h/d after compressing them by 15%, increases linearly with the increase in h/d when it is > 1.5.

8. True compression curves (up to 20%) and the subsequent stress relaxation can be obtained with sufficient accuracy by direct measurement of samples with h/d from 2 to 3, without the usual extrapolation to $h/d \to \infty$.

LITERATURE CITED

[1] G. A. Dubov and V. R. Regel', "Photoelectro-optic dynamometer," J. Tech. Phys. (USSR) 25, 14, 2542-2544 (1955).

[2] V. R. Regel' and G. A. Dubov, "A recording apparatus for compression, extension and relaxation curves," Biull. "Pribory i Stendy" (Inst. Tekhn.-Ekonomich. Informatsii AN SSSR) 2, P-56-452, 12-15 (1956).

[3] V. D. Kuznetsov, Physics of Solid Bodies 2 [in Russian] (1941).

[4] A. Nadai, Plasticity and Rupture of Solid Bodies (IL, 1954) pp. 374-401.

[5] V. R. Regel', "Extension curves of single crystals of TlBr + TlI," Trudy Inst. Krist. 11, 152-157 (1955).

[6] V. R. Regel' and A. B. Zemtsov, "The influence of crystallographic orientation of single crystals of TlBr + TlI on the yield point during extension testing," Trudy Inst. Krist. 11, 158-164 (1955).

[7] V. R. Regel' and G. E. Tomilovskii, "The dependence of the yield point of single crystals of TlBr + + TlI on speed of deformation and temperature," Trudy Inst. Krist. 12, 158-171 (1956).

[8] Iu. S. Lazurkin and R. L. Fogel'son, "Concerning the nature of large deformations of high-molecular substances in glass-like condition," J. Tech. Phys. (USSR) 21, 3, 267-287 (1951).

Received March 1, 1957

Institute of Crystallography, Academy of Sciences, USSR

EXPERIMENTS IN THE KINETICS OF SOFTENING OF TlBr–TlI CRYSTALS

V. R. Regel' and G. A. Dubov

According to the rather widely accepted views on the mechanism of plastic gliding in crystals, the investigation of the kinetics of this process must consist of separate investigations of the kinetics of two opposed processes–hardening and softening. The gathering of data on the kinetics of plastic deformation needed for building a theory of the plasticity of crystals must, according to these ideas, consist of accumulation of experimental data on the kinetics of hardening and softening [1].

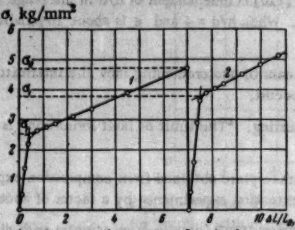

Fig. 1. Compression curves for single crystals of TlBr–TlI. 1) Compression of the original sample; 2) second compression of the same sample after relaxation.

The present work deals with experiments designed to determine the kinetics of softening in single crystals of TlBr–TlI, which are finding new uses, both in technology and in science.

To obtain the necesary data on the kinetics of softening, the method of compression of small samples was used, as described by us earlier [2-4]. All experiments were made on cylindrical samples 5 mm high (h), 2.5 mm in diameter (d) and with identical crystallographic orientation, the axis of the sample coinciding with the direction [110]. Before the experiment, the samples were annealed at 280°C for several hours.

The experimental procedure and the treatment of the results of the determination of the degree of softening may be explained by Fig. 1. Figure 1 presents compression curves obtained in two successive experiments on the same sample. In both cases the experiment was performed at room temperature (20°C) and at the same rate of deformation, $2.5 \cdot 10^{-4}$ sec^{-1}. The deformation of the samples was in all cases carried out to the same degree of hardening, corresponding to stress σ_0, or twice the limit of viscosity σ_T. After the required degree of hardening was achieved, deformation was stopped and the sample was quickly unloaded. The sample was kept in unloaded condition for a certain time t (time of relaxation) at a certain temperature T (temperature of relaxation), and was again subjected to compression. The degree of softening was determined in the usual way [5] by the formula $\eta = \frac{\sigma_1 - \sigma_T}{\sigma_0 - \sigma_T} \cdot 100\%$, on the basis of the values obtained for σ_T, σ_0, and the limit of viscosity in the second test, σ_1.

The results of measurement of the dependence of η on the time of relaxation at different temperatures in the interval from −70 to +150°C are given in Fig. 2. The maximum time of relaxation was 5 hr; the curves for these samples are given in Fig. 2, a. Longer tests were made in the temperature range from −70 to +20°C; the curves for these tests are shown in Fig. 2, b.

The curves of Fig. 2 show that it is possible by means of annealing to attain a practically complete softening of a given crystal. At 150°C this is attained in 30 min. This leads to the practical suggestion that in order to remove hardening produced by mechanical working of the crystals of TlBr–TlI it is necessary to anneal them at 150–200°C and not at higher temperatures, as was done in the past. Even at this temperature the time of annealing may be shortened.

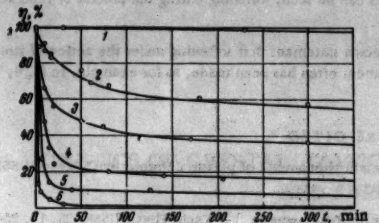

a

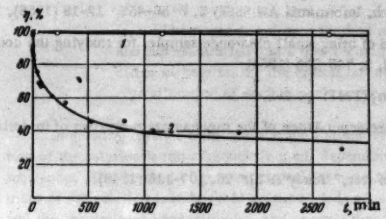

b

Fig. 2. Dependence of the degree of softening on the time of relaxation for different temperatures of relaxation. a: 1) −70°C, 2) +20°C, 3) +41°C, 4) +90°C, 5) +120°C, 6) +150°C; b: 1) −70°C, 2) +21°C.

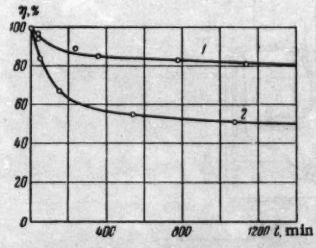

Fig. 3. The dependence of the degree of softening on time, measured during the process of relaxation (1) and in the absence of stresses (2).

The shape of the curves $\eta = \eta(t)$ given in Fig. 2 shows that relaxation in a hardened sample proceeds especially rapidly in the earlier intervals of time after unloading of the sample and then slows down substantially. The initial rate of softening is especially high at high temperatures. The character of dependence of η on t and T indicates that the hardened state is energetically unstable and that the process of softening is a process of the relaxation type. It is desirable, therefore, to find out whether or not the dependence of η on t is a simple exponential relation of the type $\eta = \eta e^{-t/\tau}$. In that case $\ln \eta$ must be a linear function of t. Actually this relation is far from being linear. This means that the kinetics of the process of softening cannot be described by a simple exponential with one relaxation time τ. In order to explain the experimental data, it is necessary to introduce an assumption that more complex phenomena are involved in the process of softening than chemical reactions of the first order. It is even more probable that several different processes of softening exist, each with its own relaxation time and corresponding energy of activation.

The existence of a set of relaxation times complicates the analysis of the experimental data and leads to a deviation from the linear relationship between $(\ln t)_{\eta = \text{const}}$ and $1/T$. For this reason at present we have evaluated the energy of activation for only rather long periods of time ($t > 60$ min) for which the relation between $(\ln t)_{\eta = \text{const}}$ and $1/T$ may be taken as approximately linear. For this region the energy of activation is about 1400 kcal/mole.

In conclusion let us review the results of measurements of the degree of softening during the process of relaxation of stresses. These measurements were made in order to determine the effect of external stresses on the rate of softening. This information is needed for correct understanding of the relation between the form of the curves of hardening and the speed of deformation and also for determining the role of the process of softening in the phenomena of relaxation of stresses in the hardened crystals.

The determination of the degree of softening attained during the process of relaxation was made in the following way. The sample was compressed to the same degree of hardening as in the preceding experiments, but when the desired hardening was attained the specimen was not unloaded but was kept under constant stress. Because of this, from the moment of attainment of stress σ_0, the sample underwent the process of relaxation of stress and at the same time remained at rest under stress; i. e., it underwent the process of softening. After a definite period of time, t, the sample was subjected to compression once more and the limit of viscosity, σ_1, was determined. The degree of softening was computed as before by the formula $\eta = \dfrac{\sigma_1 - \sigma_T}{\sigma_0 - \sigma_T} \cdot 100\%$.

The relation between η and t during relaxation has so far been investigated only at room temperature. Figure 3 shows, for comparison, two curves $\eta = \eta(t)$, one measured during the process of relaxation (curve 1) and the other in the absence of external stresses (curve 2). As can be seen, softening during the process of relaxation is much slower than in the case of simple rest.

These results, it seems to us, contradict the well-known statement that softening under the action of stresses proceeds faster than in the absence of stresses. This statement often has been made, as for example, in [1, 6, 7] and elsewhere.

LITERATURE CITED

[1] M. A. Bol'shanina, "Hardening and rest as the main phenomena of plastic deformation," Izv. AN SSSR, Ser. Fiz. 14, 2, 223-231 (1950).

[2] G. A. Dubov and V. R. Regel', "Photoelectro-optic dynamometer," J. Tech. Phys. (USSR) 25, 14, 2542-2544 (1955).

[3] V. R. Regel' and G. A. Dubov, "An apparatus for recording curves of compression, tension and relaxation," Biulleten' Pribory i Stendy (Inst. Tekhn.-Ekonomich. Informatsii AN SSSR) 2, P- 56-452, 12-16 (1956).

[4] G. A. Dubov and V. R. Regel', "On the method of using small clearance samples for studying the compression and the relaxation of stresses," Kristallografiia 2, 6, 746-755 (1955).

[5] V. D. Kuznetsov, Physics of Solids 2 [in Russian] (1941) p. 311.

[6] M. A. Bol'shanina, "Concerning the temperature dependence of the mechanical properties of materials," Trudy SFTI* 32, 170-174 (1953).

[7] L. I. Vasil'ev, "The quasi-relaxational theory of rest," Trudy SFTI* 26, 107-115 (1948).

Received March 1, 1957

Institute of Crystallography, Academy of Sciences, USSR

* Siberian Physics and Technology Institute.

KINETICS OF CRYSTALLIZATION AT CONSTANT TEMPERATURE AND SUPERSATURATION

M. I. Kozlovskii

The paper describes a method of growing crystals at constant temperature and supersaturation and a new technique of measuring linear crystallization velocities without taking the crystal out of the solution. Kinetic equations for the crystallization of Rochelle salt under constant conditions of growth are derived.

In growing crystals from solution the method of gradual lowering of temperature or the method of evaporation of the solution is most frequently used, depending on the character of the solubility curve of the crystallizing substance. The method of growing crystals at constant temperature and supersaturation with continuous enrichment of the solution is rather seldom used. It is generally believed that in this method it is more difficult to control the spontaneous appearance of seed crystals than in the other two, and for this reason it has been given less attention. At present, however, there are even industrial plants based on this method [1] (Walker and Kohman method).

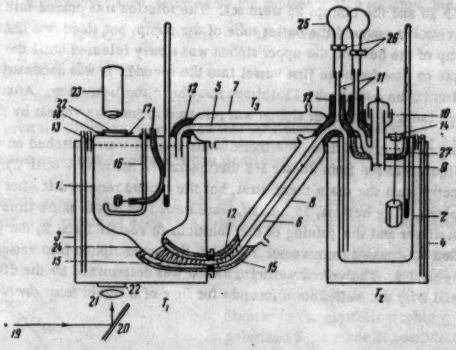

Fig. 1. Arrangement for growing crystals by the method of continuous enrichment of the solution and measuring the linear velocities of growth of the crystal faces.

For the investigation of the kinetics of crystallization at constant temperature and supersaturation, the author used the method of growing crystals by continuous enrichment of the solution.

The diagram of the arrangement devised by the author is shown in Fig. 1. The apparatus consists of two glass vessels, 1 and 2. Vessel 1 terminates in a conical funnel 24. Each vessel is placed in a thermostat 3, 4. Vessels 1 and 2 are connected by upper and lower siphons 5 and 6, and each siphon is surrounded by a glass heater 7 and 8. The upper siphon ends in a propeller pump 9 with a water seal 10. Each siphon is equipped with an

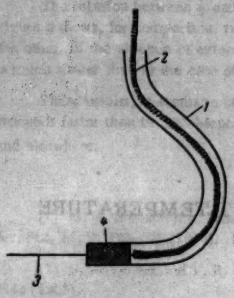

Fig. 2. Crystal carrier. 1) Glass tube, 2) elastic spiral (thin cable), 3) needle, 4) rubber stopper.

outlet tube 11 for pumping out air from the siphons. Rubber bulbs 25 with clamps 26 are used for this purpose. The ends of the siphons not enclosed within the heating tubes are wrapped in asbestos 12. The part of the lower siphon which extends beyond the thermost 3 is surrounded by a heating spiral 15 in addition to the asbestos insulation. Vessels 1 and 2 are covered with lids 13 and 14. The lid of the first vessel 13 carried a stirrer 16 which has reciprocating motion and has a window 17. The window contains a heating element 18 within the glass, which warms the glass and keeps it from fogging. This lid has holes for a thermometer and the crystal carrier. The crystal carrier is shown in Fig. 2. The lid of the second vessel also has two openings, one for the thermometer and the other for a cork which holds a crystal for maintaining the supersaturation of the solution. The lid of vessel 2 carries also a glass tube with an additional heater 27. The growing crystal is observed and photographed by means of a simple optical system consisting of a light source 19, mirror 20, condenser 21, two polaroids 22 and a camera with objective 23. The crystal carrier (Fig. 2) is a glass tube 1, containing an elastic spiral 2. The spiral terminates in a silvered needle 3, which holds the crystal. In order to prevent the solution from entering the tube, the needle is passed through a rubber stopper 4. The elastic spiral permits rotation of the crystal, thus making it possible to observe its growth in two projections.

Rochelle salt $KNaC_4H_4O_6 \cdot 4H_2O$ was used in the investigation. In all experiments the seed crystal was a small cylinder of Rochelle salt with its axis parallel to the c axis of the crystal. It was attached to the crystal carrier with the c axis perpendicular to the needle. For this purpose a hole parallel to the a axis was drilled in the crystal before it was turned into a cylinder.

The procedure was as follows. First a solution of Rochelle salt of a given concentration was prepared in an enameled vessel and the saturation point T_1 was determined by means of a special apparatus. Then an amount of salt to produce a supersaturation was added to the solution and the second saturation point, T_2, was determined. The solution was heated 10 to 15°C above T_2, filtered, and poured into the crystallizer. Just before this, air was removed from the bulb 25 and the clamps 26 were set. The solution was poured into vessel 1, then into vessel 2, so that in the second vessel it covered the outlet tube of the pump, but stood one centimeter lower than in the first vessel. The clamp of the bulb on the upper siphon was slowly released until the siphon was activated, i. e., until the solution began to flow from the first vessel into the second; it was necessary at this point to watch that the level of the solution in the outlet tube 11 did not rise above the insulation. After this, the clamp on the upper siphon was set and the clamp of the lower siphon was released to join the vessels by the lower siphon.

Before the filling of the crystallizer, the thermostats 3 and 4 were switched on and set for 10-15°C above T_2. The thermostat liquid was fed from Vobser I-8 thermostats (sensitivity = 0.01°C). The first thermostat received the liquid directly from the main thermostat, but the second received it after it had passed through the heaters on the two siphons. The heaters, 15 and 27, were turned on at the same time as the thermostats. After the filling of the crystallizer and the joining of the solutions in vessels 1 and 2, the pump and the stirrer were turned on. The solution now passed from vessel 2 through the upper siphon into vessel 1 and from vessel 1 through the lower siphon into vessel 2. The velocity of circulation was determined by the difference in the levels of the solution in vessels 1 and 2 by the well-known formula for flow of a liquid from one vessel into another through a siphon:

$$Q = \mu_3 \omega \sqrt{2gH},$$

where Q is the volume of liquid flowing per unit time, ω is the area of cross section of the lower siphon, μ_3 is the coefficient of rate of flow of the system, $\sqrt{2gH}$ is the velocity of flow of liquid through the siphon, and H the difference in levels or head.

The circulation of the liquid is made rapid at first to insure rapid exchange of solutions in vessels 1 and 2 and good mixing. Circulation and mixing at the temperature 10-15°C above T_2 are continued for two to three hours. This is done to prevent appearance of centers of crystallization before the introduction of the seed crystal.

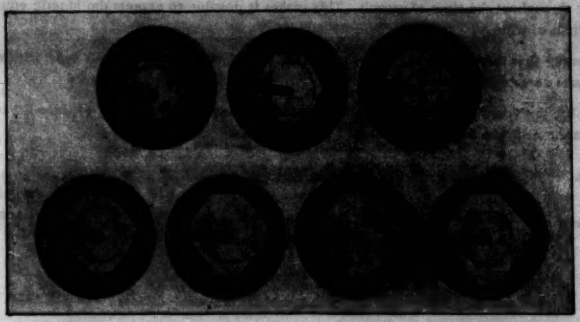

Fig. 3. Photographs of a Rochelle salt crystal in polarized light taken normal to the c axis. One hour intervals between the photographs.

After 2-3 hr, the thermostats are set to 1° above T_2 and the temperature in the vessels decreases. When it reaches $T_2 + 1°$ the stirrer and the pump are stopped and the seed crystal is introduced into vessel 1 and the feeding crystal into vessel 2. The pump is turned on again but not the stirrer. After introduction of the crystals the temperature in vessel 1 falls to T_1 and in vessel 2 to T_3. The speed of circulation is now reduced to the speed insuring continuous replacement of the impoverished solution by the supersaturated solution. After the temperature in vessel 1 becomes constant the stirrer is turned on to make 25 revolutions, first in one then in the opposite direction, at the speed of 100 rpm.

To insure exchange of the impoverished solution by the supersaturated solution, the speed of circulation must satisfy the equation $\frac{dm}{dt} = cQ$ or $cQ > \frac{dm}{dt}$, where $\frac{dm}{dt}$ is the velocity of crystallization, c is the supersaturation, Q is the rate of flow of the liquid.

In the experiments, 2.5 mm difference in levels was sufficient to insure the condition $cQ > \frac{dm}{dt}$ for the time of the growth of the crystal. Since the circulation was continuous, and under the conditions selected, $cQ > \frac{dm}{dt}$, the supersaturation in vessel 1 remained practically constant.

During each experiment, observations were made for 5-10 hr. The uniformity of conditions was checked by measuring linear velocities of growth of each face, which must be constant at any moment of measurement.

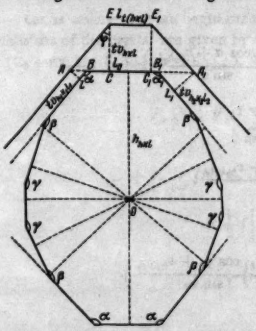

Fig. 4. Diagram to illustrate Formulas (2)-(10).

To measure the velocity of growth of each face, an optical method was used – photographing of the crystal in polarized light in the directions parallel and perpendicular to the crystallographic c axis. The use of polarized light made it possible to obtain sharp contrast between the projection of a face and the dark background. Photographs were taken every half hour or every hour. Figure 3 shows a number of successive photographs of a growing crystal at T = 40.95°C. After completion of an experiment, the photographs were projected on a screen, magnified 12 times, and the linear velocity of growth of the crystal faces was measured (error of measurement was 0.005 mm/hr). This method of measurement gives not the average but the instantaneous velocity of growth of the crystal faces.

The experiments have shown that the linear velocity of growth of crystal faces under constant conditions remains constant throughout the time of growth. This makes it possible to express the kinetic equations of crystallization as functions of time.

Let us consider first the volume change of a growing crystal of the Rochelle-salt type with the symmetry 2:2 for the general case of differential growth.

To determine the volume of a crystal it is necessary to know for each moment of time the length of the axis C_t and the area of the face (001) = S_t; then

$$V = C_t S_t; \tag{1}$$

but $C_t = C_0 + tv_c$, where C_0 is the initial length along the c axis, t is the time and v_c is the linear velocity along the c axis.

$$S_t = \frac{1}{2} \sum_{hkl} l_{t\,(hkl)} \left(h_{0(hkl)} + t v_{hkl}\right), \tag{2}$$

where $l_{t(hkl)}$ are lengths of the projections of the faces in the [001] zone on the plane perpendicular to the axis; t the time, v_{hkl} the linear velocities for the faces, $h_0(hkl)$ the initial lengths of the normals to the corresponding faces.

The magnitude $l_{t(hkl)}$ may be expressed as a function of time, linear velocities, and angles between adjacent faces. Figure 4 shows that $l_{t(hkl)} = l_0 - (BC + B_1C_1)$, $BC = AC - AB$.

From ΔAEC we obtain $AC = tv_{hkl} \operatorname{tg} \varphi = -tv_{hkl} \operatorname{ctg} \alpha$,

from ΔABL we obtain $AB = \frac{tv_{h_1k_1l_1}}{\sin \alpha}$,

Thus

$$BC = t\left(-v_{hkl} \operatorname{ctg} \alpha - \frac{v_{h_1k_1l_1}}{\sin \alpha}\right) = -t\left(\frac{v_{hkl} \cos \alpha + v_{h_1k_1l_1}}{\sin \alpha}\right).$$

Similarly

$$B_1C_1 = -t\left(\frac{v_{hkl} \cos \alpha + v_{h_2k_2l_2}}{\sin \alpha}\right).$$

Therefore

$$l_{t\,(hkl)} = l_0 + t\left(\frac{v_{hkl} \cos \alpha + v_{h_1k_1l_1}}{\sin \alpha} + \frac{v_{hkl} \cos \alpha + v_{h_2k_2l_2}}{\sin \alpha}\right).$$

For the faces forming equal angles with the adjacent faces,

$$l_{t\,(hkl)} = l_0 + t\,\frac{2v_{hkl} \cos \alpha + v_{h_1k_1l_1} + v_{h_2k_2l_2}}{\sin \alpha}.$$

But in the general case when the angles are different,

$$l_{t\,(hkl)} = l_0 + t\left(\frac{v_{hkl} \cos \varphi_1 + v_{h_1k_1l_1}}{\sin \varphi_1} + \frac{v_{hkl} \cos \varphi_2 + v_{h_2k_2l_2}}{\sin \varphi_2}\right).$$

Introducing the expression

$$\left(\frac{v_{hkl}\cos\varphi_1 + v_{h_1k_1l_1}}{\sin\varphi_1} + \frac{v_{hkl}\cos\varphi_2 + v_{h_2k_2l_2}}{\sin\varphi_2}\right) = K_{hkl}, \quad . \tag{3}$$

we may write

$$l_{t(hkl)} = l_{0\,(hkl)} + tK_{hkl}. \tag{4}$$

K_{hkl} may be either positive or negative; for the faces which do not disappear as the crystal grows, $K_{hkl} > 0$; for those which disappear, $K_{hkl} < 0$.

Substituting the value of $l_{t(hkl)}$ in (2), we get

$$S_t = \frac{1}{2}\sum_{hkl}(l_{0\,(hkl)} + tK_{hkl})(h_{0\,(hkl)} + tv_{hkl}),$$

and the final expression for the volume of the crystal is

$$V_t = \frac{1}{2}(C_0 + tv_c)\sum_{hkl}(l_{0\,(hkl)} + tK_{hkl})(h_{0\,(hkl)} + tv_{hkl}). \tag{5}$$

Transforming Eq. (5), we have

$$V_t = \frac{1}{2}v_c t^3\sum_{hkl}K_{hkl}v_{hkl} + \frac{1}{2}t^2\Big(C_0\sum_{hkl}K_{hkl}v_{hkl} + \\ + v_c\sum_{hkl}l_{0\,(hkl)}v_{hkl} + v_c\sum_{hkl}K_{hkl}h_{0(hkl)}\Big) + \frac{1}{2}t\Big(C_0\sum_{hkl}l_{0\,(hkl)}v_{hkl} + \\ + C_0\sum_{hkl}K_{hkl}h_{0\,(hkl)} + v_c\sum_{hkl}l_{0\,(hkl)}h_{0\,(hkl)}\Big) + \frac{1}{2}C_0\sum_{hkl}l_{0\,(hkl)}h_{0\,(hkl)}. \tag{6}$$

This is the equation of a cubic parabola and its last term is numerically equal to the initial volume of the growing crystal, since $\frac{1}{2}C_0\sum_{hkl}l_{0\,(hkl)}h_{0\,(hkl)} = V_0$. It may seem that, with a different initial volume, a different curve would be obtained. It is easy to show, however, that the volume change of the seed crystal does not change the form of the curve but merely shifts the origin of the coordinates to the right or left of the axis t.

Let us assume that we begin measuring the linear velocity of growth not at the moment when the initial dimensions of the crystal are given by the values C_0, $l_{0}(hkl)$, $h_0(hkl)$ but after an interval τ, when the conditions are $(C_0 + \tau v_c)$, $(l_0(hkl) + \tau K_{hkl})$, $(h_0(hkl) + \tau v_{hkl})$, so that Eq. (6) has the form

$$V_\tau = \frac{1}{2}V_c t^3\sum_{hkl}K_{hkl}v_{hkl} + \frac{1}{2}t^2\Big[(C_0 + \tau v_c)\sum_{hkl}K_{hkl}v_{hkl} + \\ + v_c\sum_{hkl}(l_{0(hkl)} + \tau K_{hkl})\cdot v_{hkl} + v_c\sum_{hkl}K_{hkl}(h_{0\,(hkl)} + \tau v_{hkl})\Big] + \\ + \frac{1}{2}t\Big[(C_0 + \tau v_c)\sum_{hkl}(l_{0(hkl)} + \tau K_{hkl})v_{hkl} + \\ + (C_0 + \tau v_c)\sum_{hkl}K_{hkl}(h_{0(hkl)} + \tau v_{hkl}) +$$

(more)

(continued)

$$+ v_c \sum_{hkl} (l_{0(hkl)} + \tau K_{hkl})(h_{0(hkl)} + \tau v_{hkl})\Big] +$$

$$+ \frac{1}{2}(C_0 + \tau v_c) \sum_{hkl} (l_{0(hkl)} + \tau K_{hkl})(h_{0(hkl)} + \tau v_{hkl}). \quad (7)$$

If in Eq. (6) the origin is shifted by τ, the following equation is obtained:

$$V'_\tau = \Big(\frac{1}{2} v_c \sum_{hkl} K_{hkl} v_{hkl}\Big)(t+\tau)^3 + \frac{1}{2}\Big(C_0 \sum_{hkl} K_{hkl} v_{hkl} +$$

$$+ v_c \sum_{hkl} l_{0(hkl)} v_{hkl} + v_c \sum_{hkl} K_{hkl} h_{0(hkl)}\Big)(t+\tau)^2 +$$

$$+ \frac{1}{2}\Big(C_0 \sum_{hkl} l_{0(hkl)} v_{hkl} + c_0 \sum_{hkl} k_{hkl} h_{0(hkl)} + v_c \sum_{hkl} l_{0(hkl)}\, h_{0(hkl)}\Big)\cdot(t+\tau) +$$

$$+ \frac{1}{2} c_0 \sum_{hkl} l_{0(hkl)} h_{0(hkl)}. \quad (8)$$

Expanding the parentheses in both equations, we can easily verify that $V_\tau = V'_\tau$, i. e., that the initial volume does not change the character of the curve, but shifts the origin along axis t to the right if the initial volume is increased, and to the left if it is decreased.

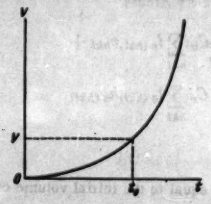

Fig. 5. Volume change of the crystal as a function of time.

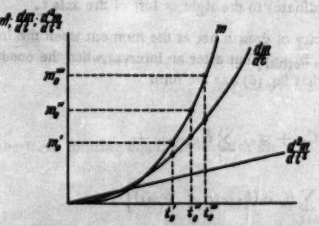

Fig. 6. Change of mass, velocity of crystallization and acceleration of crystallization as functions of time.

Having shifted the origin to the left by the interval of time τ for which C_0, $l_{0(hkl)}$ and $h_{0(hkl)}$ become zero, we obtain Eq. (6) in a simplified form:

$$v_l = \frac{1}{2} v_c t^3 \sum_{hkl} k_{hkl} v_{hkl}. \quad (9)$$

Equation (9) makes it possible to determine the volume of a growing crystal at any moment of time by the measured linear velocities of growth of its faces. It is necessary for this to determine the coefficient

$$a = \frac{1}{2} v_c \sum_{hkl} k_{hkl} v_{hkl},$$

to draw the curve $V = at^3$ (Fig. 5), to calculate the initial volume V_0, to plot this value on the curve, to find the corresponding point on the t axis and to count time from it.

From Eq. (9) the mass of the growing crystal and the velocity and acceleration of growth also can be determined:

$$m = \frac{1}{2} \gamma v_c t^3 \sum_{hkl} k_{hkl} v_{hkl}, \quad (10)$$

$$\frac{dm}{dt} = \frac{3}{2} \gamma v_c t^2 \sum_{hkl} k_{hkl} v_{hkl}, \quad (11)$$

$$\frac{d^3m}{dt^3} = 3\gamma v_c^2 \sum_{hkl} k_{hkl} v_{hkl}, \tag{12}$$

where γ is the density.

As can be seen from Eqs. (9)-(12), the increase in volume and mass of the crystal is represented by a cubic parabola, change in velocity of crystallization by a quadratic parabola, and acceleration of crystallization by a straight line (Fig. 6). Examination of Fig. 6 shows that velocity of crystallization increases with the size of the crystal, and this confirms the well-known statement that large crystals grow faster than small ones [2].

For calculating the mass of a crystal of Rochelle salt growing from an aqueous solution by the method of gradual decrease of temperature, Koptsik [3] derived the following formula:

$$m = 0.53\,\gamma b^2 c. \tag{13}$$

It is easy to see that this formula is a special case of Eq. (10) for these particular conditions of crystal growth. Using similar arguments, it is possible to derive from the formula $m = 0.53\,\gamma b^2 c$ the following equation:

$$m = 0.53\gamma t^3 v_b^2 v_c. \tag{14}$$

Equation (10) is also reduced to this form for these conditions of growth.

Equation (14) gives

$$\frac{dm}{dt} = 1.59\,\gamma t^2 v_b^2 v_c. \tag{15}$$

Comparing Eq. (15) with the equation of velocity of crystallization obtained from (13):

$$\frac{dm}{dt} = 0{,}53\,\gamma b^2 \frac{dc}{dt} + 1.06\,\gamma bc \frac{db}{dt}, \tag{16}$$

it is not difficult to see that with $dc/dt = \text{const}$, $db/dt = \text{const}$ and the initial conditions $b_0 = 0$, $c_0 = 0$, $b = b_0 + tv_b$, $c = c_0 + tv_c$.

TABLE 1

Linear Velocities of Growth of Faces of Rochelle Salt Crystals at T = 33.35°C and T = 40.95°C

Indices of faces	T = 33.35°C		T = 40.95°C	
	linear velocity, mm/hr	K	linear velocity, mm/hr	K
(010)	0.2348	+0.0101	0.2966	+0.0328
(0$\bar{1}$0)	0.2759	−0.0217	0.3518	−0.0647
(1$\bar{1}$0)	0.1517	+0.6190	0.1708	+0.8808
($\bar{1}$10)	0.1738	+0.2819	0.2277	+0.4837
(2$\bar{1}$0)	0.2483	−0.0646	0.2759	−0.1564
($\bar{2}$10)	0.1793	+0.2156	0.2759	+0.2891
(100)	0.3173	−0.3038	0.3311	−0.1567
($\bar{1}$00)	0.2483	−0.2437	0.4201	−0.4421
($\bar{2}$10)	0.1862	+0.1696	0.3311	−0.0694
(210)	0.2207	+0.0542	0.2759	−0.1505
(110)	0.1379	+0.5222	0.1724	+0.6585
($\bar{1}$10)	0.1655	+0.2770	0.2207	+0.6536
c axis	0.5518	—	0.6895	—

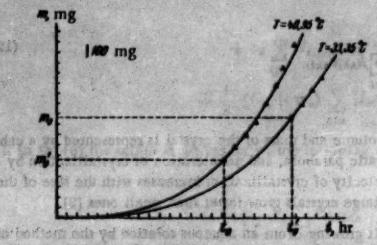

Fig. 7. Volume of a growing crystal of Rochelle salt as a function of time at T = 33.35°C and T = 40.95°C.

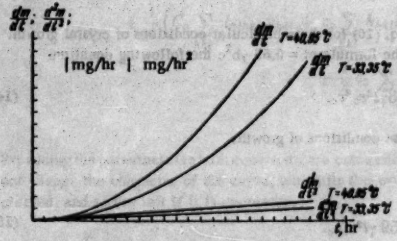

Fig. 8. Velocity and acceleration of crystallization of Rochelle salt as functions of time for T = 33.35°C and T = 40.95°C.

$$\frac{dm}{dt} = 0.53\,\gamma b^3 \frac{dc}{dt} + 1.06\,bc\frac{db}{dt} = 1.59\,\gamma l^2 v_b^2 v_c.$$

To illustrate what has been said, we shall review the course of crystallization at temperatures of 33.35°C and 40.95°C with constant supersaturation of 80 g/liter. Table 1 gives the velocities of growth and the calculated

TABLE 2

Values of $\underline{a}$ and a_γ for T = 33.35°C and T = 40.95°C

T, °C	$\underline{a}$	a_γ
33.35	0.0465	0.0823
40.95	0.0742	0.1313

values of K_{hkl} for each face. The table shows that, all other conditions being equal, the linear velocities of growth of the faces increase with increasing temperature. Examining the values of K_{hkl}, we may determine in advance which faces will appear in the final crystal and which ones will disappear during growth. The fastest growing faces are (100) and $(\bar{1}00)$ since for them the values of K are negative and have larger absolute values than the other negative values of K.

Table 2 gives the values of the coefficient $\underline{a}$ and the product a_γ for the temperatures of 33.35°C and 40.95°C.

Figures 7 and 8 are curves of change of mass, velocity of crystallization and acceleration of a growing crystal. In Fig. 7 triangles represent experimentally obtained points. The curves are drawn according to the formulas

$$m = a\gamma l t^3; \quad \frac{dm}{dt} = 3a\gamma l^2; \quad \frac{d^2m}{dt^2} = 6a\gamma l.$$

SUMMARY

1. It has been verified experimentally that under constant conditions of crystallization (T = const and C = const) the linear velocity of growth of individual crystal faces remains constant.

2. It has been shown that the growth of individual faces depends not only on the linear velocity of growth of these faces and their nearest neighbors but also on the angles between a given face and its neighbors.

3. A formula has been derived which makes it possible to predetermine whether a given face will appear on the grown crystal or disappear during growth and to calculate the time required for complete disappearance of a face.

4. A kinetic equation of growth of crystals of the Rochelle-salt type under constant conditions has been derived.

5. It has been shown that the velocity of crystallization depends on the size of the seed crystal.

6. A new method of measuring the velocity of growth of crystal faces during the growth of the crystal, i. e., without taking it out of the solution, has been worked out.

The author expresses his gratitude to Professor G. G. Lemmlein and Dr. V. A. Koptsik for their interest in his work and valuable advice and criticism.

LITERATURE CITED

[1] H. E. Buckley, Crystal Growth [Russian translation] (IL, 1954).

[2] A. V. Shubnikov, "Dependence of the velocity of crystal growth on the size of the crystal," Doklady Akad. Nauk SSSR 1135-1142 (1919).

[3] V. A. Koptsik, "Certain problems of the kinetics of crystal growth," Coll.: Growth of Crystals [in Russian] (1957) pp. 359-366.

Received November 27, 1956

M. V. Lomonosov Moscow State University

PRODUCTION OF ORIENTED FIGURES ON METALS BY IONIC BOMBARDMENT

V. E. Iurasova

The paper points out the advantages of using cathode sputtering to develop oriented figures on metal surfaces and gives the conditions needed for obtaining the best results on crystals of different metals. The possibility of revealing glide planes in metal crystals is pointed out also. The mechanism of formation of faceted figures by ionic bombardment is discussed in the light of modern theories of cathode sputtering.

In a glow discharge the cathode undergoes destruction by the gas ions bombarding it; this is the phenomenon of cathode sputtering [1]. Those areas of the cathode surface in which atomic bonds are weakest are most easily destroyed. Therefore, during cathode sputtering the boundaries of metal grains are outlined [2] and the interiors of the grains are etched into relief. In some cases the relief of the metal surface which has undergone cathode sputtering consists of regular crystalline figures. It was shown earlier [3] that the oriented figures obtained in this way from single metal crystal are similar to the "etch figures" produced by chemical action on the metal surface [4] and possess the symmetry of the face on which they are formed. Therefore, oriented figures obtained by cathode sputtering, just as the usual "etch figures," can serve to determine the symmetry of a crystal face or of a grain in a crystal aggregate and to reveal the degree of distortion of the lattice in the surface layer of the metal, etc.

Cathode sputtering has a number of advantages for obtaining oriented figures as compared with chemical etching.

1) In chemical etching it is necessary to select a special etching agent for each metal or alloy, which is often quite difficult. The cathode sputtering method reveals the structure of any metal or alloy.

2) Unlike the chemical method, cathode sputtering makes it possible to obtain oriented figures on crystal faces within a large range of temperatures (from 20-30°C to within 0.6° of the melting temperature of the crystal). This makes it possible, for example, to study the disappearance of distortions in the surface layer of the metal on heating, as well as other processes.

3) The surface of the metal subjected to sputtering does not become covered with an oxidation film, as happens in chemical etching. Sputtered surfaces give good replicas for electron microscope study and thus make possible a more detailed view of the surface relief.

4) Finally, by changing the number and velocity of ions bombarding the surface, it is easy to control the process of sputtering and the depth of the "etch figures."

Since cathode sputtering is a universal method of obtaining oriented figures, it is advisable to find out under what conditions the clearest figures on the surface of the metal are obtained.

In order to determine the effect of the duration of sputtering and of the number and velocity of ions on the relief surface, the {513} plane of an aluminum crystal was subjected to bombardment by neon ions under different conditions in a glow discharge. The experiment was performed in a glass tube whose construction is shown in Fig. 1. The specimen was attached to a molybdenum holder cooled with water. Figure 2, a is a photograph of the {513} plane of an aluminum crystal after sputtering (2 kv potential difference between cathode and anode,

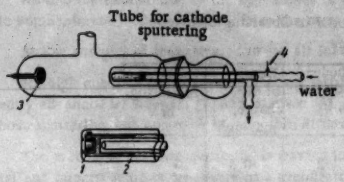

Fig. 1. Tube for cathode sputtering of metals. 1) Sample, 2) junction between copper and glass, 3) anode, 4) connection for supplying voltage to the sample.

density of discharge 1.2 ma/cm^2, pressure of neon $1 \cdot 10^{-1}$ mm Hg, duration of sputtering 3 hr). The surface shows a pattern with oriented areas which probably correspond to the {110} planes. This is confirmed by the fact that sputtering of planes of the {110} type on an aluminum crystal gives similar oriented figures whose flat areas are parallel to the surface, i. e., represent the {110} plane (Fig. 3). Evidently ionic bombardment most easily etches a surface with the least atomic density [5].

When the duration of sputtering is increased to six hours the oriented figures are slightly fused, and after ten hours no regular pattern is observed on the {513} plane (Fig. 2, b).

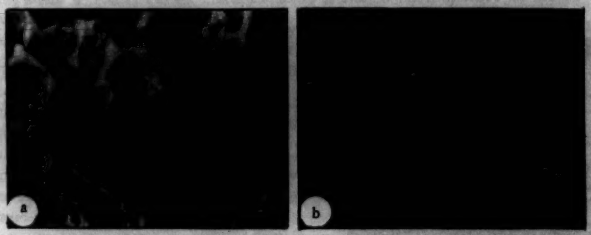

Fig. 2. The {513} plane of an aluminum crystal after cathode sputtering. (V = 2 kv; j = 1.2 ma/cm^2, $P_{neon} = 1 \cdot 10^{-1}$ mm Hg; x 1000). a) Duration of sputtering 3 hr; b) duration of sputtering 10 hr.

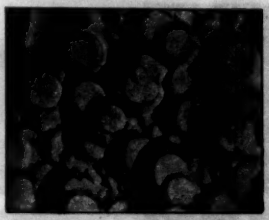

Fig. 3. The {110} plane of an aluminum crystal after cathode sputtering. (x 720, V = 2 kv, j = 0.8 ma/cm^2, $P_{neon} = 8 \cdot 10^{-2}$ mm Hg, t = 1.5 hr.)

The same effect is achieved by increasing the voltage between the cathode and the anode to over 3 kv or by increasing the density of discharge to 2.5 ma/cm^2. Thus, to obtain clear-cut oriented figures on the surface of aluminum, the following conditions may be recommended: voltage between cathode and anode 2 kv, density of discharge 1.2 ma/cm^2, pressure of neon $1 \cdot 10^{-1}$ mm Hg, duration of bombardment about 3 hr.

The conditions used in ionic etching to reveal the crystal structure of some metals are given in Table 1.

Besides producing oriented figures, cathode sputtering reveals the glide planes of metallic crystals. The glide planes of a cadmium crystal are shown in Fig. 4. Glide planes have been observed also in zinc crystals.

The crystalline figures which form on the surface of a crystal after ionic bombardment may be either depressions or prominences of regular form. For example, oriented depressions are produced on the planes of aluminum crystals, hexagonal depressions are formed on the {0001} plane of zinc single crystals. Prominences in the form of regular trigonal pyramids are etched on the {111} plane of a silver crystal. Minute hexagonal pyramids form on the {0001} planes of bismuth crystals.

After numerous metal crystals had been subjected to cathode sputtering and the effects carefully studied, certain regularities in the formation of oriented figures came to light. There are crystals, for example, on which faceted pits are produced, but not oriented prominences. Aluminum crystals are among these. (This statement

TABLE 1

Sample Conditions for Ionic Etching Used in Obtaining Oriented Figures on the Surfaces of Some Metals

Metal	Face subjected to sputtering	Cathode-anode voltage, kv	Density of discharge, ma/cm²	Duration of sputtering, hr
Aluminum	{110}; {513}	2	0.8	3
Bismuth	{0001}	2	0.1	2
Cadmium	{0111} {0001}	2	1.2	0.5; 1.5
Cobalt	{0001}	1.8	1	1
Magnesium	cryst. aggreg.	1.2	1	6
Copper	—»—	2	2	3.5
Tin	—»—	1.5	0.2	0.5
Zinc	{0001}	2	0.5	3

Fig. 4. Glide planes in a cadmium crystal revealed by bombardment with neon ions. (× 450, V = 2 kv, $j = 1\ ma/cm^2$, $P \sim 1 \cdot 10^{-1}$ mm Hg, t = 40 min.)

refers to those conditions of sputtering under which the mass of pulverized material is carried off the cathode and not condensed upon it.)

In some metals, closely packed planes of a given symmetry give oriented prominences, and in others identical planes give oriented depressions. In zinc and bismuth crystals the {0001} plane is the most closely packed, yet bismuth gives hexagonal prominences, while zinc gives hexagonal pits. The relief produced on the {0001} planes of bismuth and zinc crystals is shown in Fig. 5.

Some crystal planes give both prominences and depressions at the same time. For example, on the surfaces of a cadmium crystal sputtering produces rounded prominences covered with small clear-cut hexagonal pits.

a b

Fig. 5. a) {0001} plane of a bismuth crystal after sputtering (V = 2kv, j = 0.1 ma/cm^2, $P_{neon} = 8 \cdot 10^{-3}$ mm Hg, t = 1.5 hr, × 600); b) {0001} plane of a zinc crystal after sputtering (V = 2 kv, j = 0.5 ma/cm^2, $P \approx 3 \cdot 10^{-2}$ mm Hg, t = 3 hr, × 600).

What is the explanation of the appearance of oriented figures on the surfaces of metal crystals subjected to ionic bombardment? Does it follow from the current theories of cathode sputtering?

At low energies of ions (about 300 ev) all features of sputtering are well explained by the impact theory [5].

For high energies the impact theory is unsatisfactory. In this case good results are obtained from the theories recently advanced by Keywell [7] and Harrison [8]. Both theories give the same explanation of the mechanism of cathode sputtering, but approach the problem differently.

The process of cathode sputtering is treated in these theories as follows. An ion strikes the surface of a metal and imparts some of its energy to a metal atom. If this energy exceeds that needed to displace the metal atom (this energy is a few tens of electron volts for most metals), the atom begins to move from its position in the lattice and the metal acquires a so-called "primary" displaced atom. The ion, moving deeper into the metal, may collide with other atoms and produce new "primary" atoms until its energy finally becomes insufficient to displace more atoms. The "primary" atoms, during their movement through the metal, may collide with other atoms in the lattice and displace them, causing the appearance of "secondary" displaced atoms, and so forth. Thus a group of moving atoms is produced in the metal and some of these atoms may leave the metal.

The theories of Keywell and Harrison consider only the elastic interaction of particles, which is true, of course, only for some energies of the impinging ions. At higher energies (for example, for Ne ions with energies greater than 4000 ev) inelastic interactions appear and the theories become untenable.

The shortcomings of these theories lie in disregarding the crystalline structure of matter; they do not consider the dependence of the coefficient of sputtering on the crystallographic direction (observed at low energies of bombarding ions) and do not explain the formation of oriented figures on the surfaces of the sputtered metal.

Meanwhile, accepting the mechanism suggested by these theories [7, 8] the formation of oriented figures can be qualitatively explained. Those metal atoms which occupy positions of weakest bonding are more likely to be ejected from the surface of the metal, since smaller energy is required on the part of the "displaced" atoms to move them. On the surface of the metal those atoms are weakly bonded which lie at the boundaries of grains; after prolonged sputtering these boundaries are etched into deep grooves. Other atoms are weakly bonded at the surface, because they belong to the planes of low packing density which are exposed at the surface. Such planes are quickly etched and faceted pits form on the surface of the crystal.

Surface diffusion of atoms may also play a role in the formation of oriented figures, as well as the settling of the sputtered material back on the surface of the metal. Very probably these processes play an important role in the formation of faceted prominences. The formation of faceted depressions is due mainly to the easier sputtering of some planes than others. This is confirmed by examination of the relief of the sputtered surfaces. Figure 5, b, for example, shows clearly a number of stages in the formation of hexagonal pits on the {0001} plane of a zinc crystal. First a groove is etched along the sides of the hexagon (hexagon 1, Fig. 5, b), probably because of the sputtering of the $\{11\bar{2}0\}$ planes, which have a less dense packing of atoms; then the metal within the hexagon is sputtered, possibly because of destruction of the $\{11\bar{2}0\}$ planes within it, and the hexagons are deepened (2 in Fig. 5, b). Most of the atoms are displaced in this case in the direction parallel to the surface (6 directions of close packing $[11\bar{2}0]$ parallel to {0001}); they stop at the sides of the hexagon and form edges, as for example, on the hexagons 3, Fig. 5, b. The profile of such a hexagon is shown in Fig. 6. Thus, in the formation of oriented figures on the {0001} plane of a zinc crystal the main role is played by differential sputtering of the least closely packed planes, but migration of the atoms and their redeposition on the surface also play a role.

Fig. 6. Profile of a hexagon formed on the {0001} plane of a zinc crystal (hexagon 3, Fig. 5, b).

From the example of sputtering of the {0001} plane of a zinc crystal it is clear that the formation of oriented figures cannot be ascribed to a single process; to differential sputtering, or to migration or to redeposition of the sputtered matter. All these processes always take place. However, in some cases (in the formation of faceted pits) the first process predominates, while in other cases (formation of oriented prominences), migration and redeposition of the sputtered matter on the irregularities of the surface play the more important role.

In conclusion, the author expresses her gratitude to A. V. Shubnikov for many valuable comments and also to G. V. Spivak and V. R. Regel' for their interest in this work and useful advice.

LITERATURE CITED

[1] N. D. Morgulis, "Cathode sputtering," Uspekhi Fiz. Nauk 28, 203 (1946).

[2] G. V. Spivak, I. N. Prilezhaeva and M. I. Malkina, "On etching steel by ionic bombardment," J. Tech. Phys. (USSR) 24, 225 (1954).

[3] G. V. Spivak, V. E. Iurasova, I. N. Prilezhaeva and E. K. Pravdina, "On the processes occurring on the surfaces of metals in cathode sputtering," Izv. AN SSSR, Ser. Fiz. 20, 1184 (1956).

[4] A. P. Honess, The Nature, Origin, and Interpretation of the Etch Figures of Crystals (New York, 1927).

[5] G. K. Wehner, "Sputtering of metal single crystals by ion bombardment," J. Appl. Phys. 26, 1056 (1955); G. K. Wehner, "Controlled sputtering of metals by low-energy Hg ions," Phys. Rev. 102, 690 (1956).

[6] A. V. Shubnikov, "New photographic method for crystal research," Z. Krist. 78, 3 (1931).

[7] F. Keywell, "Measurements and collision-radiation damage theory of high-vacuum sputtering," Phys. Rev. 97, 1611 (1955).

[8] Don E. Harrison, Jr., "Theory of the sputtering process," Phys. Rev. 102, 1473 (1956).

[9] G. Seitz, "On the disordering of solids by action of fast massive particles," Discuss. Farad. Soc. 5, 271 (1949).

[10] J. Tamman and A. Müller, "Über Verfahren zur Bestimmung der Orientierung der Kristallite in metallischen Konglomeraten," Z. Metallkunde 18, 69 (1926); G. Tamman and H. H. Meyer, "Die Änderung der Kristallitenorientierung bei der Rekristallisation von Kupfer," Z. Metallkunde 18, 176 (1926).

Received February 21, 1957

M. V. Lomonosov Moscow State University

BRIEF COMMUNICATIONS

ON THE ELASTIC ANISOTROPY OF ISOMETRIC CRYSTALS IN THE (hkl) PLANE

S. E. Shtepan

For crystals of the isometric system

$$s'_{11} = s_{11} - (2s_{11} - 2s_{12} - s_{44}) \cdot \Psi_1,$$
$$s'_{12} = s_{12} - (2s_{11} - 2s_{12} - s_{44}) \cdot \Psi_2,$$
$$s'_{44} = s_{44} + (4s_{11} - 4s_{12} - 2s_{44}) \cdot \Psi_3,$$

where

$$\Psi_1 = \alpha_1^2\alpha_2^2 + \alpha_2^2\alpha_3^2 + \alpha_1^2\alpha_3^2,$$
$$\Psi_2 = \alpha_1\alpha_2\beta_1\beta_2 + \alpha_1\alpha_3\beta_1\beta_3 + \alpha_2\alpha_3\beta_2\beta_3,$$
$$\Psi_3 = \beta_1^2\gamma_1^2 + \beta_2^2\gamma_2^2 + \beta_3^2\gamma_3^2,$$

and α_1, α_2, α_3, β_1, β_2, β_3, γ_1, γ_2, γ_3 are direction cosines of a coordinate system which determines the directions of the elastic coefficients s'_{11}, s'_{12}, s'_{44} in relation to the crystallographic axes. If these directions lie in a certain plane(hkl), then the functions Ψ_1, Ψ_2, Ψ_3 may be conveniently represented by its indices. The following expressions have been obtained for these functions:

$$\Psi_1 = A_1\mu^2 + B_1\mu^4 + C_1\mu\sqrt{1-\mu^2} + D_1\mu^3\sqrt{1-\mu^2} + E_1,$$
$$\Psi_2 = A_2\mu^2 + B_2\mu^4 + C_2\mu\sqrt{1-\mu^2} + D_2\mu^3\sqrt{1-\mu^2} + E_2,$$
$$\Psi_3 = A_3\mu^2 + C_3\mu\sqrt{1-\mu^2} + E_3,$$

where

$$A_1 = \frac{J_2^2(k^2+l^2-h^2) + h^2[(l^4+k^4-4k^2l^2)J_3 - 2h^2k^2l^2}{J_2^2J_3^2},$$

$$B_1 = \frac{-J_2^4 - h^2[(l^4+k^4-4k^2l^2)J_3 - h^2k^2l^2] + l^2k^2J_3^2}{J_2^2J_3^2},$$

$$C_1 = \frac{2h^2kl(k^2-l^2)}{\sqrt{J_2^2J_3^2}}, \quad D_1 = \frac{2hkl(k^2-l^2)(2h^2+k^2+l^2)}{J_2^2},$$

$$E_1 = \frac{h^2[J_2^2 + h^2k^2l^2]}{J_2^2J_3^2},$$

$$A_3 = -B_3 = -\frac{J_2}{J_3} + \frac{h^2 J_3}{J_2^2} - \frac{h^2 (h^4 - 4h^2 l^2 + l^4)}{J_2^2 J_3} + \frac{l^2 h^2}{J_2^2} + \frac{h^4 h^2 l^2}{J_2^2 J_3},$$

$$C_3 = \frac{hkl\,(h^2 - l^2)\,(2h^2 + k^2 + l^2)}{J_2^2 \sqrt{J_3^2}}, \quad D_3 = \frac{-2hkl\,(k^2 - l^2)\,(2h^2 + k^2 + l^2)}{J_2^2 \sqrt{J_3^2}},$$

$$E_3 = \frac{-h^2 k^2 l^2}{J_2^2 J_3}, \quad A_3 = \frac{2h^2\,(h^4 + l^4) - 2l^2 h^2\,(h^2 + l^2)}{J_2 J_3^2}, \quad C_3 = \frac{2hkl\,(l^2 - k^2)}{J_2 \sqrt{J_3^2}},$$

$$E_3 = \frac{2l^2 h^2}{J_2 J_3}, \quad J_2 = k^2 + l^2, \quad J_3 = h^2 + k^2 + l^2.$$

Here μ is the cosine of the angle formed by a given direction with a certain constant direction in the plane (hkl).

An analysis of these functions shows that in relation to the elasticity coefficients s_{11} and s_{22}, those planes are isotropic for which $h = k = l$.

For the coefficient s_{44}, besides these planes, the plane of the type (001) is also isotropic.

Received April 2, 1956

M. V. Lomonosov Zaporozhye Pedagogical Institute

AN APPARATUS FOR THE STUDY OF CRYSTAL GROWTH UNDER THE MICROSCOPE

T. G. Petrov

Microscopic methods are widely used in the study of crystal formation. But the absence of special apparatus and well-developed techniques makes work in this field difficult.

In the Crystallography Department of the Leningrad State University an apparatus has been assembled which is a combination of a specially constructed thermostat with three interchangeable vessels designed for different types of crystallization. Measurement of the velocity of growth of different crystal faces by means of a motion picture camera or a micrometer ocular, as well as of the temperature of saturation of the solution in the vessel, can be made with this apparatus, and later the crystal can be studied on a goniometer, or by means of x-rays, etc.

The thermostat has a one-liter capacity and, on being heated to 50°C, attains stability of temperature within 10-12 min with variations not exceeding 0.05°C. Cooling by 3°C and subsequent stabilization are achieved in 4-5 min. After some experience with the thermostat, it is possible to shorten the period of stabilization considerably.

A diagram of the apparatus is shown in Fig. 1. The thermostat liquid, distilled water in this case, is moved by a centrifugal pump 1. From the pump it passes into the inner tubes of two coolers 2 (the tubes contain heating elements) and then flows through a bulb with a heat regulator 3. From the bulb, the water, still of rather inconstant temperature, because of the considerable thermal inertia of the mercury heat regulator, passes into the outer tube of the second cooler, where portions of water with different temperatures are mixed. Finally, after flowing through the bulb with the thermometer, the water passes through the outer tube of the crystallizing dish and returns to the centrifugal pump. Tap water is passed through the outer tube of the first cooler for rapid cooling of the distilled water. By using other sufficiently transparent and mobile liquids instead of distilled water, and by filling the first cooler with a cooling mixture, the range of temperatures obtained with the thermostat can be considerably extended.

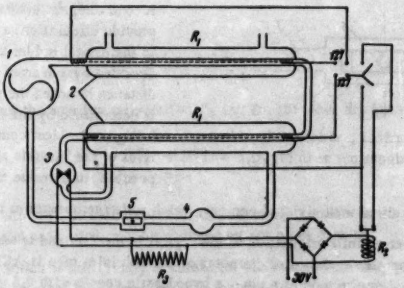

Fig. 1. Diagram of the apparatus.

The electrical circuit of the thermostat consists of two parts – heating and relay. Heating is done by two 55 ohm (R_1) heating coils. As can be seen on the diagram, one of the elements can be switched directly into a 127 volt circuit. The other heater used in work with constant temperature is switched in through a relay by means of a knife switch, and, for work with higher temperatures, directly into the 127 volt circuit. This circuit allows return to the required temperature after the temporary temperature increase needed for partial solution of the crystal or for washing and filling of the crystallizing dish without changing the position of the heat regulator contact.

The relay part of the circuit is fed from a 30 v transformer (not shown). A bridge of two selenium rods provides a 10 v dc voltage, which is sufficient to work the telephone relay of type RM with a 400 ohm resistor (R_3). The heat regulator 3 is a standard contact thermometer with graduations from 0 to 100°C. A 600 ohm resistance(R_4)is connected in parallel with the heat regulator, thus eliminating sparking of the mercury contact. It should be mentioned that the use of a 4 μf condenser in place of the resistance coil, as recommended by Chmutov [1] leads to increased sparking and rapid destruction of the regulator.

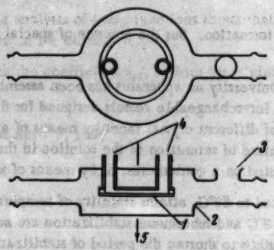

Fig. 2. Dish for the horizontal position of the microscope stage. 1) Dish, 2) housing, 3) opening for thermocouple, 4) tubes for introducing solution and seeds, 5) optic axis of the microscope.

In assembling the thermostat, it is desirable to keep the volume of circulating hot water at a minimum by shortening the tubes containing heating elements and to bring the heat regulator as close to the element connected to the relay as possible.

Three types of crystallizing dishes were made. One dish was designed for study of crystal growth in transparent or nearly opaque solutions and melts between cover glasses in a layer less than 1 mm thick, observations being made with the microscope stage in horizontal position (Fig. 2). A dish of this type permits observation on the spontaneous formation of seed crystals and their growth. The position and orientation of such crystals cannot be predetermined. Because of the shallowness of the dish, the effect of convection currents is negligible and diffusion is almost entirely responsible for crystal growth. The dish is washed by means of rubber tubes and a rubber bulb attached to the extensions of the glass tubes.

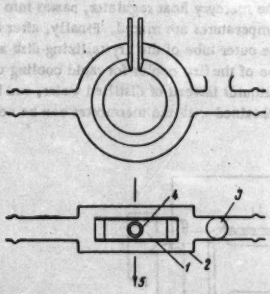

Fig. 3. Dish for the vertical position of the microscope stage. Same designations as in Fig. 2.

A second type of dish was designed for observation of a crystal growing on a crystal holder in a transparent solution more than 4 mm deep, with the microscope stage in a vertical position (Fig. 3).

The third type of dish is a modification of the second one, but used with a circulating solution. To provide circulation, a second tube is introduced parallel to the crystal holder tube, which contains a glass stirrer operated by a Warren or some other slow motor. The distance between the cover of the housing and the dish is determined by the focal distance of the objectives being used. Most convenient are the long-focus objectives of the "Russkie samotsvety" make, which make it possible to increase this distance to 7-10 mm.

The dishes were glued with glyphtal cement, which resists temperatures up to 200°C.

The crystal holder permits orientation of the crystal in the dish and is assembled in the following manner. A hole of the same diameter as the outer diameter of the dish inlet tube is drilled part way through a rubber stopper which is then placed on the tube as a cap; a hypodermic needle with 0.5 mm opening is pushed through the

stopper and a length of wire is introduced into the needle. The end of the wire is capped with nitrolac, which holds the seed crystal.

In working with anisotropic crystals between crossed nicols, monochromatic light is used, so that the changes in the growing crystal can be more easily observed by the shape of the interference bands.

In designing a dish of the second or third type, it is necessary to calculate the minimum volume which would permit growth of a crystal without substantial decrease in the initial supersaturation of the solution. A formula may be derived for determining the minimum volume of a dish, v, in which crystals of maximum volume u can be grown at the temperature of crystallization T_{cr} from a solution saturated at T_1.

Let n/100 be the amount of possible change in the initial supersaturation, where n is expressed in percent; let C_{T_1} be the amount of substance needed to saturate 100 g of water at temperature T_1, and C_{T_2} the amount of substance needed for saturation at the nearest lower temperature for which data are available. (for substances with the usual direct relation between solubility and temperature.) Then, the excess of substance P, in cooling from T_1 to T_{cr}, will be:

$$P = \frac{C_{T_1} - C_{T_2}}{T_1 - T_2}(T_1 - T_{cr}). \tag{1}$$

The value of P obtained in this way is accurate enough, if the solubility curve is nearly straight. If it is not, and greater accuracy is required, P is best determined directly from the curve.

If V is the volume of solution containing 100 g of water, C_{T_1} g the weight of substance and P the weight of the excess of the substance in the dish at T_{cr}, then

$$P = \frac{V \cdot p}{v}, \tag{2}$$

and, if P = du, where d is the specific gravity of the substance, then equating (1) and (2), we get

$$\frac{(C_{T_1} - C_{T_2})(T_1 - T_{cr})}{T_1 - T_2} = \frac{Vdu}{v},$$

hence, the volume of the dish, taking into consideration the degree of possible initial supersaturation, n/100, is determined by the formula

$$v = \frac{T_1 - T_2}{(C_{T_1} - C_{T_2})(T_1 - T_{cr})} \cdot \frac{Vdu}{n} \cdot 100. \tag{3}$$

The value of V may be determined experimentally within 1%, but if the specific gravities of saturated solutions for different temperatures are available,

$$V = \frac{C_{T_1} + 100}{D},$$

where D is the specific gravity of the solution saturated at T_1 and Eq. (3) takes the form

$$v = \frac{(C_{T_1} + 100)du}{PDn} \cdot 100. \tag{4}$$

It is easy, by using Expression (4), to calculate also the maximum volume of the crystal, u, which can be grown in a given dish if the initial saturation may be changed by not more than n%.

The temperature control which is sufficiently accurate for the solution of many problems and the rapidity with which the temperature can be stabilized, together with the simplicity of construction and operation of the

apparatus make it useful in many studies of crystal growth under the microscope at constant temperature, and also in taking still and motion picture photographs of the process.

LITERATURE CITED

[1] K. V. Chmutov, Technique of Physicochemical Research [in Russian] (1954).

Received February 2, 1957

A. A. Zhdanov Leningrad State University

SOVIET PHYSICS – CRYSTALLOGRAPHY: AUTHOR INDEX FOR Vol. 2, 1957

(Russian Original Vol. 2, 1957, The Journal Crystallography of the Academy of Sciences, USSR)

Abdullaev, G. K. Some New Simple Forms of Pyrite - 307.

Abov, Iu. G., see Liashchenko, B. G. - 59.

Akishin, P. A. and V. P. Spiridonov. Electron Diffraction Analysis of the Molecular Structures of Halides of Group II Elements - 472.

Akulenok, E. M., Kh. S. Bagdasarov and V. Ia. Khaimov-Mal'kov. The Problem of the Effect of Mechanical Agitation and Ultrasonic Vibrations on the Process of Impurity Trapping by Single Crystals - 193.

Aleksandrov, K. S. Propagation of Elastic Shear Waves in a Crystal Bent Around a Specific Direction - 134.

Aleksandrov, K. S., see Chumakov, A. A. - 699.

Alfavdin, N. V., N. N. Sheftal' and Z. I. Frolova. Growing Uniform Crystals of Rochelle Salt from Strongly Supersaturated Solutions - 188.

Andreeva, N. S., N. G. Esipova and M. I. Millionova. Concerning the Peculiarities of Collagen Structure - 467.

Anikin, L. N. Hydrothermal Synthesis of Scheelite - 191.

Antsishkina, A. S., see Porai-Koshits, M. A. - 366.

Bagariatskii, Iu. A. Crystal Structure of the Metastable Phase Formed During the Tempering of Cu – Sn Alloys Containing 24-27% Sn - 277.

Bagariatskii, Iu. A. and Iu. D. Tiapkin. The Mechanism of Structure Transformations in Agehardening Alloys Based on Nickel - 414.

Bagdasarov, Kh. S., see Akulenok, E. M. - 193.

Bagdasarov, Kh. S. and V. Ia. Khaimov-Mal'kov. Some Experimental Data on the Nature of the Formation of Etched Figures in an Ultrasonic Field - 309.

Baranskii, K. N. Excitation of Ultrasonic Vibrations in Quartz - 296.

Batsanov, S. S. and V. I. Pakhomov. On the Change in the Nature of the Chemical Bond When the Coordination Number is Changed - 176.

Batsanov, S. S. Refractometric Determination of the Structure of Complex Cobalt Compounds - 259.

Bazhenov, V. A. Wood as a Piezoelectric Texture - 104.

Beliaev, L. M., V. A. Perl'shtein and V. P. Panova. Activator Distribution in Alkali Halide Crystals Studied With Radioactive Tracers - 435.

Beliustin, B. V. On the Equilibrium Form of Crystals in a Gravitational Field - 583.

Belov, N. V. and E. N. Belova. Mosaics for 46 Plane (Shubnikov) Antisymmetry Groups and for 15 (Fedorov) Color Groups - 16.

Belov, N. V., N. N. Neronova and T. S. Smirnova. Shubnikov Groups - 311.

Belov, N. V. New Silicate Structures - 361.

Belov, N. V. Concerning the Course in Geometric Crystallography for Physicists - 667.

Belov, N. V. Concerning the Tetrahedral (T = 23) and Gyrohedral (O = 432) Groups - 712.

Belov, N. V. A Theorem on the Primitiveness (Emptiness) of the Unit Cell of a Crystal Lattice - 715.

Belova, E. N., see Belov, N. V. - 16.

Bleidelis, Ia. Ia. Crystalline Structure of Cis – $[Pt(NH_3)_2(SCN)_2]$ - 270.

Bleidelis, Ia. Ia. and G. B. Bokii. The Crystalline Structure of the Trans-Diamminedithiocyanide of Divalent Platinum - 274.

Bogdanov, S. V., B. M. Vul, R. Ia. Razbash. Piezoelectric Shear Modulus of Polarized Barium Titanate - 111.

Boiarskaia, Iu. S. Investigation of the Anisotropy of Hardness of Single Crystals of PbS by Scratching - 702.

Bokii, G. B. and Kozlova, O. G. Crystallographic Criteria in Selecting Fluorspar for Growing Artificial Crystals of Optical Fluorite - 152.

Bokii, G. B., see Bleidelis, Ia. Ia. - 274.

Bokii, G. B. and G. A. Kukina. Crystallochemistry of Complex Divalent Platinum Compounds (The Effect of Transinfluence in Crystalline Substances) - 395.

Bokii, G. B. and N. A. Parpiev. X-Ray Structural Analysis of Crystals of $[Ru(NH_3)_4(NO)(OH)Cl_2$ - 681.

Boksha, S. S. New Method of Producing Very High Gas Pressures - 195.

Breido, L. Ia., see Leiteizen, L. G. - 286.

Briatov, L. V., see Butuzov, V. P. - 659.

Bublik, A. I. Electron Diffraction Study of the Structure of Thin Films of Molten Tin - 240.

Bublik, A. I. and A. G. Buntar', Determination of the Radial-Distribution Function for Atoms in a Liquid Metallic Alloy from Electron-Diffraction Data - 246.
Buntar', A. G., see Bublik, A. I. - 246.
Butuzov, V. P., Study of Phase Transformations at Very High Pressures - 533.
Butuzov, V. P. and L. V. Briatov. An Investigation of Phase Equilibria in a Part of the System $H_2O - SiO_2 - Na_2CO_3$ at High Temperatures and Pressures - 659.
Bykov, V. N., S. I. Vinogradov, V. A. Levdik and V. S. Golovkin. A Double Crystal Neutron Spectrometer - 626.

Chernov, A. A., see Lemmlein, G. G. - 426.
Chernysheva, M. A., see Indenbom, V. L. - 522.
Chistiakov, Iu. D. and M. V. Mal'tsev. Electron-Diffraction Study of the Oxidation of Aluminum Alloys - 620.
Chumakov, A. A., I. M. Sil'vestrova and K. S. Aleksandrov. The Dielectric, Elastic and Piezoelectric Properties of Single Crystals of Benzophenone - 699.

Dikareva, L. M., see Porai-Koshits, M. A. - 366.
Dubov, G. A. and V. R. Regel'. Concerning a Method of Testing Small Samples in Compression and Stress Relaxation - 734.
Dubov, G. A., see Regel', V. R. - 742.
Dukova, E. D., see Lemmlein, G. G. - 426.

Eisner, L. Ia. Some Alterations in the Dielectric Properties of Rochelle Salt Crystals Exposed to X-Rays - 293.
Eliutina, V., see Umanskii, Ia. - 500.
Enikeeva, M. G., see Grum-Grzhimailo, S. V. - 180.
Ermolina, A. V., G. S. Markova and V. A. Kargin. Electron-Diffraction Investigation of Polymers. IV. A Study of the Structural Changes in Polychlorotrifluoroethylene in the Crystalline Melting Point Range - 615.
Esipova, N. G., see Andreeva, N. S. - 367.
Ezhek, Dr. I., I. Koritta and K. Lebl'. On the Morphology of Spherulitic Graphite in High-Strength Cast Iron - 653.

Fotchenkov, A. A. Apparatus for Measuring Very Small Displacements of Oscillating Crystals - 643.
Frank-Kamenetskii, V. A. Oriented Crystallization of $KMnO_4$ and $KClO_4$ on Barytes - 706.
Frank-Kamenetskii, V. A. In Memoty of Osip Markovich Ansheles - 709.
Fridkin, V. M. Electrophotography on Photoelectrets - 125.
Fridkin, V. M., see Zheludev, I. S. - 697.
Frolova, Z. I., see Aliavdin, N. V. - 188.

Gal'perin, E. I. and Iu. S. Terminasov. On the State of Carbon in Annealed Silicon Steel - 684.
Gal'perin, E. I. and Iu. S. Terminasov. Change in the Crystal Structure of Steel During Cold Work and Heat Treatment - 515.
Gladyshevskii, E. I. and P. I. Kripiakevich. Crystal Structure of the Compounds $MoBe_{12}$, WBe_{12} and $TaBe_{12}$ - 730.
Glukhovskoi, B. M., see Leiteizen, L. G. - 286.
Gol'der, G. A., see Ozerov, R. P. - 211.
Golovkin, V. S., see Bykov, V. N. - 626.
Grum-Grzhimailo, S. V. and M. G. Enikeeva. On the Vibrational "Structure" of Absorption Spectra of Crystals Whose Coloration is Due to Isomorphic Impurities - 180.

Ignatov, D. V. Electron Diffraction Investigation of Phase Transitions in Thin Films of Metals and Oxides - 480.
Indenbom, V. L. On the Possibility of Optical Detection of Dauphine Twinning in Quartz - 79.
Indenbom, V. L. and G. E. Tomilovskii. Macroscopic Edge Dislocations in a Corundum Crystal - 183.
Indenbom, V. L. and M. A. Chernysheva. Significance for the Theory of Ferroelectricity of the Optical Study of Domains in Rochelle Salt - 522.
Indenbom, V. L. The Macroscopic Theory of the Formation of Dislocations in Crystal Growth - 587.
Iukhno, E. K. and M. A. Porai-Koshits. The Crystal Structures of Trans-Diisothiocyanotetrammine-Nickel - 230.
Iukhno, E. K., see Porai-Koshits, M. A. - 366.
Iurin, V. A., see Konstantinova, V. P. - 290.
Iveronova, V. I., A. P. Zviagina and A. A. Katsnel'son. Distortions of the Crystal Lattice in Solid Solutions - 408.
Iveronova, V. I., see Zviagina, A. P. - 606.

Kagan, A., see Umanskii, Ia. - 500.
Kapyshev, A. G., see Venevtsev, Iu. N. - 225.
Kargin, V. A., see Ermolina, A. V. - 615.
Katsnel'son, A. A., see Iveronova, V. I. - 408.
Katsnel'son, A. A. Monochromatization of the Reflected X-Ray Beam - 692.
Kaverin, S. V., see Pinsker, Z. G. - 169.
Kaverin, S. V., see Pinsker, Z. G. - 380.
Kel'ner, N. A., see Vertsner, V. N. - 494.

Kgol', Dr. Frantishek. An Instrument for the Mechanical Determination of the Separation Between Lattice Planes - 597.
Khaimov-Mal'kov, V. Ia., see Akulenok, E. M. - 193.
Khaimov-Mal'kov, V. Ia., see Bagdasarov, Kh. S. - 309.
Khodashova, T. S. The Structure of Crystals of Cobaltous Hexafluogermanate Hexahydrate $[Co(H_2O)_6][GeF_6]$ - 602.
Khotsianova, T. L. The Crystal Structures of Diphenyliodonium Halides - 45.
Khotsianova, T. L., see Struchkov, Iu. T. - 376.
Khotsianova, T. L. and Iu. T. Struchkov. The Crystal Structures of Diphenyl Halogen Compounds - 378.
Kitaigorodskii, A. I. The Theory of the Relation Between Structure Amplitudes and Methods of Direct Analysis of Crystal Structures - 346.
Kitaigorodskii, A. I. Concepts of Organic Crystallography - 454.
Kitaigorodskii, A. I. The Packing of Chain Molecules. II. The Layers of Paraffin Molecules - 637.
Klassen-Nekliudova, M. V. and A. A. Urusovskaia. Plastic Deformation of Crystals Caused by Rotation of the Lattice Without Formation of Glide Lines - 128.
Kochnov, V. E. and M. P. Shaskol'skaia. Study of Slip Lines in Silver Chloride Crystals - 265.
Kochnov, V. E. Inhomogeneity of Stress Distribution in the Grain of a Polycrystal in the Initial Stage of Plastic Deformation - 301.
Kolontsova, E. V. and L. V. Telegina. The Influence of Deformation Conditions on the Mechanism of the Formation of Slip Bands - 648.
Konobeevskii, S. T. On the Representation of Crystal Atoms as Symmetrical Bodies - 445.
Konstantinova, V. P. and V. A. Iurin. The Nature of Polarization in Crystals of Impure Rochelle Salt - 290.
Koptsik, V. A. On the Superposition of Symmetry Groups in Crystal Physics - 95.
Koritta, I., see Ezhek, Dr. I. - 653.
Kozlova, O. G., see Bokii, G. B. - 152.
Kozlovskii, M. I. Observations on Layered-Spiral Growth of Crystals from Solutions - 146.
Kozlovskii, M. I. Kinetics of Crystallization at Constant Temperature and Supersaturation - 745.
Kripiakevich, P. I., see Gladyshevskii, E. I. - 730.
Kukina, G. A., see Bokii, G. B. - 395.
Kurov, G. A., S. A. Semiletov and Z. G. Pinsker. Electrical Properties and Real Structure of Single-Crystal Germanium Films Producted by Evaporation in Vacuum - 53.
Kuz'min, R. N., G. S. Zhdanov and N. N. Zhuravlev. Metallographic and X-Ray Diffraction Study of Alloys in the Antimony-Iridium System - 42.
Kvitka, S. S. and M. M. Umanskii. X-Ray Diffraction Camera for Precise Measurement of the Unit Cell Parameters of Single Crystals RKM-114 - 694.

Leiteizen, L. G., B. M. Glukhovskoi and I. Ia. Breido. Photoelectric Multiplier for Scintillation Gamma-Spectrometers - 286.
Lemmlein, G. G., E. D. Dukova and A. A. Chernov. The Dynamics of Certain Elementary Crystal Growth and Evaporation Processes - 426.
Levdik, V. A., see Bykov, V. N. - 626.
Liashchenko, B. G., D. F. Litvin, I. M. Puzei and Iu. G. Abov. Neutron Diffraction Study of Iron – Nickel Alloys of the Permalloy Class - 59.
Litvin, D. F., see Liashchenko, B. G. - 59.

Malinovskii, T. I. X-Ray Diffraction Structure Determination of Cobalt Diparatoliudin-Dichloride - 723.
Mal'tsev, M. V., see Chistiakov, Iu. D. - 620.
Markova, G. S., see Ermolina, A. V. - 615.
Melankholin, N. M. Anomalous Bisectrix Dispersion in Organic Pigment Crystals - 75.
Mikheev, V. I. and I. I. Shafranovskii. Edge Forms and Striation on Crystals - 158.
Mikheev, V. I. X-Ray Diffraction Determinative Table of Minerals - 463.
Millionova, M. L., see Andreeva, N. S. - 467.
Mindukshev, V. F., see Terminasov, Iu. S. - 510.
Mokievskii, V. A. and I. I. Shafranovskii. Symmetry, Antisymmetry and Pseudosymmetry of Nucleation Surfaces - 19.

Neronova, N. N., see Belov, N. V. - 311.

Ozerov, R. P., G. A. Gol'der and G. S. Zhdanov. X-Ray Diffraction Study of Sodium and Potassium Oxygen Vanadium Bronzes $Me_{0.33}V_2O_5$ - 211.
Ozerov, R. P. Crystal Chemistry of the Oxygen Vanadium Bronzes - 219.

Pakhomov, V. I., see Batsanov, S. S. - 176.
Panova, V. P., see Beliaev, L. M. - 435.
Parpiev, N. A., see Bokii, G. B. - 681.
Perl'shtein, V. A., see Beliaev, L. M. - 435.
Petrov, T. G. An Apparatus for the Study of Crystal Growth Under the Microscope - 761.
Pinsker, Z. G., see Kurov, G. A. - 53.

Pinsker, Z. G., S. V. Kaverin and N. V. Troitskaia. Electron Diffraction Study of Molybdenum Nitrides - 169.
Pinsker, Z. G. and S. V. Kaverin. Electron Diffraction Study of Nitrides and Carbides of Transition Metals - 380.
Pinsker, Z. G. and B. K. Vainshtein. A Survey of Electron Diffraction Structural Analysis - 551.
Pinsker, Z. G. and N. A. Skobel'styna. Electron Diffraction Analysis of the Processes of Decomposition of Supersaturated Solid Solutions in Systems Al – Cu and Ag – Cu - 610.
Pivovarov, L., see Umanskii, Ia. - 500.
Porai-Koshits, M. A., see Iukhno, E. K. - 230.
Porai-Koshits, M. A., E. K. Iukhno, A. S. Antsishkina and L. M. Dikareva. The Atomic Crystal Structures of Complex Acid-Amine Nickel Compounds - 366.
Puzei, I. M., see Liashchenko, B. G. - 59.

Razbash, R. Ia., see Bogdanov, S. V. - 111.
Regel', V. R., see Dubov, G. A. - 734.
Regel', V. R. and G. A. Dubov. Experiments in the Kinetics of Softening of TlBr-TlI Crystals - 742.
Rozsibal, M., see Semiletov, S. A. - 281.

Sakvarelidze, L. G. and L. M. Utevskii. Concerning Procedures of Studying the Structures and Phase Composition of Grain Boundaries - 687.
Semenchenko, V. K. Plant Transitions and Critical Phenomena in Anisotropic Phases - 139.
Semiletov, S. A., see Kurov, G. A. - 53.
Semiletov, S. A. and M. Rozsibal. Electron Diffraction Study of InSb Films - 281.
Shafranovskii, I. I., see Mokievskii, V. A. - 19.
Shafranovskii, I. I., see Mikheev, V. I. - 158.
Shafranovskii, I. I. and N. N. Stulov. Memorial to Viktor Ivanovich Mikheev - 199.
Shafranovskii, I. I. Development of the Study of Crystal Forms - 323.
Shakhova, R. A., see Zviagin, B. B. - 173.
Shamba, N. A. and N. N. Sheftal'. Spiral Growth of Silicon Crystals - 439.
Shamburov, V. A. Dividing Mechanisms Based on the Crystallographic Principle of the Close Packing of Geometrically Identical Bodies - 163.
Shaskol'skaia, M. P., see Kochnov, V. E. - 265.
Shaskol'skaia, M. P. and Iu. Kh. Vekilov. Etch Pits on Slip Lines and on the Boundaries of Polygonal Blocks in Silver Chloride Crystals - 544.
Sheftal', N. N., see Aliavdkin, N. V. - 188.
Sheftal', N. N., see Shamba, N. A. - 439.
Shishakov, N. A. On the Structure of the Oxide Au_2O_3 - 674.
Shishakov, N. A. On the Structure of the Oxide PtO_2 - 677.
Shishakov, N. A. A Simple Method for the Determination of Crystal Lattice Constants by Electron Diffraction Patterns from the Surface of an Object - 679.
Shtepan, S. E. On the Elastic Anisotropy of Isometric Crystals in the (hkl) Plane - 759.
Shubnikov, A. V. On the Formation of Spherulites - 422.
Shubnikov, A. V. On the Initial Forms of Spherulites - 578.
Shumov, Iu. V., see Venevtsev, Iu. N. - 225.
Shuvalov, L. A. Dielectric and Piezoelectric Properties of Polarized Ceramic $BaTiO_3$ in its Various Ferroelectric Phases - 115.
Sil'vestrova, I. M. Determination of Temperature-Conductivity Coefficients in Crystals of Ethylene Diamine Tartrate - 303.
Sil'vestrova, I. M., see Chumakov, A. A. - 699.
Skolbel'styna, N. A., see Pinsker, Z. G. - 610.
Smirnova, T. S., see Belov, N. V. - 311.
Sokolov, E. I., see Zamorzaev, A. M. - 5.
Solov'ev, A. M., see Vertsner, V. N. - 494.
Solov'ev, S. P., see Zhdanov, G. S. - 630.
Spiridonov, V. P., see Akishin, P. A. - 472.
Stepanova, A. A., see Zhdanov, G. S. - 284.
Struchkov, Iu. T. and T. L. Khotsianova. X-Ray Investigation of Crystals of Some Ferrocene Derivatives - 376.
Struchkov, Iu. T., see Khotsianova, T. L. - 378.
Stulov, N. N., see Shafranovskii, I. I. - 199.

Tarasov, V. V. Atomic Chains and the Fine structure of Glass - 487.
Tashpulatov, Iu., Z. V. Zvonkova and G. S. Zhdanov. X-Ray Examination of Captax (2-Mercaptobenzothiazole) - 33.
Tatarinova, L. I. Electron Diffraction Study of Amorphous Antimony Sulfide - 251.
Telegina, I. V., see Kolontsova, E. V. - 648.
Terminasov, Iu. S. and V. F. Mindukshev. X-Ray Diffraction Study of the Structural Distortion of Metals Under Static and Dynamic Compression at Room Temperature and Low Temperature - 510.
Terminasov, Iu. S., see Gal'perin, E. L. - 515.
Terminasov, Iu. S., see Gal'perin, E. L. - 684.
Tiapkin, Iu. D., see Bagariatskii, Iu. A. - 414.
Tomilovskii, G. E., see Indenbom, V. L. - 183.
Troitskaia, N. V., see Pinsker, Z. G. - 169.

Tsukerman, L. L., see Vedeneeva, N. E. - 68.

Umanskii, M. M., see Zhdanov, G. S. - 284.
Umanskii, Ia., V. Eliutina, A. Kagan and L. Pivovarov. X-Ray Diffraction Analysis of the Changes in Mosaic Structure During the Ageing of Beryllium Copper - 500.
Umanskii, M. M., see Zubenko, V. V. - 505.
Umanskii, M. M., see Kvitka, S. S. - 694.
Urusovskaia, A. A., see Klassen-Nekliudova, M. V. - 128.
Utevskii, L. M., see Sakvarelidze, L. G. - 687.

Vainshtein, B. K. On the Theory of the Radial Distribution Method - 24.
Vainshtein, B. K. Intensity of Electron Diffraction Pattern Reflections (General Case) - 334.
Vainshtein, B. K., see Pinsker, Z. G. - 551.
Vedeneeva, N. E. and L. L Tsukerman. The State of Fixation of the Cations of Methylene Blue on the Crystals of Montmorillonite and the Capacity of the Latter to Form Oriented Aggregates - 68.
Vekilov, Iu. Kh., see Shaskol'skaia, M. P. - 544.
Venevtsev, Iu. N., A. G. Kapyshev and Iu. V. Shumov. X-Ray Study of the System $PbTiO_3$–$BaSnO_3$ - 225.
Venevtsev, Iu. N., see Zhdanov, G. S. - 630.
Vertsner, V. N., N. A. Kel'ner and A. M. Solov'ev. Oxide Formation and Photoresistance of Lead Sulfide Films - 494.
Vinogradov, S. L., see Bykov, V. N. - 626.
Vlasenko, V. I. and G. S. Zhdanov. The Automatic Synthesis of a Two-Dimensional Representation of Atomic Structures - 353.
Vul, B. M., see Bogdanov, S. V. - 111.

Zamorzaev, A. M. and E. I. Sokolov. Symmetry and Various Kinds of Antisymmetry of Finite Bodies - 5.
Zamorzaev, A. M. Generalization of Fedorov Groups - 10.
Zheludev, I. S. Symmetry of Homogeneous, Continuous Isotropic Media in Tensor, Vector and Scalar Fields - 330.
Zhdanov, G. S., see Tashpulatov, Iu. - 33.
Zhdanov, G. S., see Kuz'min, R. N. - 42.
Zhdanov, G. S., see Ozerov, R. P. - 211.
Zhdanov, G. S., N. N. Zhuravlev, A. A. Stepanova and M. M. Umanskii. Crystal Chemistry of the Metal Hexaborides - 284.
Zhdanov, G. S., see Vlasenko, V. I. - 353.
Zhdanov, G. S., S. P. Solov'ev and Iu. N. Venevtsev. Structural Coefficients of the Internal Field in Ferroelectrics with the Perovskite-Type Structure - 630.
Zheludev, I. S. Symmetry and Piezoelectric Properties of Crystals and "Textures," - 86.
Zheludev, I. S. Symmetry of Scalars, Vectors, and Tensors of Second Rank - 202.
Zheludev, I. S. and V. M. Fridkin. Concerning the Two Limiting Point Groups of Symmetry of Polycrystalline Photoelectrets - 697.
Zheludev, I. S. The Point Groups of Symmetry of Crystals and Their Physical Interpretation - 718.
Zhuravlev, N. N., see Kuz'min, R. N. - 42.
Zhuravlev, N. N., see Zhdanov, G. S. - 284.
Zubenko, V. V. and M. M. Umanskii. The X-Ray Diffraction Determination of the Thermal Expansion of Single Crystals - 505.
Zviagin, B. B. and R. A. Shakhova. Electron Diffraction Study by Reflection of Powder Samples of Celadonite - 173.
Zviagin, B. B. Determination of the Structure of Celadonite by Electron Diffraction - 388.
Zviagina, A. P., see Iveronova, V. I. - 408.
Zviagina, A. P. and V. I. Iveronova. A Method for Determining the Amplitudes of the Thermal Vibrations of the Various Kinds of Atoms in Solid Solution - 606.
Zvonkova, Z. V., see Tashpulatov, Iu. - 33.
Zvonkova, Z. V. A Crystallochemical Investigation of the Structure of Some Complex Compounds - 403.

SOVIET PHYSICS – CRYSTALLOGRAPHY: SUBJECT INDEX FOR Vol. 2, 1957

(Russian Original Vol. 2, 1957, The journal Crystallography of the Academy of Sciences, USSR)

Absorption spectra of crystals containing isomorphic impurities, vibrational structure of - 180.
Acid-amine complexes of nickel, crystal structures of - 366.
Activator distributions in alkali halide crystals studied with radioactive tracers - 435.
Adsorption of methylene blue on montmorillonite - 68.
AgCl crystals, etch pits on - 544.
AgCl crystals, slip lines in - 265.
Ag-Cu, electron diffraction study of decomposition of supersaturated solid solutions - 610
Al-Cu, electron diffraction study of decomposition of supersaturated solid solutions - 610.
Age-hardening alloys, nickel, mechanism of structure transformation - 414.
Alkali halide crystals, activator distribution, study by radioactive tracers - 435.
Alloys, aluminum, electron diffraction study of oxidation - 620.
Alloys, Sb-Ir, metallographic and x-ray study - 42.
Alterations in the dielectric properties of Rochelle salt crystals exposed to x-rays - 293.
Aluminum alloys, electron diffraction study of oxidation - 620.
Anisotropic phases, plant transitions and critical phenomena in - 139.
Anisotropy of hardness in PbS crystals - 702.
Anomalous bisectrix dispersion in organic pigment crystals - 75.
Ansheles, Osip Markovich, in memory of - 709.
Antimony-iridium system, metallographic and x-ray study - 42.
Antimony sulfide, amorphous, electron diffraction study - 251.
Antisymmetry groups, mosaics for - 16.
Antisymmetry of finite bodies - 5.
Antisymmetry of nucleation surfaces - 19.
Apparatus for measuring very small displacements of oscillating crystals - 643.
Apparatus for the study of crystal growth under the microscope - 761.
Atomic chains and the fine structure of glass - 487.
Atomic crystal structures of complex acid-amine nickel compounds - 366.
Atoms, in crystals, representation as symmetrical bodies - 445.
Au_2O_3, structure - 674.
Automatic synthesis of a two-dimensional representation of atomic structures - 353.

Barytes, epitaxy of $KMnO_4$ and $KClO_4$ on - 706.
Barium titanate, piezoelectric shear modulus - 111.
Barium titanate, polarized ceramic, dielectric and piezoelectric properties - 115.
$BaSnO_3$-$PbTiO_3$ system - 225.
$Be_{12}Mo$, $Be_{12}W$ and $Be_{12}Ta$, structures - 730.
Bent crystal, propagation of shear waves in - 134.
Benzophenone, dielectric, elastic and piezoelectric properties - 699.
Beryllium-copper, changes in mosaic structure during ageing - 500.
Bisectrix dispersion, anomalous, in organic pigment crystals - 75.
Boundaries of polygonal blocks and slip lines, etch pits on, in silver chloride crystals - 544.

Camera, single-crystal x-ray diffraction, for precise determination of lattice parameters - 694.
Captax - 33.
Carbides of transition metals, electron diffraction study of - 380.
Carbon, state of, in annealed silicon steel - 684.
Cast iron, high-strength, morphology of spherulitic graphic in - 653.
Celadonite, electron diffraction study - 173.
Celadonite, structure determination by electron diffraction - 388.
Chain molecules, packing of - 637.
Change in the nature of the chemical bond when the coordination number is changed - 176.
Close packing, dividing mechanisms based on - 163.
Cobalt complexes, refractometric determination of structure - 259.
Cobalt di(p-toluidine) dichloride, structure - 723.
$[Co(H_2O)_6]$ $[GeF_6]$, structure - 602.
Collagen, peculiarities of structure - 467.
Color groups, mosaics for - 16.
Complex compounds, crystal structures of - 403.
Complexes, Pt (II), crystal chemistry - 395.
Concepts of organic crystallography - 454.
Coordination number and nature of the chemical bond - 176.
Copper-aluminum, electron diffraction study of decomposition of supersaturated solid solutions - 610

Copper-beryllium, changes in mosaic structure during ageing - 500.
Copper-silver, electron diffraction study of decomposition of supersaturated solid solutions - 610.
Copper-tin alloys, crystal structure of metastable phase - 277.
Corundum, macroscopic edge dislocations in - 183.
Course in geometric crystallography for physicists - 667.
Critical phenomena and plant transitions in anisotropic phases - 139.
Crystal chemistry of the metal hexaborides - 284.
Crystal chemistry of the oxygen vanadium bronzes - 219.
Crystal chemistry, organic - 454.
Crystal form , study of - 323.
Crystal growth and evaporation, dynamics of - 426.
Crystal growth, macroscopic theory of formation of dislocations in - 587.
Crystalline structure of Cis-$[Pt(NH_3)_2(SCN)_2]$ - 270.
Crystalline structure of the trans-diammine-dithiocyanide of divalent platinum - 274.
Crystallization at constant temperature and supersaturation, kinetics of - 745.
Crystallization, oriented, $KMnO_4$ and $KClO_4$ on barytes - 706.
Crystallochemical investigation of the structure of some complex compounds - 403.
Crystallochemistry of complex divalent platinum compounds (the effect of transinfluence in crystalline substances) - 395.
Crystallographic criteria in selecting fluorspar for growing artificial crystals of optical fluorite - 152.
Crystallography, development in USSR in last 40 years - 573.
Crystallography, geometric, course for physicists - 667.
Crystal physics, superposition of symmetry groups in - 95.
Crystals, equilibrium form in a gravitational field - 583.
Crystal-structure analysis, direct methods of, in relation to structure amplitudes - 346.
Crystal structure of steel during cold work and heat treatment - 515.
Crystal structure of the compounds $MoBe_{12}$, WBe_{12} and $TaBe_{12}$ - 730.
Crystal structure of the metastable phase formed during the tempering of Cu - Sn alloys containing 24-27 % Sn - 277.
Crystal structures of complex compounds - 403.
Crystal structures of diphenyl halogen compounds - 378.
Crystal structures of diphenyliodonium halides - 45.
Crystal structures of trans-diisothiocyanotetrammine-nickel - 230.
Cu-Ag, electron diffraction study of decomposition of supersaturated solid solutions - 610.
Cu-Al, electron diffraction study of decomposition of supersaturated solid solutions - 610.
Cubic space groups - 712.
Cu-Sn, crystal structure of metastable phase formed during tempering of alloys containing 24-27% Sn - 277.

Dauphine twinning in quartz, optical detection of - 79.
Decomposition of supersaturated solid solution, Al-Cu and Ag-Cu - 610.
Deformation conditions and mechanism of formation of slip bands - 648.
Deformation, plastic, by lattice rotation of crystals - 128.
Determination of the radial-distribution function for atoms in a liquid metallic alloys from electron-diffraction data - 246.
Determination of the structure of celadonite by electron diffraction - 388.
Determination of temperature-conductivity coefficients in crystals of ethylene diamine tartrate - 303.
Development of crystallography in the USSR in the last forty years - 573.
Development of the study of crystal forms - 323.
Dielectric, elastic and piezoelectric properties of single crystals of benzophenone - 699.
Dielectric and piezoelectric properties of polarized ceramic $BaTiO_3$ in its various ferroelectric phases - 115.
Dielectric properties, alteration on exposure to x-rays in Rochelle salt - 293.
Dielectric properties of barium titanate - 115.
Diphenylhalogen compounds, crystal structures of - 378.
Diphenyliodonium halides - 45.
Dislocations in corundum, macroscopic - 183.
Dislocations, macroscopic theory of formation in crystal growth - 587.
Distortions of the crystal lattice in solid solutions - 408.
Distortion, structural, of metals under static and dynamic compression at room and low temperatures - 510.
Dividing mechanisms based on the crystallographic principle of the close packing of geometrically identical bodies - 163.
Domains in Rochelle salt, optical study of, and theory of ferroelectricity - 522.

Double crystal neutron spectrometer - 626.
Dynamics of certain elementary crystal growth and evaporation processes - 426.

Edge forms and striation on crystals - 158.
Elastic anistropy of isometric crystals in the (hkl) plane - 759.
Elastic, dielectric, and piezoelectric properties of benzophenone - 699.
Elastic shear waves, propagation in a bent crystal - 134.
Electrical properties and real structure of single-crystal germanium films produced by evaporation in vacuum - 53.
Electron diffraction analysis of the molecular structures of halides of group II elements - 472.
Electron diffraction analysis of the processes of decomposition of supersaturated solid solutions in systems Al – Cu and Ag – Cu, - 610.
Electron-diffraction data, use in determining the radial distribution function in a liquid alloy - 246.
Electron diffraction, determination of the structure of celadonite by - 388.
Electron diffraction investigation of phase transitions in thin films of metals and oxides - 480.
Electron diffraction investigation of polymers. IV. A study of the structural changes in poly-chlorotrifluoroethylene in the crystalline melting point range - 615.
Electron-diffraction method of determination of lattice constants - 679.
Electron-diffraction pattern reflections, intensity of - 334.
Electron-diffraction structural analysis - 551.
Electron diffraction study by reflection of powder samples of celadonite - 173.
Electron diffraction study of amorphous antimony sulfide - 251.
Electron diffraction study of InSb films - 281.
Electron diffraction study of molybdenum nitrides - 169.
Electron diffraction study of nitrides and carbides of transition metals - 380.
Electron-diffraction study of the oxidation of aluminum alloys - 620.
Electron diffraction study of the structure of thin films of molten tin - 240.
Electron diffraction, theory of the radial distribution method - 24.
Electrophotography on photoelectrets - 125.
Epitaxy of $KMnO_4$ and $KClO_4$ on barytes - 706.
Equilibrium form of crystals in a gravitational field - 583.
Etch figures, formation in an ultrasonic field - 309.
Etch pits on slip lines and on the boundaries of polygonal blocks in silver chloride crystals - 544.
Ethylenediamine tartrate, temperature-conductivity coefficients - 303.
Evaporation and crystal growth, dynamics of - 426.
Excitation of ultrasonic vibrations in quartz - 296.
Experimental data on the nature of the formation of etched figures in an ultrasonic field - 309.
Experiments in the kinetics of softening of TlBr-TlI crystals - 742.

Fedorov groups, generalization of - 10.
Fedorov groups, mosaics for - 16.
Fe-Ni alloys, neutron diffraction study - 59.
Ferrocene derivatives, x-ray study of - 376.
Ferroelectricity, theory of, and optical study of domains in Rochelle salt - 522.
Ferroelectric phases of barium titanate - 115.
Ferroelectrics, perovskite-type, structural coefficients of the internal field - 630.
Fibrous proteins - 467.
Films, germanium, single-crystal, electrical properties and structure - 53.
Films, InSb, electron diffraction study of - 281.
Films of metals and oxides, electron diffraction study of phase transitions - 480.
Films, PbS, oxide formation and photoresistance of - 494.
Finite bodies, symmetry and antisymmetry - 5.
Fluogermanate, cobaltous, hexahydrate, structure - 602.
Fluorite, crystallographic criteria for selection for growing crystals of optical - 152.
Formation of spherulites - 422.
Fourier synthesis, two-dimensional, automatic method for - 353.

Gamma-spectrometers, scintillation, photoelectric multiplier for - 286.
Generalization of Fedorov groups - 10.
Geometric crystallography, course for physicists - 667.
Germanium, single-crystal films, electrical properties and structure - 53.
Glass, fine structure of, and atomic chains - 487.
Glide lines, plastic deformation of crystals without formation of - 128.
Gold oxide, Au_2O_3, structure - 674.
Grain boundaries, methods of studying structures and phase composition - 687.
Graphite, spherulitic, in high-strength cast-iron - 653.
Gravitational field, equilibrium form of crystals in - 583.

Group II elements, electron-diffraction study of halides - 472.
Growing uniform crystals of Rochelle salt from strongly supersaturated solutions - 188.
Growth, spiral, silicon crystals - 439.

Halides of group II elements, electron-diffraction determination of structure - 472.
Halogen diphenyl compounds - 45, 378
Hardness, anisotropy in PbS crystals - 702.
Hexaborides, crystal chemistry of - 284.
H_2O-SiO_2-Na_2CO_3, phase equilibria at high temperatures and pressures - 659.
Hydrothermal synthesis of scheelite - 191.

Impurity spectra of crystals, vibrational structure of - 180.
Impurity trapping in single crystals, mechanical agitation and ultrasonic vibrations - 193.
Indium antimonide films, electron diffraction study - 281.
Influence of deformation conditions on the mechanism of the formation of slip bands - 648.
Inhomogeneity of stress distribution in the grain of a polycrystal in the initial stage of plastic deformation - 301.
Initial forms of spherulites - 578.
Instrument for the mechanical determination of the separation between lattice planes - 597.
Intensity of electron diffraction pattern reflections (general case) - 334.
Investigation of the anisotropy of hardness of single crystals of PbS by scratching - 702.
Investigation of phase equilibria in a part of the system $H_2O - SiO_2 - Na_2CO_3$ at high temperatures and pressures - 659.
Iridium-antimony system, metallographic and x-ray study - 42.
Iron, cast, high-strength, morphology of spherulitic graphite in - 653.
Iron-nickel alloys, neutron diffraction study - 59.
Internal field in perovskite-type ferroelectrics, structural coefficients of - 630.

Kinetics of crystallization at constant temperature and supersaturation - 745.
Kinetics of softening of TlBr-TlI crystals - 742.
$KMnO_4$ and $KClO_4$, epitaxy on barytes - 706.

Lattice constants, method of determination by electron diffraction - 679.
Lattice parameters of single crystals, x-ray diffraction camera for precise measurement - 694.
Lattice planes, instrument for mechanical determination of spacing between - 597.
Lattice rotation, plastic deformation of crystals caused by - 128.
Layered-spiral growth - 146.
Lead sulfide crystals, anisotropy of hardness in - 702.
Lead sulfide films, oxide formation and photoresistance - 494.
Lead titanate-barium stannate system - 225.
Liquid alloy structure, determination of the radial distribution function from electron-diffraction data - 246.

Macroscopic edge dislocations in a corundum crystal, 183.
Macroscopic theory of the formation of dislocations in crystal growth - 587.
Mechanical agitation and impurity trapping in single crystals - 193.
Mechanism of structure transformations in age-hardening alloys based on nickel - 414.
Mechanisms, dividing, based on close packing - 163.
Melting of poly(chlorotrifluoroethylene), electron diffraction study - 615.
Memorial to Viktor Ivanovich Mikheev - 199.
2-Mercaptobenzothiazole - 33.
Metal and oxide films, electron diffraction study of phase transitions - 480.
Metals, structural distortion of, under static and dynamic compression at room and low temperatures - 510.
Metallographic and x-ray diffraction study of alloys in the antimony-iridium system - 42.
Method for the determination of crystal lattice constants by electron diffraction patterns from the surface of an object - 679.
Method for determining the amplitudes of the thermal vibrations of the various kinds of atoms in solid solution - 606.
Methods of studying structure and phase composition of grain boundaries - 687.
Method of testing small samples in compression and stress relaxation - 734.
Methylene blue, adsorption on montmorillonite - 68.
Minerals, x-ray diffraction determinative table of - 463.
Mikheev, Viktor Ivanovich, memorial to - 199.
$MoBe_{12}$, structure - 730.
Molybdenum nitrides, electron diffraction study - 169.
Monochromatization of the reflected x-ray beam - 692.
Montmorillonite, adsorption of methylene blue on, and oriented aggregation of - 68.
Morphology, development of study - 323.

Morphology of spherulitic graphite in high-strength cast iron - 653.
Mosaics for 46 plane (Shubnikov) antisymmetry groups and for 15 (Fedorov) color groups - 16.
Mosaic structure in Be-Cu, changes during ageing - 500.

Na_2CO_3-H_2O-SiO_2, phase equilibria at high temperatures and pressures - 659.
Nature of chemical bond and coordination number - 176.
Nature of polarization in crystals of impure Rochelle salt - 290.
Neutron diffraction study of iron — nickel alloys of the permalloy class - 59.
Neutron spectrometer, double crystal - 626.
New method of producing very high gas pressures - 195.
New silicate structures - 361.
New simple forms of pyrite - 307.
Nickel alloys, age-hardening, mechanism of structure transformation - 414.
Nickel complexes, acid-amine, crystal structures of - 366.
Nickel-iron alloys, neutron diffraction study - 59.
$Ni(NH_3)_4(SCN)_2$, trans, crystal structures of - 230.
Nitrides, molybdenum, electron diffraction study - 169.
Nitrides of transition metals, electron diffraction study of - 380.
Nucleation surfaces, symmetry, antisymmetry, and pseudosymmetry of - 19.

Observation on layered-spiral growth of crystals from solutions - 146.
Optical detection of Dauphine twinning in quartz - 79.
Optical fluorite, crystallographic criteria for selecting fluorspar for growing - 152.
Optical study of domains in Rochelle salt and theory of ferroelectricity - 522.
Organic crystal chemistry, concepts of - 454.
Organic pigment crystals, anomalous bisectrix dispersion in - 75.
Oriented aggregation of montmorillonite - 68.
Oriented crystallization of $KMnO_4$ and $KClO_4$ on barytes - 706.
Oscillating crystals, apparatus for measuring very small displacement of - 643.
Oxide formation and photoresistance of lead sulfide films, - 494.

Packing of chain molecules. II. The layers of paraffin molecules - 637.
Paraffin molecules, packing in layers of - 637.
PbS crystals, anisotropy of hardness in - 702.
PbS films, oxide formation and photoresistance - 494.
$PbTiO_3$-$BaSnO_3$ system - 225.
Peculiarities of collagen structure - 467.
Permalloy, neutron diffraction study - 59.
Perovskite-type ferroelectrics, structural coefficients of the internal field - 630.
Phase composition and structure of grain boundaries - 687.
Phase equilibria at high temperatures and pressures in system H_2O-SiO_2-Na_2CO_3 - 659.
Phase transitions at very high pressures - 533.
Phase transitions in thin films of metals and oxides, electron diffraction study - 480.
Photoelectric multiplier for scintillation gamma-spectrometers - 286.
Photoelectrets, electrophotography on - 125.
Photoelectrets, polycrystalline, limiting point groups of - 697.
Photoresistance of PbS films and oxide formation - 494.
Piezoelectric, dielectric, and elastic properties of benzophenone - 699.
Piezoelectricity of wood - 104.
Piezoelectric properties of barium titanate - 115.
Piezoelectric shear modulus of polarized barium titanate - 111.
Piezoelectric properties of crystals, symmetry, and textures - 86.
Physical interpretation of the point groups - 718.
Plane groups, antisymmetric and colored, mosaics for - 16.
Plant transitions and critical phenomena in anisotropic phases- 139.
Plastic deformation of crystals caused by rotation of the lattice without formation of glide lines - 128.
Plastic deformation of polycrystals - 301.
Platinum dioxide, structure - 677.
Point groups with antisymmetry operations- 5.
Point groups and their physical interpretation - 718.
Point groups of polycrystalline photoelectrets - 697.
Point groups of symmetry of crystals and their physical interpretation - 718.
Polarization, nature of, in crystals of impure Rochelle salt - 290.
Poly(chlorotrifluoroethylene), structural changes in melting point range, electron diffraction study - 615.
Polycrystals, plastic deformation of - 301.
Polymers, electron-diffraction study - 615.
Possibility of optical detection of Dauphine twinning in quartz - 79.

Potassium permanganate and perchlorate, epitaxy on barytes - 706.
Pressure, very high, phase transitions at - 533.
Pressures, very high, method of production in gas - 195.
Primitiveness of unit cells of lattices - 715.
Problem of the effect of mechanical agitation and ultrasonic vibrations on the process of impurity trapping by single crystals - 193.
Procedures of studying the structures and phase compo ition of grain boundaries - 687.
Propagation of elastic shear waves in a crystal bent around a specific direction - 134.
Proteins, fibrous - 467.
Pseudosymmetry of nucleation surfaces - 19.
Pt (II) complexes, crystal chemistry - 395.
$Pt(NH_3)_2(SCN)_2$, cis, crystal structure - 270.
$Pt(NH_3)_2(SCN)_2$, trans, crystal structure - 274.
PtO_2, structure - 677.
Pyrite, some new simple forms of - 307.

Quartz, excitation of ultrasonic vibrations in - 296.
Quartz, optical detection of Dauphine twinning in - 79.

Radial distribution function, determination in a liquid metallic alloy from electron-diffraction data - 246.
Radial distribution method, theory of - 24.
Radioactive tracers, study of activator distributions in alkali halide crystals - 435.
Refractometric determination of the structure of complex cobalt compounds - 259.
Representation of crystal atoms as symmetrical bodies - 445.
Rochelle salt crystals, alteration in dielectric properties on exposure to x-rays - 293.
Rochelle salt, growing uniform crystals of - 188.
Rochelle salt, impure, nature of polarization in - 290.
Rochelle salt, optical study of domains, and theory of ferroelectricity - 522.
$[Ru(NH_3)_4(NO)(OH)]Cl_2$, structure - 681.

Sb-Ir system, metallographic and x-ray study - 42.
Sb_2S_3, amorphous, electron diffraction study - 251.
Scalar fields, effect on symmetry of isotropic media - 330.
Scheelite, hydrothermal synthesis of - 191.
Scintillation gamma-spectrometers, photoelectric multiplier for - 286.
Shfranovskii, Illarion Illarionovich, 50th birthday - 665.
Shear modulus, piezoelectric, of polarized barium titanate - 111.
Shear waves, propagation in a bent crystal - 134.
Shubnikov, Aleksei Vasil'evich - 1.
Shubnikov groups - 311.
Shubnikov groups, mosaics for - 16.
Significance for the theory of ferroelectricity of the optical study of domains in Rochelle salt - 522.
Silicate structures, new - 361.
Silicon crystals, spiral growth of - 439.
Silicon steel, annealed, state of carbon in - 684.
Silver chloride crystals, etch pits on - 544.
Silver chloride crystals, slip lines in - 265.
Silliver-copper, electron diffraction study of decomposition of supersaturated solid solutions - 610.
Single-crystal films, germanium, electrical properties and structure - 53.
Single crystals, impurity trapping by, and mechanical agitation and ultrasonic vibrations - 193.
Single crystals, x-ray diffraction determination of thermal expansion - 505.
SiO_2-Na_2CO_3-H_2O, phase equilibria at high temperatures and pressures - 659.
Single crystal x-ray diffraction camera for precise determination of lattice parameters - 694.
Slip lines in silver chloride crystals - 265.
Sodium potassium tartrate crystals, alteration in dielectric properties on exposure to x-rays - 293.
Sodium potassium tartrate, growing uniform crystals of - 188.
Sodium potassium tartrate, impure, nature of polarization in - 290.
Sodium potassium tartrate, optical study of domains, and theory of ferroelectricity - 522.
Softening of TlBr-TlI crystals, kinetics - 742.
Solid solutions, determination of amplitudes of thermal vibrations in - 606.
Solid solutions, supersaturated, decomposition of, Al-Cu and Ag-Cu - 610.
Slip bands, influence of deformation conditions on mechanism of formation - 648.
Slip lines and boundaries of polygonal blocks etch pits on, in silver chloride crystals - 544.
Sodium potassium tartrate, optical study of domains, and theory of ferroelectricity - 522.
Solid solutions, lattice distortions in - 408.
Space groups, generalization of - 10.
Space-group theory - 311, 712.
Spacing between lattice planes, instrument for mechanical determination of - 597.
Spectra, absorption, of crystals containing isomorphic impurities, vibrational structure of - 180.
Spectrometer, neutron, double crystal - 626.
Spherulites, formation of - 422.
Spherulites, initial forms of - 578.
Spiral growth, layered - 146.
Spiral growth of silicon crystals - 439.

Stannate, barium-lead titanate system - 225.
State of carbon in annealed silicon steel - 684.
State of fixation of the cations of methylene blue on the crystals of montmorillonite and the capacity of the latter to form oriented aggregates - 68.
Steel, change in crystal structure during cold work and heat treatment - 515.
Steel, silicon, annealed, state of carbon in - 684.
Stress distribution, inhomogeneity in the grain of a polycrystal during plastic deformation - 301.
Striations and edge forms on crystals - 158.
Structural analysis by electron diffraction - 551.
Structural changes in poly(chlorotrifluoroethylene) in melting point range, electron diffraction study - 615.
Structural coefficients of the internal field in ferroelectrics with the perovskite-type structure - 630.
Structure amplitudes and methods of direct crystal-structure analysis - 346.
Structure and phase composition of grain boundaries - 687.
Structure of crystals of cobaltous hexafluogermanate hexahydrate $[Co(H_2O)_6][GeF_6]$ - 602.
Structure of the oxide Au_2O_3 - 674.
Structure of the oxide PtO_2 - 677.
Structure transformations in age-hardening nickel alloys - 414.
Study of phase transformations at very high pressures - 533.
Study of slip lines in silver chloride crystals - 265.
Superposition of symmetry groups in crystal physics - 95.
Survey of electron diffraction structural analysis - 551.
Symmetry, antisymmetry and pseudosymmetry of nucleation surfaces - 19.
Symmetry groups in crystal physics, superposition of - 95.
Symmetry groups of polycrystalline photoelectrets - 697.
Symmetry of homogeneous, continuous isotopic media in tensor, vector and scalar fields - 330.
Symmetry and piezoelectric properties of crystals and "textures" - 86.
Symmetry of scalars, vectors, and tensors of second rank - 202.
Symmetry and various kinds of antisymmetry of finite bodies - 5.
Synthesis, hydrothermal, of scheelite - 191.

$TaBe_{12}$, structure - 730.
Table of x-ray diffraction determinative data for minerals - 463.
Tartrate, ethylenediamine, temperature-conductivity coefficients - 303.
Tartrate, sodium potassium, alteration in dielectric properties of crystals on exposure to x-rays - 293.
Tartrate, sodium potassium, growing uniform crystals of - 188.
Tartrate, sodium potassium, impure, nature of polarization in - 290.
Tartrate, sodium potassium, optical study of domains, and theory of ferroelectricity - 522.
Temperature-conductivity coefficients in crystals of ethylenediamine tartrate - 303.
Tempering of Cu-Sn alloys, crystal structure of metastable phase from alloys containing 24-27% Sn - 277.
Tensor and vector symmetry - 202.
Tensor fields, effect on symmetry of isotropic media - 330.
Testing small samples in compression and stress relaxation - 734.
Tetrahedral (T = 23) and gyrohedral (O = 432) groups - 712.
Textures, symmetry, and piezoelectric properties of crystals - 86.
Theorem on the primitiveness (emptiness) of the unit cell of a crystal lattice - 715.
Theory of the radial distribution method - 24.
Theory of the relation between structure amplitudes and methods of direct analysis of crystal structures - 346.
Thermal expansion of single crystals, x-ray diffraction determination - 505.
Thermal vibrations, determination of amplitudes in solid solutions - 606.
Thin films, tin, structure of - 240.
Tin, structure of thin films - 240.
Tin-copper alloys, crystal structure of metastable phase - 277.
Titanate, barium, piezoelectric shear modulus - 111.
Titanate, barium, polarized ceramic, dielectric and piezoelectric properties of - 115.
Titanate, lead-barium stannate system - 225.
TlBr-TlI crystals, kinetics of softening - 742.
Trans-diisothiocyanotetrammine-nickel, crystal structures of - 230.
Trans-effect and crystal chemistry of platinum complexes - 395.
Transition metal nitrides and carbides, electron diffraction study of - 380.
Transitions, plant, and critical phenomena in anisotropic phases - 139.
Transverse vibrations, propagation in a bent crystal - 134.
Twinning, Dauphine, optical detection in quartz - 79.

Two-dimensional syntheses, automatic method for - 353.
Two limiting point groups of symmetry of polycrystalline photoelectrets - 697.

Ultrasonic field, formation of etch figures in - 309.
Ultrasonic vigrations and impurity trapping in single crystals - 193.
Ultrasonic vibrations, excitation in quartz - 296.
Unit cells, primitiveness of - 715.
USSR, development of crystallography in last 40 years - 573.

Valence theory and coordination number - 176.
Vanadium bronzes, crystal chemistry of - 219.
Vanadium bronzes, sodium and potassium - 211.
Vector and tensor symmetry - 202.
Vector fields, effect on symmetry of isotropic media - 330.
Very high gas pressures, method of producing - 195.
Vibrational "structure" of absorption spectra of crystals whose coloration is due to isomorphic impurities - 180.
Vibrations, thermal, determination of amplitudes in solid solutions - 606.

WBe_{12}, structure - 730.
Wood as a piezoelectric texture - 104.

X-ray beam, reflected, monochromatization of - 692.
X-ray diffraction analysis of the changes in mosaic structure during the ageing of beryllium copper - 500.
X-ray diffraction camera for precise measurement of the unit cell parameters of single crystals RKM-114 - 694.
X-ray diffraction determination of the thermal expansion of single crystals - 505.
X-ray diffraction determinative table of minerals - 463.
X-ray diffraction structure determination of cobalt diparatoluidin-dichloride - 723.
X-ray diffraction study of sodium and potassium oxygen vanadium bronzes $Me_{0.33}V_2O_5$ - 211.
X-ray diffraction study of the structural distortion of metals under static and dynamic compression at room temperature and low temperature - 510.
X-ray examination of captax (2-mercaptobenzothiazole) - 33.
X-ray investigation of crystals of some ferrocene derivatives - 376.
X-rays, alteration in dielectric properties of Rochelle crystals on exposure to - 293.
X-ray structural analysis of crystals of $[Ru(NH_3)_4(NO)(OH)]Cl_2$ - 681.
X-ray study of the xyxtem $PbTiO_3 - BaSnO_3$ - 225.

SOVIET PHYSICS — CRYSTALLOGRAPHY

(Translation of the journal "Crystallography" of the USSR, Vol. 2, No. 6
published by the American Institute of Physics, May 1958)

Volume 2, Number 6 November-December 1957

CONTENTS

	PAGE	RUSS. PAGE
In Memory of Osip Markovich Ansheles	709	719
Concerning the Tetrahedral (T = 23) and Gyrohedral (O = 432) Groups. N. V. Belov	712	722
A Theorem on the Primitiveness (Emptiness) of the Unit Cell of a Crystal Lattice. N. V. Belov	715	725
The Point Groups of Symmetry of Crystals and Their Physical Interpretation. L. S. Zheludev	718	728
X-ray Diffraction Structure Determination of Cobalt Diparatoluidine Dichloride. T. I. Malinovskii	723	734
Crystal Structure of the Compounds $MoBe_{12}$, WBe_{12} and $TaBe_{12}$. E. I. Gladyshevskii and P. I. Kripiakevich	730	742
Concerning a Method of Testing Small Samples in Compression and Stress Relaxation. G. A. Dubov and V. R. Regel'	734	746
Experiments in the Kinetics of Softening of TlBr—TlI Crystals. V. R. Regel' and G. A. Dubov	742	756
Kinetics of Crystallization at Constant Temperature and Supersaturation. M. I. Kozlovskii	745	760
Production of Oriented Figures on Metals by Ionic Bombardment. V. E. Iurasova	754	770
Brief Communications		
On the Elastic Anisotropy of Isometric Crystals in the (hkl) Plane. S. E. Shtepan	759	776
An Apparatus for the Study of Crystal Growth Under the Microscope. T. G. Petrov	761	777
Author Index for Vol. 2, 1957	765	
Subject Index for Vol. 2, 1957	770	

SIGNIFICANCE OF ABBREVIATIONS MOST FREQUENTLY ENCOUNTERED IN SOVIET CRYSTALLOGRAPHY LITERATURE

AN SSSR	*Academy of Sciences, USSR*
FIAN	*Physics Institute, Academy of Sciences USSR*
GITI	*State Scientific and Technical Press*
GITTL	*State Press for Technical and Theoretical Literature*
GOI	*State Optical Institute*
GONTI	*State United Scientific and Technical Press*
Gosfizkhimizdat	*State Physical Chemistry Press*
Gozkhimizdat	*State Chemistry Press*
GOST	*All-Union State Standard*
Goztekhizdat	*State Technical Press*
GTTI	*State Technical and Theoretical Press*
GUPIAE	*State Office for Utilization of Atomic Energy*
IF KhI	*Institute of Physical Chemistry Research*
IFP	*Institute of Physical Problems*
IK	*Institute of Crystallography*
IL	*Foreign Literature Press*
IPF	*Institute of Applied Physics*
IPM	*Institute of Applied Mathematics*
IREA	*Institute of Chemical Reagents*
ISN (Izd. Sov. Nauk)	*Soviet Science Press*
IIaP	*Institute of Nuclear Studies*
Izd	*Press (publishing house)*
KISO	*Solar Research Commission*
LETI	*Leningrad Electrotechnical Institute*
LFTI	*Leningrad Institute of Physics and Technology*
LIM	*Leningrad Institute of Metals*
LITMiO	*Leningrad Institute of Precision Instruments and Optics*
MATI	*Moscow Aviation Technology Institute*
MGU	*Moscow State University*
Metallurgizdat	*Metallurgy Press*
MOPI	*Moscow Regional Pedagogical Institute*
NIAFIZ	*Scientific Research Association for Physics*
NIFI	*Scientific Research Institute of Physics*
NIIMM	*Scientific Research Institute of Mathematics and Mechanics*
NII ZVUKSZAPIOI	*Scientific Research Institute of Sound Recording*
NIKFI	*Scientific Institute of Motion Picture Photography*
OIIaI	*Joint Institute of Nuclear Studies*
ONTI	*United Scientific and Technical Press*
OTI	*Division of Technical Information*
OTN	*Division of Technical Science*
RIAN	*Radium Institute, Academy of Sciences of the USSR*
SPB	*All-Union Special Planning Office*
Stroiizdat	*Construction Press*
TsNIIChERMET	*Central Scientific Research Institute for Ferrous Metallurgy*
URALFTI	*Ural Institute of Physics and Technology*

NOTE: Abbreviations not on this list and not explained in the translation have been transliterated, no further information about their significance being available to us.—*Publisher.*

The expanded program of the American Institute of Physics comprises translation of six leading Soviet physics journals, as listed below. These translations, by competent, qualified scientists, provide all research laboratories and libraries with accurate and up-to-date information of the results of research in the U.S.S.R.

Soviet Physics—Technical Physics

A translation of the "Journal of Technical Physics" of the Academy of Sciences of the U.S.S.R. The translation began with the 1956 issues. Twelve issues per year, approximately 3,000 Russian pages. Annually $75.00 domestic, $79.00 foreign. Libraries* $35.00 domestic, $39.00 foreign. Back numbers, all issues $8.00.

Soviet Physics—Acoustics

A translation of the "Journal of Acoustics" of the Academy of Sciences of the U.S.S.R. The translation began with the 1955 issues. Four issues per year, approximately 400 Russian pages. Annually $12.00 domestic, $14.00 foreign. (No library discounts.) Back numbers, all issues $4.00.

Soviet Physics—Doklady

A translation of all of the "Physics Sections" of the Proceedings of the Academy of Sciences of the U.S.S.R. The translation began with the 1956 issues. Six issues per year, approximately 1,500 Russian pages. Annually $35.00 domestic, $38.00 foreign. Libraries* $15.00 domestic, $18.00 foreign. Back numbers for Volumes 1 and 2, $5.00 per issue; Volume 3 and subsequent, $7.00 per issue.

Soviet Physics—JETP

A translation of the "Journal of Experimental and Theoretical Physics" of the Academy of Sciences of the U.S.S.R. The translation began with the 1955 issues. Twelve issues per year, approximately 4,000 Russian pages. Annually $75.00 domestic, $79.00 foreign. Libraries* $35.00 domestic, $39.00 foreign. Back numbers, all issues $8.00.

Soviet Physics—Crystallography

A translation of the journal "Crystallography" of the Academy of Sciences of the U.S.S.R. The translation began with the 1957 issues. Six issues per year, approximately 1,000 Russian pages. Annually $25.00 domestic, $27.00 foreign. Libraries* $10.00 domestic, $12.00 foreign. Back numbers, all issues $5.00.

Soviet Astronomy—AJ

A translation of the "Astronomical Journal" of the Academy of Sciences of the U.S.S.R. The translation began with the 1957 issues. Six issues per year, approximately 1,100 Russian pages. Annually $25.00 domestic, $27.00 foreign. Libraries* $10.00 domestic, $12.00 foreign. Back numbers, all issues $5.00.

Subscriptions should be addressed to the American Institute of Physics, 335 East 45th Street, New York 17, N.Y.

* For libraries of non-profit academic institutions.